This project is implemented through the CENTRAL EUROPE Programme co-financed by the ERDF.

http://transenergy-eu.geologie.ac.at

Summary Report „Geothermal Models at Supra-Regional Scale"

Title: Summary report "Geothermal Models at Supra-Regional Scale"

Authors: **Goetzl Gregor & Zekiri Fatime (GBA) editor** in cooperation with MFGI, GEO-ZS, ŠGÚDŠ.

Austria: Goetzl Gregor, Hoyer Stefan, Zekiri Fatime

Hungary: Lenkey Laszlo

Slovakia: Švasta Jaromir

Slovenia: Rajver Dušan

Date: 30-SEPTEMBER-2012

Status: Final

Type: Text

Description: This report covers the elaboration on various geothermal models covering the entire Transenergy project area at a scale of 1:500.000. The results are presented in terms of maps showing amongst others the Surface Heatflow Density, subsurface temperatures at various depth levels, depths of 3 different temperature levels as well as maps showing the geothermal potential.

Format: PDF

Language: En

Project: TRANSENERGY –Transboundary Geothermal Energy Resources of Slovenia, Austria, Hungary and Slovakia.

Work package: WP5 Cross-border geoscientific models, task 5.2.4. Geothermal maps covering the entire project area (supra-regional model)

Contents

Abstract

The aim of the Transenergy project is to enable the sustainable utilization of hydrogeothermal systems, based on the elaboration of interconnected geological, geothermal and hydrogeological models.

The summary report “Geothermal models at a supra-regional scale” deals with the elaboration and results of geothermal modelling at the scale of 1:500.000 covering the entire Transenergy project area. One of the goals of the geothermal modelling at supra-regional scale was to present an overview of the geothermal conditions for the entire project area in order to enhance the awareness and understanding about existing resources. Furthermore geothermal boundary conditions could be determined for regional scale geothermal models within the pilot areas. Based on that, the geothermal potentials and resources within the area could be estimated to allow a sustainable (and balanced) utilization of the existing hydrogeothermal resources.

The main input parameters for geothermal modelling were derived by re-processing data of existing geothermal and hydrocarbon exploration wells and additional data obtained by laboratory measurements and literature research. The following parameters represent the dominating influencing factors on the used modelling: surface heat flow density (HFD), rock temperatures at different depths, depth contours of different temperature levels, natural geothermal recharge, Specific Heat in Place (Specific HIP) and Specific Identified Resources.

The developed geothermal models were published in terms of maps at a scale of 1:500.000. Additionally the 16 individual maps were grouped according to their aims (heat flow density, temperature maps, contour maps, potential maps) stated above. They indicate prosperous areas in terms of local to regional scaled geothermal anomalies (high HFD, Temperature or Specific HIP values). Examples for these regions are the south-western part of the Transenergy project area covering parts of the Styrian and Mura – Zala Basin and the central part of the Danube Basin.

The elaborated potential maps provide a first perspective on available geothermal resources and the actual degree of exploitation within the project area, irrespective to known or estimated geothermal plays and reservoirs. However, the achieved results imply that only a very small amount of the supposedly available geothermal resources is already utilized (<1%). Therefore hydrogeothermal utilization may be able to play an important role in future energy supply schemes of the Transenergy project area.

1 Introduction

The following report deals with the elaboration and outcomes of geothermal modelling at a supra-regional scale 1:500.000 covering the entire Transenergy project area. These models describe the natural geothermal conditions and resources with a clear emphasize on hydro-geothermal utilization.

1.1 Definitions and Nomenclature

Table 1: Mathematic symbols

Symbol	Parameter	Unit	Comment
q	Heat Flow Density	mW/m^2	
T	Subsurface Temperature	°C	
T_0	Temperature at Surface	°C	
z	Depth	m	
m	Thickness	m	
P	Percentage	%	
∂T/∂z	Temperature Gradient	°C/m	
A	Area	m^2	
λ	Thermal Conductivity	W/(m*K)	
C_p	Specific Heat Capacity	J/(kg*K)	
c	relative proportion of rock type	-	within geological unit
ρ	Density	kg/m^3	
ϕ	Porosity	-	
ΔH_0	Heat in Place	J	see definition in Table 2
H_1	Identified Resources	J	see definition in Table 2
R	Recovery Factor	-	see definition in Table 2
S	Data Class of Temperature	-	

Table 2: Definition of technical terms

Thermal Water	▪ **Austria & Slovenia**: Natural flowing groundwater with a constant temperature above 20°C. ▪ **Hungary**: Natural flowing groundwater with a constant temperature above 30°C. ▪ **Slovakia**: Natural thermal water is groundwater, which is heated by the action of heat in the earth's rock environment with minimal

	temperature of water at 20 ° C. (Geological Act. 569/2007 Coll.).
Thermomineral water	▪ **Slovenia:** thermal water containing > 1000 mg/l of total dissolved solids or 250 mg/l of free CO_2.
Hydrogeothermal Use	Utilization of naturally occurring thermal water for energetic or balneologic purposes.
Heatflow Density (HFD)	Amount of heat per time unit flowing across a unit area using the physical unit (W/m²) or (J/(s^xm²).The governing transport process is constituted by either conductive heat transport and/or convective heat transport or/and radiant heat transport.
Surface Heatflow Density (SHFD)	Terrestrial HFD flowing to the surface of the Earth's interior either by conduction or convection. In practice the SHFD is calculated for an observed section of a borehole or a well and reflects the geothermal condition of the subsurface.
Heat in Place (HIP)	Heat stored in a specified volume of subsurface porous rock and the associated pore water using the physical unit (J) or (Wh during a specified time period).
Specific HIP	Heat in Place referred to a unit area.
Specific Identified Resources	Fraction of specific HIP regarding a Heat Recovery Factor. Note, that not the entire heat amount stored in a defined rock volume can be recovered by technical measures.
Heat Recovery Factor	Ratio of recoverable heat to stored HIP. During Transenergy a constant Heat Recovery Factor of 0.33 (equals to 33% of the stored heat technically recovered) has been assumed.

Table 3: Subscripts and Indices

Symbol	Description
eff	effective value
r	rock
w	water
m	matrix
i	i-th component
sp	specific
inj	injected
form	formation
sh	Shale/clay
ss	sandstone

1.2 Aims and deliverables

One of the main subjects of Transenergy is the elaboration of geothermal models, which enable the sustainable utilization of hydrogeothermal systems. The models cover all aspects of heat transfer due to conduction and advection (heat transport by externally driven forces, e.g. gravitational or technical water flow) and intend to provide information about the initial and actual geothermal conditions of existing thermal water reservoirs in terms of temperature distributions and thermal balances. Naturally these models are closely linked to the also elaborated geological- and hydrogeological models.

In general three different operating scales are applied in Transenergy:

i. Supra-regional scale 1:500.000 covering the entire project area
ii. Regional scale (1:100.000 up to 1:200.000) for selected pilot areas
iii. Local scale (<1:100.000) for selected geothermal reservoirs within the pilot areas.

Considering the different operating scales, the elaborated geothermal models certainly pursue different goals. The actual report only treats the supra-regional scale geothermal models, regional scale and local scale geothermal models will be discussed in subsequent, individual reports.

Generally the following goals were defined for the supra-regional scale geothermal models:

- Description of the overall geothermal conditions for the entire project area in order to enhance the awareness and understanding about the existing resources.
- Elaboration of geothermal boundary conditions for the regional scale geothermal models at the pilot areas.
- Estimation of existing geothermal potentials and resources at a supra-regional scale in order to distinguish between prosperous and non-prosperous regions with respect to hydrogeothermal utilization as well as to enable an overall hydrogeothermal balancing for the entire project area.

To achieve the already mentioned goals, the following thematic aspects have been investigated for the entire project area:

- Observed Surface Heat flow Density
- Rock temperatures at different depth intervals and depth contours of different temperature levels.
- Natural geothermal recharge
- Specific Heat in Place
- Specific identified resources which equal the specific Heat in Place combined with an invariant Heat Recovery Factor irrespective of hydrogeothermal reservoirs.

All achieved geothermal models have been published in terms of maps at a scale of 1:500.000 covering the entire project areas. The individual maps are grouped in different map series, which picture the different aspects and aims mentioned above.

Table 4: **Overview of achieved geothermal maps at a supra-regional scale of 1:500.000 covering the entire project area.**

Thematic Aspect (Map Series)	Title of Map and Content
Heat Flow Density	▪ Surface Heatflow Density Map
Temperature distribution in several depth levels	▪ Temperature at a depth of 1000m below surface ▪ Temperature at a depth of 2500m below surface ▪ Temperature at a depth of 5000m below surface ▪ Temperature at the depth of top Pre-Tertiary basement
Contour Maps of different temperature levels	▪ Contour map of 50°C isotherm ▪ Contour map of 100°C isotherm ▪ Contour map of 150°C isotherm
Potential- and resource maps	▪ Heat in Place in sedimentary basin fillings ▪ Heat in Place in top 50m at basement ▪ Heat in Place in uppermost 5km of Earth's crust ▪ Heat in Place in uppermost 7km of Earth's crust ▪ Specific identified resources in sedimentary basin fillings ▪ Specific identified resources in top 50m at basement ▪ Specific identified resources in uppermost 5km of Earth's crust ▪ Specific identified resources in uppermost 7km of Earth's crust

1.3 Project Area

The following chapter gives an introduction to the Transenergy project area with respect to already existing knowledge about the geothermal conditions.

1.3.1 General overview

The Pannonian Basin and its adjacent areas cover the most prominent geothermal anomalies of central Europe showing values of Surface Heat flow Densities up to 150mW/m², while the global average is around 70mW/m². Although the major terrestrial Heat flux anomalies are located at the eastern part of the Pannonian Basin, enhanced geothermal conditions are also observed at its western part, which is covered by the Transenergy project area.

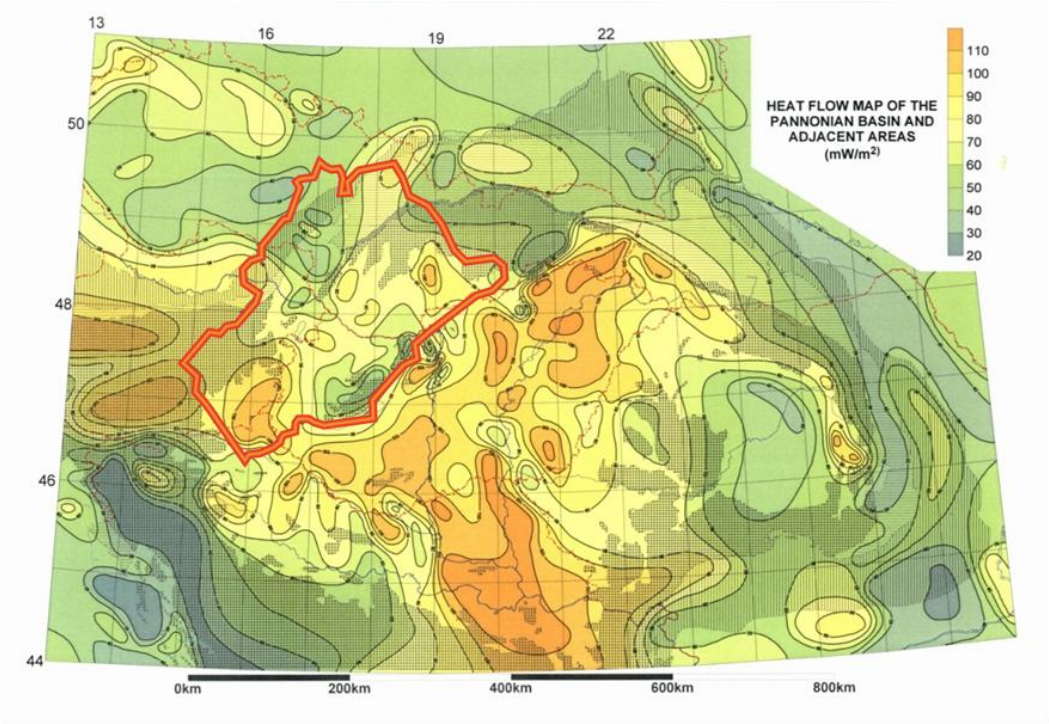

Above: Distribution of the Surface Heatflow Density at the Pannonian Basin with respect to the outline of the Transenergy project area. Taken from Horváth (2005).

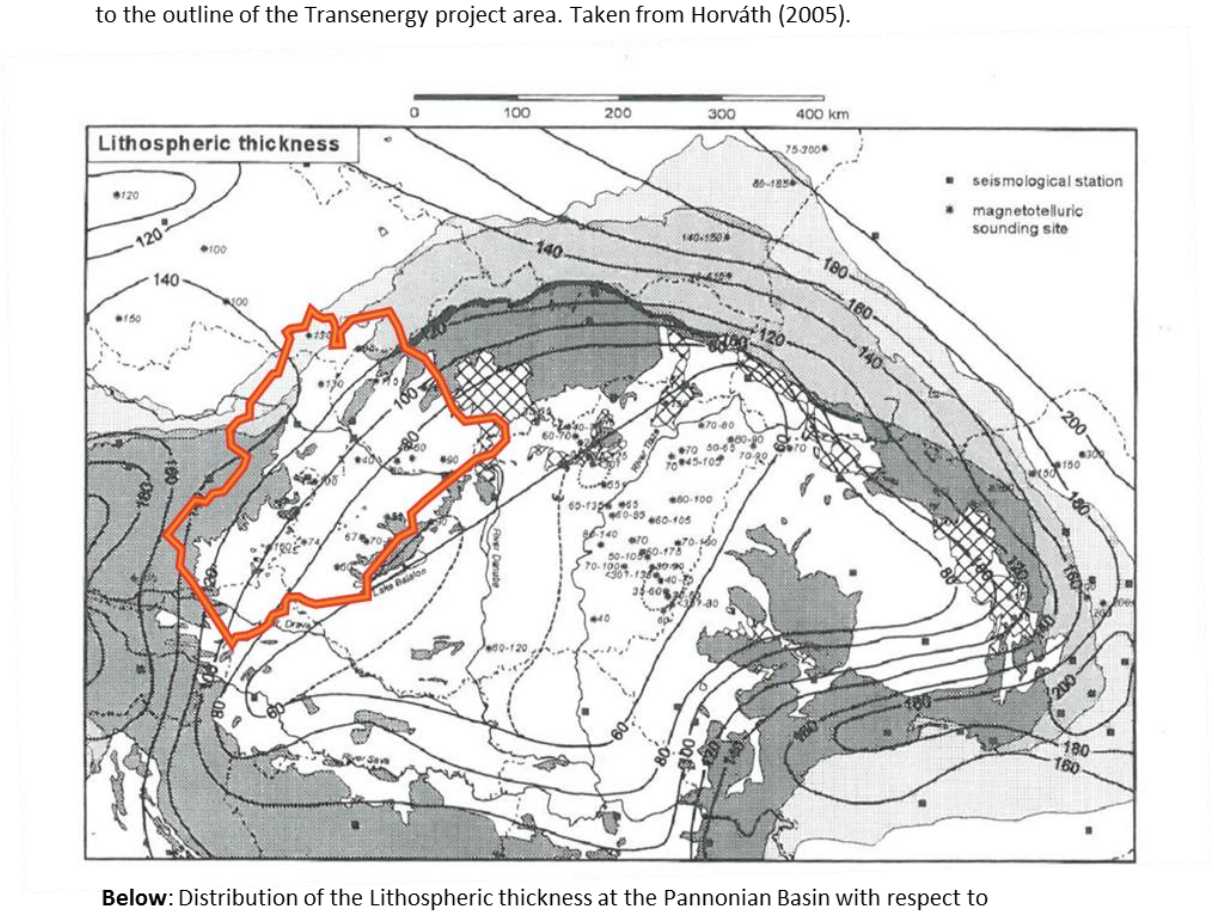

Below: Distribution of the Lithospheric thickness at the Pannonian Basin with respect to the outline of the Transenergy project area. Taken from Lenkey (1999).

Figure 1: **Overview of the geothermal condition at the Pannonian Basin regarding the distribution of Surface heat flow Density and lithospheric thickness.**

The main reason for the enhanced geothermal conditions is understood as related lithospheric thinning, which is a consequence of plate tectonics (dilatation of the ALCAPA microplate). As shown in Figure 1 the thickness of the lithosphere is gradually decreasing from more than 120km to a minimum of less than 60km at the eastern part of the Pannonian Basin. In addition there are several local to regional scale heat flow anomalies superimposed to the long scale variations of the terrestrial heat flow density. These anomalies are predominantly related to hydrodynamic systems, which lead to lowered geothermal conditions in recharge and descent areas, where “cold” meteoric waters are infiltrating, and effect positive anomalies in the area of ascending and discharging “hot” thermal water. Further variations of the terrestrial heat flow density are related to sedimentary and topographic effects, especially at the margin areas of the western Pannonian Basin.

The geothermal conditions with respect to hydrogeothermal use in the project area have already been partly investigated in several previous studies. In general, these studies have to be divided into:

i. High scale international geothermal atlases (e.g. Hurter & Haenel 2002, or Hurtig et al 1992).
ii. Transnational initiatives: DANREG between Austria, Slovakia and Hungary (1987 – 1997), Transthermal between Austria and Slovenia (2005 – 2008) and T-Jam between Slovenia and Hungary (2009 – 2011).
iii. National geothermal studies.

International geothermal atlases (i) are covering the entire project area but they generally show a very low resolution at scales above 1:500.000. Furthermore it has to be pointed out, that such geothermal maps depict the geothermal conditions at a very general and rudimentary level.

The transnational activities (ii) mentioned above concentrated on the development of geothermal maps with higher resolution (mostly scale 1:200.000), without covering the entire project area (see also Figure). The DANREG project represents the first transnational activity regarding hydrogeothermal conditions in the western Pannonian Basin with emphasis on the so called Danube Basin sub-region. A major outcome of DANREG was achieved by providing a simplified map of maximum expected subsurface water temperatures above the crystalline basement of the Danube Basin (see also Kollmann 1997). During the period 2005 to 2008 the bilateral study Transthermal has been carried out between Austria and Slovenia, which led to the elaboration of high quality hydrogeothermal potential maps outlining relevant hydrogeothermal reservoirs of the Styrian Basin and the Slovenian Basin (see also Domberger et a, 2008). A quantitative mapping of the available hydrogeothermal resources at the trans-boundary Mura – Zala Basin has been achieved during the bilateral project T-Jam, which has been conducted by Slovenia and Hungary and was accomplished in 2011 (for more details visit http://en.t-jam.eu/project/).

Within the Transenergy project area a number of different scale national geothermal studies without an Implementation of trans-boundary data are available. The previously accomplished national studies will partly be presented in the subsequent chapters of this report.

Transenergy is the first project offering harmonized datasets for the entire western Pannonian basin and its adjacent regions. However, the previously accomplished national and transnational studies provide a crucial data basis for Transenergy project and should therefore not be neglected.

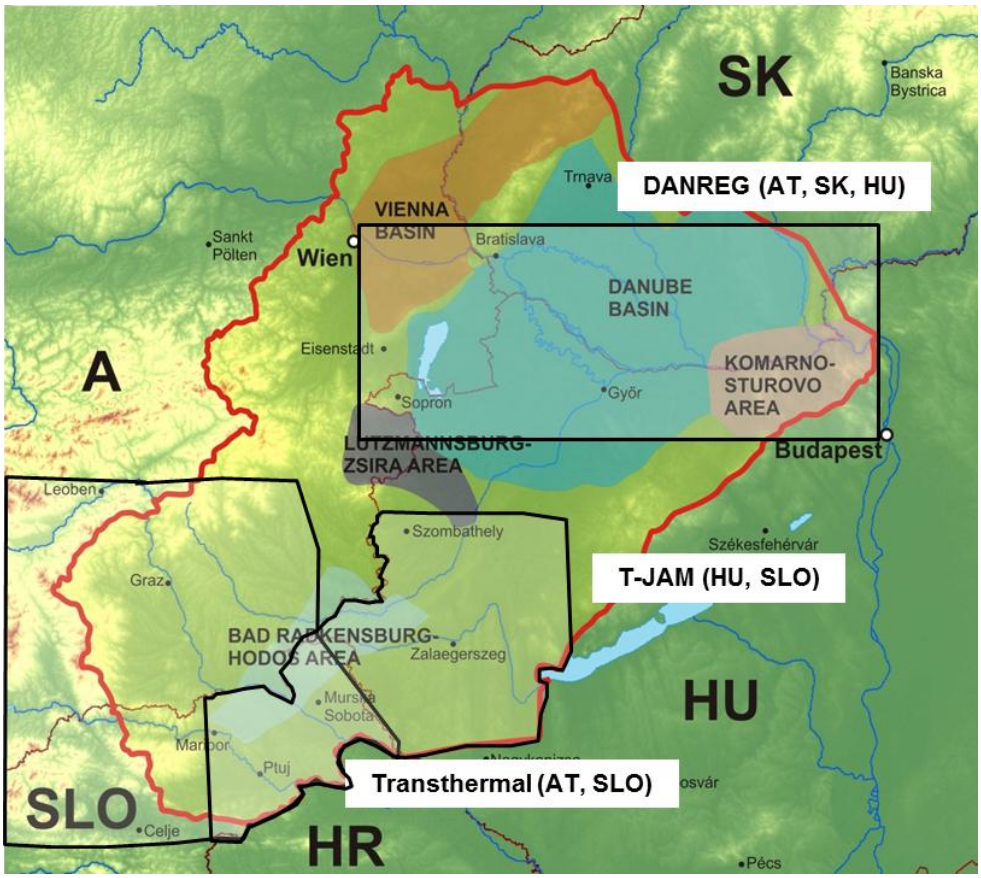

Figure 2: **Overview of the project areas of previous transnational geothermal initiatives within the Transenergy project area, combined with the outlines of the different pilot areas of Transenergy.**

1.3.2 Austria

In general a detailed geothermal atlas covering the entire area of Austria is still lacking. However, a first comprehensive Heat flow Density map for Austria at a scale of 1:1.5 Mio was published in 2007 (see also Figure 3) by Goetzl (2007). At large scale Austria offers average geothermal conditions, which may vary significantly within the different regions. The south-eastern parts of Austria clearly show enhanced heat flow densities due to the geothermal influence of the adjacent Pannonian Basin. In this area maximum HFD values of up to 120mW/m² were registered. Opposed to that moderate to low conditions can be observed at the northern Alpine front (Northern Calcareous Alps) as a consequence of crustal thickening combined with significant inflow of meteoric waters. In this area SHFD values down to as less as 30mW/m² were measured. Due to lacking temperature measurements the geothermal conditions within the Central Alpine Belt are not entirely cleared. An existence of local to regional scale positive HFD anomalies caused by rapid

exhumation of deeply buried crustal segments is assumed for the area of the so called Tauern Window.

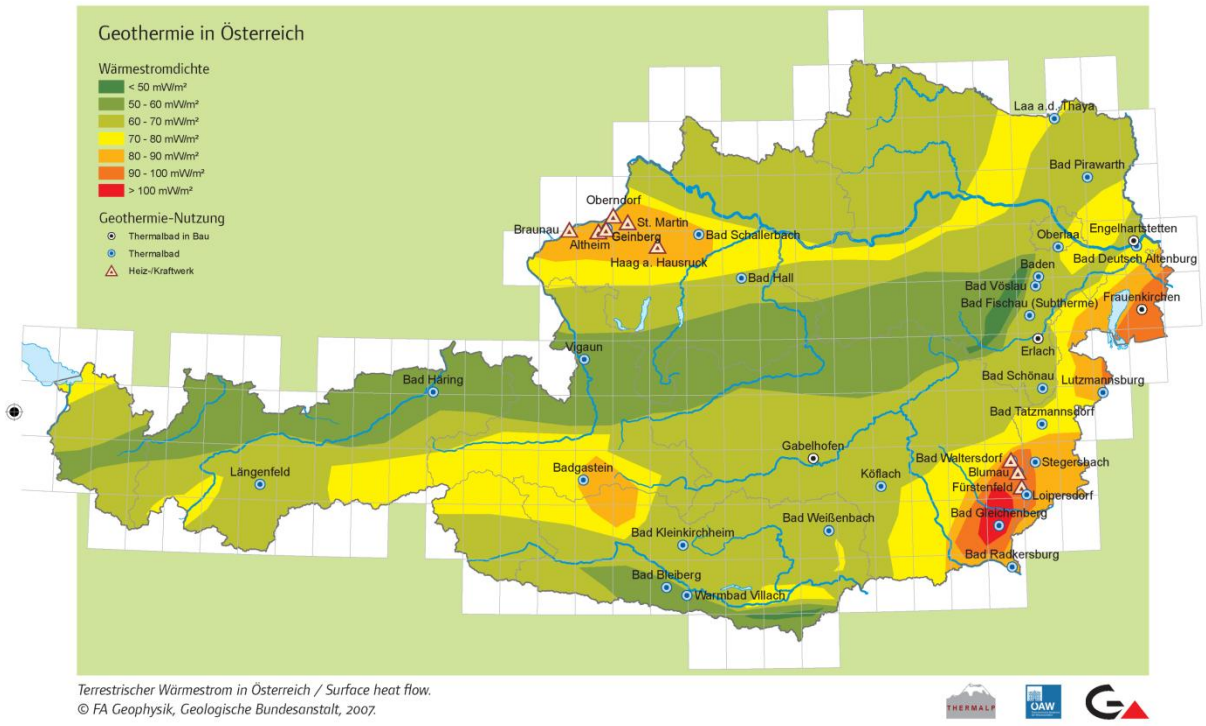

Figure 3: **Supra-regional Surface Heat flow Density map of Austria at the scale of 1:1.5 Mio, taken from Goetzl (2007).**

The Austrian part of the supra-regional area covers the Vienna Basin, the Styrian Basin and the western margin of the Pannonian Basin (see Figure 2). Several previous geothermal studies were accomplished at the Austrian part of the Transenergy project area because of previous and current (central and northern Vienna Basin) hydrocarbon exploration.

The first regional scale geothermal investigations are based on temperature measurements at artesian wells in eastern Styria and southern Burgenland (Zojer 1977, Zötl & Zojer 1979). These studies resulted in temperature maps at a depth of 1000 meter below surface and other maps showing the distribution of the geothermal gradient. The investigated aquifers were limited to depths of approximately 200 meters below surface. Therefore it can be supposed that the extrapolated geothermal conditions shown in these maps have significantly been influenced by the conditions at the uppermost part of the underground. During the bilateral Interreg IIIA Study Transthermal (2005 – 2008) the results of the above mentioned studies have been re-evaluated using corrected BHT and DST datasets from hydrocarbon exploration wells and temperature measurements at geothermal wells in the Styrian Basin. These datasets were compiled to several geothermal maps including a Heat flow Density map and additional map series showing the temperature distribution at several depth levels. Furthermore major geothermal reservoirs have been outlined and classified for a qualitative evaluation of available hydrogeothermal resources. The elaborated so called Hydrogeothermal Potential Map series covers reservoirs in sedimentary basin fillings and basement rocks. An excerpt of these maps is shown in chapter

4. All maps are available at a scale of 1:200.000 and provide the distinction between prosperous and non-prosperous regions for hydrogeothermal utilization. They have been published by Goetzl et al 2008.

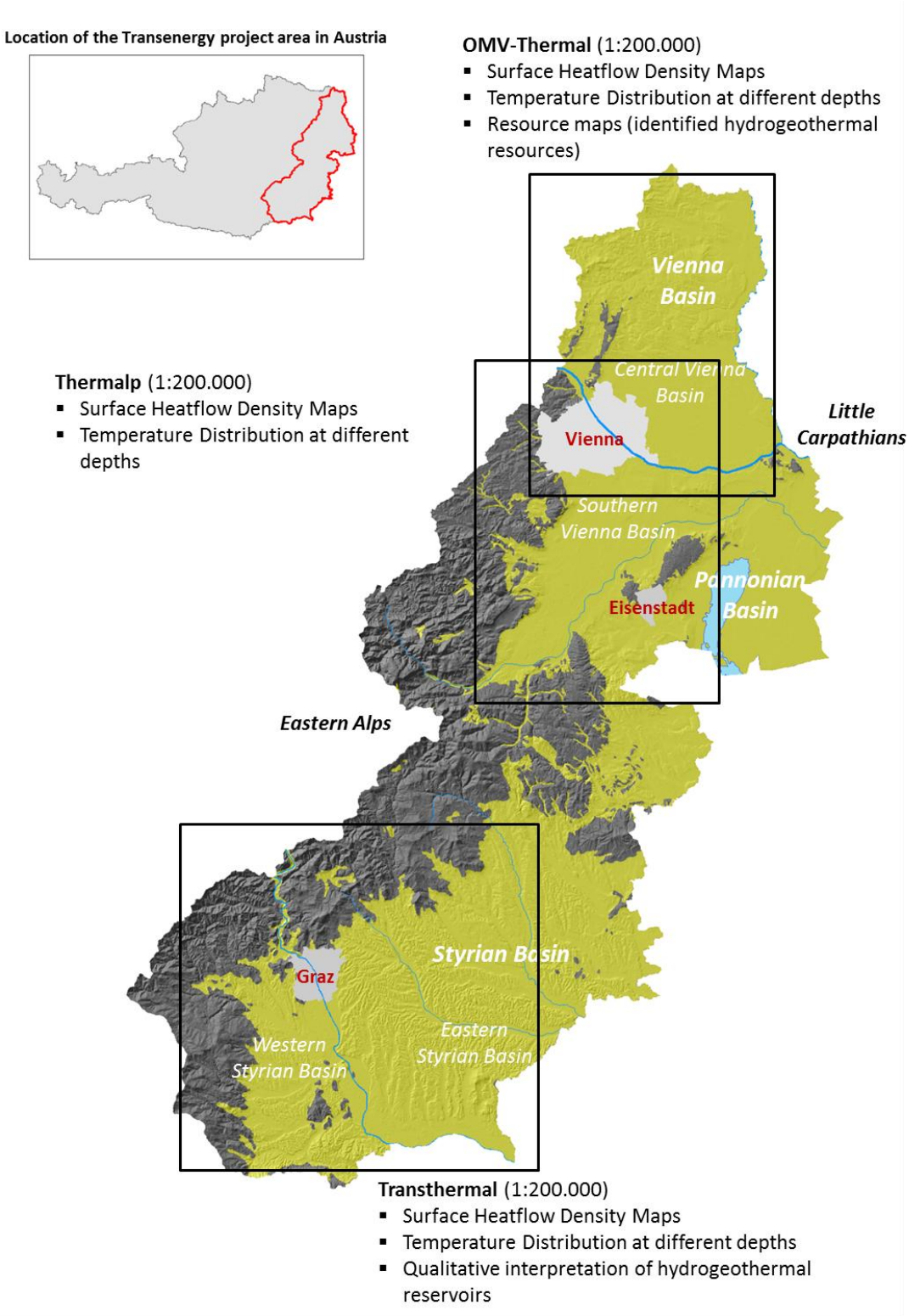

Figure 4: **Overview on the Austrian part of the Transenergy project area with respect to selected previous studies**

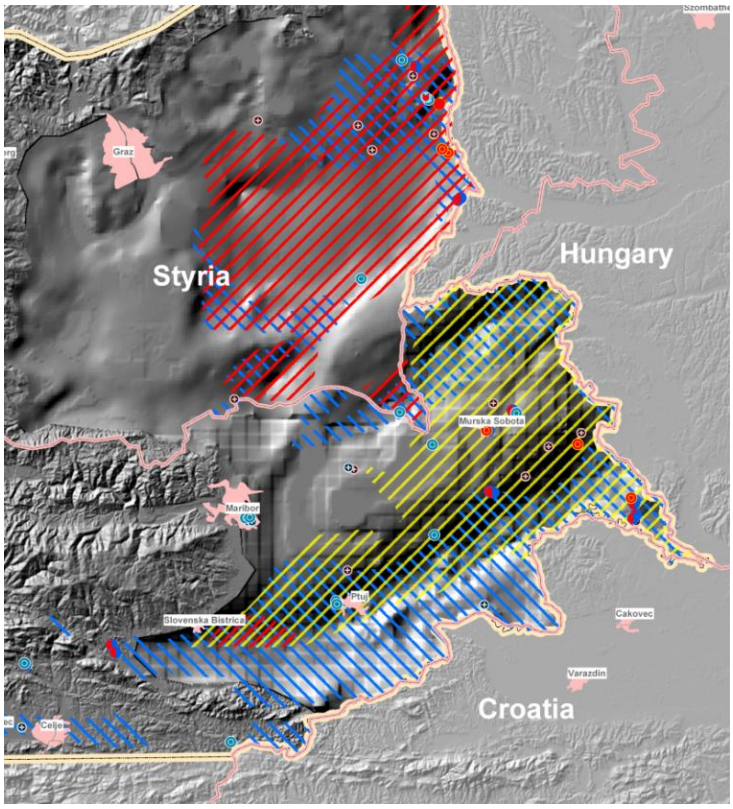

Figure 5: **Geothermal potential map showing the outline of hydrogeothermal reservoirs in tertiary basin fillings (blue scattered lines) and at the pre-tertiary basement (red scattered lines) in the Styrian Basin and the Slovenian part of the Mura – Zala Basin.** The yellow scattered lines mark regions of intensive hydrogeothermal utilization. These results were gained at the bilateral Interreg IIIA study Transthermal (Goetzl et al, 2008).

Due to the large geothermal potential in the Vienna Basin several projects were executed at the Geological Survey of Austria in the past 8 years. The scientific study THERMALP (2004 – 2012), financed by the Austrian Academy of Sciences – OEAW, investigated active hydrodynamic systems at the southern Vienna Basin and pictured locally varying positive and negative geothermal anomalies. By applying 3D geological and numerical modelling several geothermal maps showing the distribution of the Heat flow Density and subsurface temperatures at different depths have been elaborated for this region (see also Figure 6). Furthermore a regional scale geothermal and hydrothermal balance has been calculated for the most prominent hydrodynamic[1] reservoir at the southern Vienna Basin. They showed that the mentioned reservoir offers a utilizable heat content of approximately 50MW_{th}[2] for predominantly balneological purposes which already is confronted with a degree of exploitation of almost 50% of the available resources.

The central and northern parts of the Vienna Basin have been investigated during the industrial cooperative study OMV-Thermal (2008 – 2011). Based on water inflow observations at hydrocarbon exploration wells in the Vienna Basin, hydrogeothermal resources for energetic utilization in the range of 500MW_{th} have been estimated for this region.

[1] In this context hydrodynamic systems are defined as naturally circulating, actively recharged thermal water reservoirs, which lead to local to regional scale geothermal anomalies.
[2] Related to an ambient temperature of 10°C.

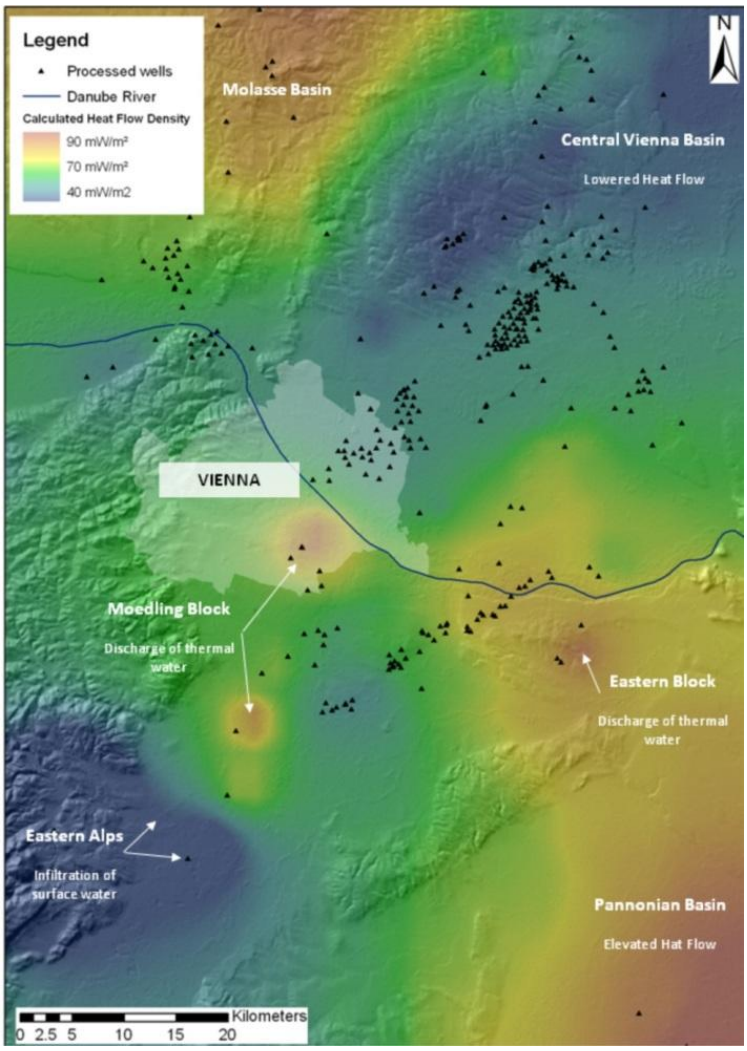

Figure 6: **Surface Heat flow Density (SHFD) map for the southern and central Vienna Basin at a scale of 1:200.000 (taken from Goetzl et al, 2010).** The regions with significantly lowered SHFD values down to as less as 40mW/m² are related to crustal thickening at the Alpine thrust zone in combination with significant inflow of "cold" meteoric water. The gradually enhanced geothermal conditions toward the East are already related to the geothermal regime at the Pannonian Basin. Toward the central and northern part of the Vienna Basin lowered geothermal conditions are assumed to be related to transient geothermal conditions caused by rapid sedimentation. Locally confined positive heat flow anomalies are in turn linked to ascent paths and discharge areas of naturally circulating thermal water (hydrodynamic systems).

The results from the previous studies mentioned above, which were performed at the Geological Survey of Austria, were compiled and re-evaluated using recently acquired additional data and improved processing algorithms in order to elaborate the supra-regional scale geothermal maps presented in this report.

1.3.3 Hungary (Lenkey L.)

Due to intensive hydrocarbon exploration many boreholes and wells were drilled in the Little Hungarian Plain and the Zala basin, in which BHTs, drill stem tests and other types of temperature measurements were carried out. In the hilly parts of the Transenergy project area, like e.g. the Transdanubian Central Range, temperature measurements in mining exploration boreholes were conducted. Additionally the temperature of in- and outflow in thermal water

wells was recorded. These temperature data are stored in the Geothermal Database of Hungary (Dövényi, 1994), which is continuously updated. The temperature data are corrected for the transient effects of the drilling and represent the “true” formation temperature. The database also contains the lithology of the boreholes and wells in order to estimate the thermal conductivity of rocks. The thermal conductivity of the rocks is known from laboratory measurements on core samples (Dövényi et al., 1983). Functions of the variation of the thermal conductivity versus depth were established for neogene sands and shales (Dövényi and Horváth, 1988).

In the area of the Transenergy project heat flow density was determined in five wells (Table 5). In these wells both temperature and thermal conductivity measurements were carried out. In other boreholes and wells the heat flow density was estimated using thermal conductivity values of Dövényi et al. (1983) and Dövényi and Horváth (1988), depending on the rock types.

Table 5: **Hungarian wells within the TE project area, where heat flow density determination was carried out.** For location of the wells see Figure 8. The expression No. of λ measurements means thermal conductivity measurements on core samples from the well. References, a: Horváth et al., 1977, b: Horváth and Dövényi, 1987, c: Boldizsár, 1959, d: Horváth et al., 1989.

Name of well	Short name	No. of λ measur.	HFD (mW/m^2)	Error	Reference
Bárszentmihályfa-1	Bm-1	26	92	± 20 %	a
Bősárkány-1	Bős-1	17	83	± 15 %	b
Kerkáskápolna-1	Ker-1	12	90	± 15 %	b
Nagylengyel-62	Nl-62	12	84	± 20 %	c
Szombathely-II	Sz-II	56	108	± 15 %	d

Heat flow density and temperature maps were elaborated for a larger area than the Transenergy project area. A heat flow density map of Hungary is presented in the Atlas of Geothermal Resources in Europe (Dövényi et al., 2002), and in the assessment of geothermal energy resources in Hungary (Rezessy et al., 2005). The heat flow density in the Pannonian basin and surrounding area is shown in Figure 7 (Horváth et al., 2005), which represents an updated version of the former heat flow density maps of the region (Dövényi, 1994, Lenkey et al., 2002).

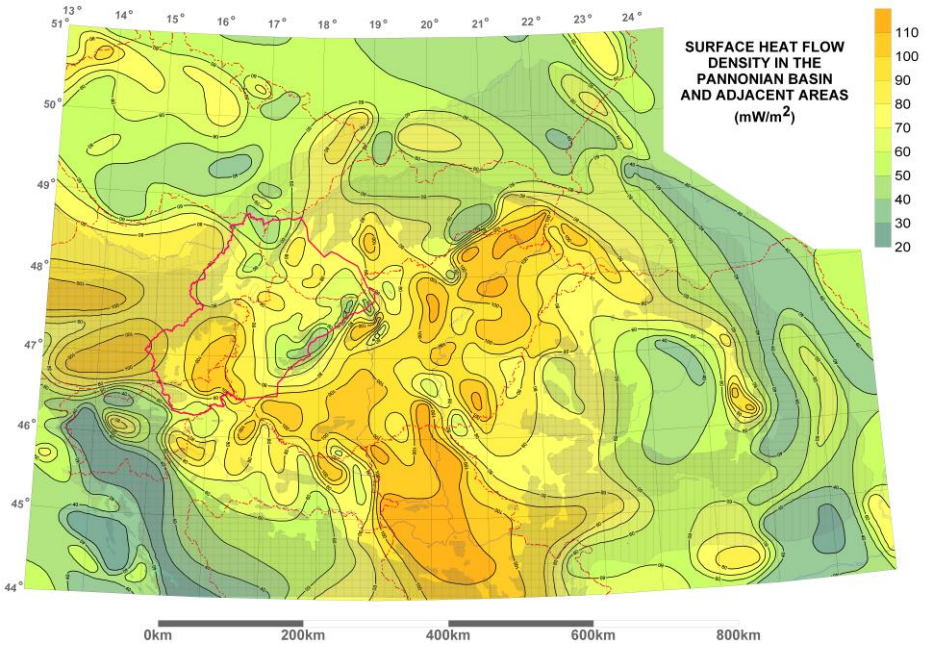

Figure 7: **Heat flow density in the Pannonian basin and surrounding areas (after Horváth, 2005).** The boundary of the TE project area is depicted by the thick red line.

The temperature at 2000m depth was calculated by an extrapolation of temperatures measured in different depths assuming conductive heat transport. The temperature in 2000m depth in the western part of Hungary is shown in Figure 8 (after Mádlné Szőnyi et al., 2008). Other temperature maps, compiled for the same depth and area (Dövényi et al., 2002, Rezessy et al., 2005) are very similar: the amplitudes of the geothermal anomalies are identic; the shape of the isolines is slightly different.

The map in Figure 7 shows the large scale variations in the heat flow density. In general, the heat flow density in the Pannonian basin is higher (80-100mW/m^2) than in the surrounding areas (50-70mW/m^2). In the area of the Transenergy project the heat flow is highest (over 100mW/m^2) in the southern region (Styrian basin, Zala-Mura basin) and lowest in the Transdanubian Central Range (TCR) (50mW/m^2). The Little Hungarian Plain-Danube basin is characterized by medium values (70-80mW/m^2). The heat flow density in the Vienna basin increases from 50mW/m^2 to 80mW/m^2 from north to south. The subsurface temperature in Hungary varies in accordance with the heat flow density, temperature is high where the heat flow density is high, and vice versa (Figure 8).

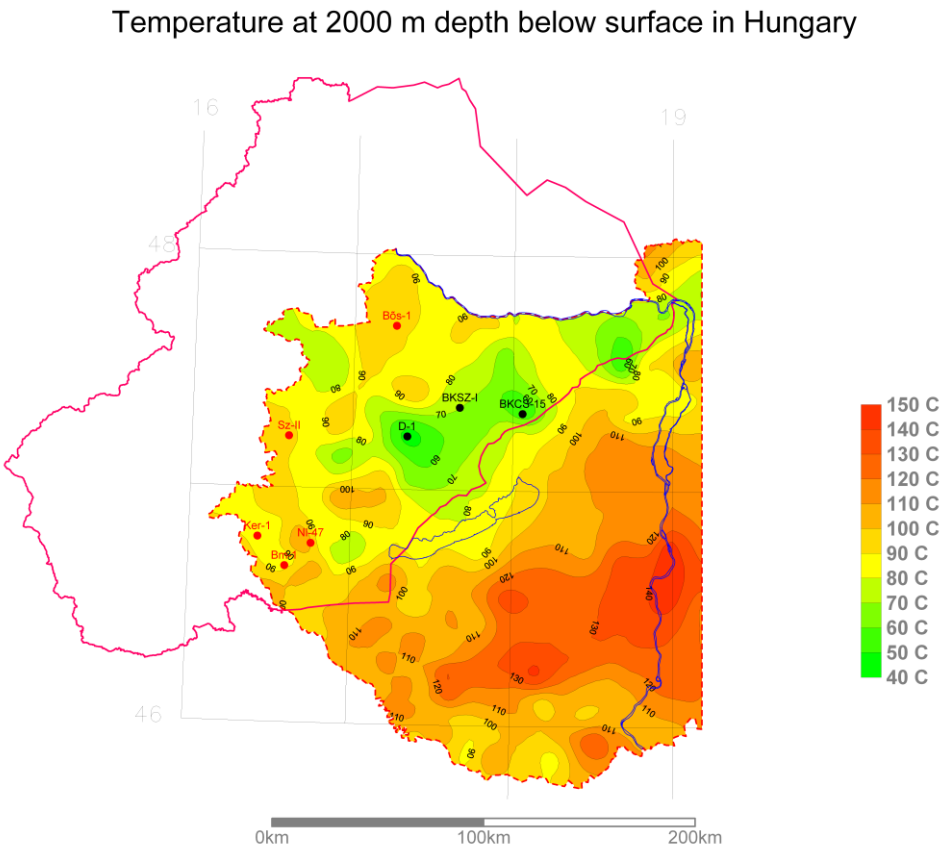

Figure 8: **Temperature at 2000m depth below surface in western part of Hungary.** The boundary of the Transenergy project area is depicted by the thick red line. Wells with temperature measurements are shown by black colour: D-1: Dabrony-1, BKSZ-I: Bakonyszűcs-I, BKCS-15: Bakonycsernye-15. Wells with heat flow density determination are shown by red colour: Bm-1: Bárszentmihályfa-1, Bős-1: Bősárkány-1, Ker-1: Kerkáskápolna-1, Nl-62: Nagylengyel-62, Sz-II: Szombathely-II.

The low temperature and heat flow density values in the TCR are caused by groundwater flow occurring in karstified Mesozoic carbonates. The area of the TCR is a recharge area, where meteoric water precipitates. The groundwater seepages towards northwest and cools the karstic aquifer in the basement of the Little Hungarian Plain (LHP) and the overlying neogene sediments as it is observed in several wells (Figure 9). At the Rába line in the centre of the LHP, which is the north-western boundary of the carbonatic rocks, the karstic flow turns to northeast and southwest, and the discharge areas (the Komárom-Esztergom-Sturovo area and the Hévíz area) are heated by the upwelling warm groundwater.

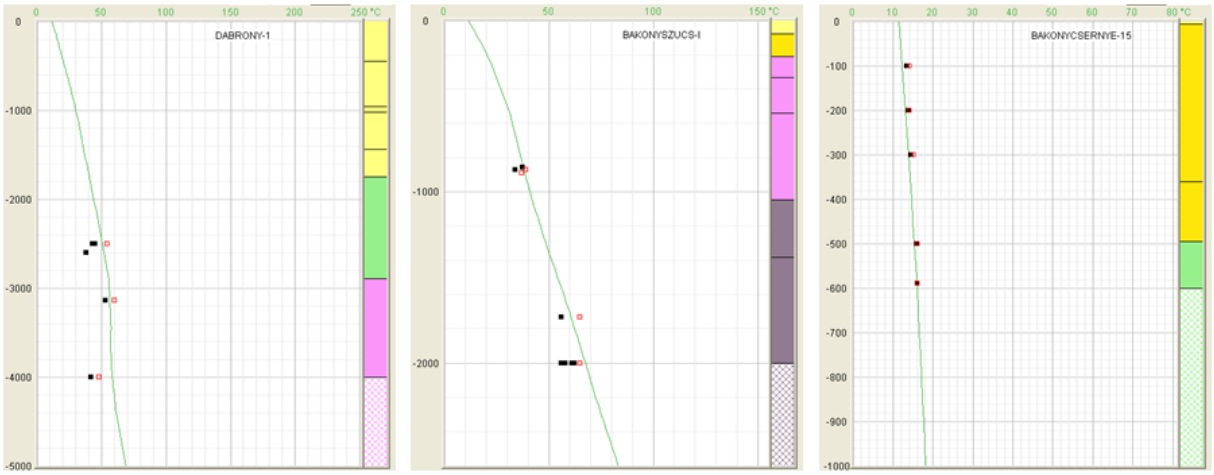

Figure 9: **From Left to Right: Temperature in the Dabrony-1, Bakonyszűcs-1 and Bakonycsernye-15 wells.** Black rectangles: measured temperature, red squares: corrected temperatures, green line: temperature-depth curve calculated assuming heat conduction, right column: stratigraphy – the colour code is the following: yellow: Neogene, green: Cretaceous, purple: Triassic, dark purple: Permian, blue: Palaeozoic.

Groundwater flow also occurs in the porous Upper Pannonian sediments. The heat flow density in the Szombathely-II well increases with depth from 90mW/m^2 in the upper 1500m to 108mW/m^2 below 1500m (Figure 10). The increase of heat flow density is interpreted by groundwater flow in the Upper Pannonian sediments (Horváth et al., 1989). The sedimentary layers are tilted towards east, the centre of the LHP, and the recharge area is located in a distance of about 10.000-30.000m in the west where the Upper Pannonian sediments outcrop to the surface.

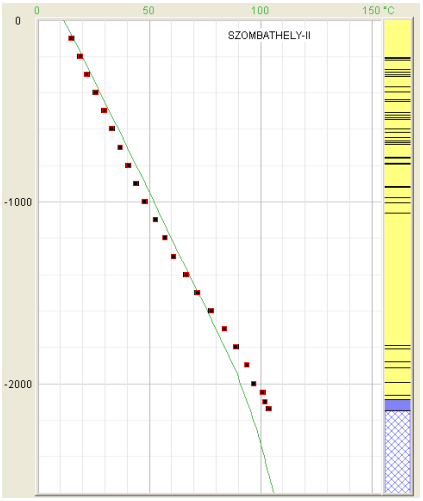

Figure 10: **Temperature and stratigraphy in the Szombathely-II well (Horváth et al., 1989).** The explanations see at Figure 9.

The LHP-Danube basin is characterized by smaller heat flow density values than the southern regions in the TE project area. Solely based on observations it is difficult to say whether the lower HFD values are due to groundwater flow in the carbonatic basement and in the porous Upper Pannonian sediments, or due to reduced heat flow density coming from the

mantle. This question can only be answered by coupled modelling of groundwater flow and heat transport. The results should be compared with results of pure thermal conduction models and observations.

1.3.4 Slovakia

The Slovak part of the supra-regional area includes the northern part of the Vienna Basin, the northern part of the Danube Basin and a part of the Komarno-Sturovo area. In these regions regional studies were already published, describing the geothermal conditions along with calculations of geothermal water reserves, description of geothermal water circulation and regimes. The main source for a general overview on pilot areas of the Transenergy project is provided by the Atlas of Geothermal Energy of Slovakia (Franko, Remšík, Fendek, (eds), 1995), which summarizes the existing knowledge from detailed studies until the end of 1994. The Atlas consists of detailed texts, maps, cross-sections and figures. This geothermal atlas is based on temperature data from 376 boreholes, observed heat flow densities in 136 boreholes and hydrogeothermal data from 61 boreholes. The geothermal conditions at the territory of Slovakia are represented in six different map series:

i. thematic geothermal map
ii. map of heat flow density at the surface
iii. map of heat flow density at the Moho-discontinuity
iv. geothermal maps of Slovakia
v. geothermal maps of delimited geothermal areas
vi. hydrogeothermal maps of delimited geothermal areas

All maps are accompanied by cross-sections, figures and well log profiles of geothermal boreholes with outlines aquifers of geothermal plays at various geothermal areas. The text part mainly points out the purpose of the Atlas as well as a description of the applied compilation methods. Furthermore it comprises a general hydrogeothermal characterization of both the entire territory of Slovakia as well as of individual geothermal areas at different regions. It provides explanatory notes on technical aspects regarding the production of geothermal water and possibilities for waste water disposal. The text is accompanied by tables and diagrams containing data about temperatures and heat flow density in boreholes, geothermal installations and the chemical properties of geothermal waters. The Atlas is fundamental knowledge for scientists, teachers, engineers, for governmental and industrial decision makers involved in exploring and exploiting geothermal energy and for the general public interest. The Atlas is in bilingual Slovak – English edition.

In the following the geothermal areas situated at the Transenergy project area will be described in detail:

(a) Vienna Basin

The pre-Tertiary relief (see Figure 11) of the Slovak part of the Vienna Basin is represented by the slope of the Male Karpaty Mts. which in the west plunges to a depth of as much as 500m - 600m. It is dissected by numerous faults running NE-SW and W-E. The structure of the pre-Neogene substratum is very complex. It has two essential elements - West Carpathi-

an and Eastern Alpine units. The two elements are separated by an abrupt change in the earth's crust thickness. The geothermal characteristics are rather inhomogeneous, showing areas with lowered and enhanced heat flow densities which seem to be trending roughly along NW-SE axis. The lowered areas (heat flow density less than 45mW/m^2) are located at a south-western depression zone, whereas enhanced heat flow densities (exceeding 65mW/m^2) have been observed at the Laksarska Nova Ves high block. The temperature regime at existing hydrogeothermal reservoirs seems to be more homogeneous and shows an antithetic trend compared to the distribution of terrestrial heat flow densities:

At the margin of the Male Karpaty temperature reaches less than 40°C and in the Rohoznik area even less than 35°C. Temperature increases with distance from the mountains to more than 45°C. In the Lab-Malacky block it exceeds 50°C while the highest reservoir temperatures associated to naturally circulating water are observed in the Laksarska Nova Ves elevation with a maximum of 55°C. The basin has no natural geothermal springs, therefore e geothermal waters are tapped by two geothermal wells - RGL-1 at Laksarska Nova Ves and RGL-2 at Sastin-Straze (Remšík et al, 1985 and 1989).

In addition, heated formation water has been observed in several hydrocarbon exploration wells. These structures underlie the basin's neogene filling and are composed of several different tectonic nappes (predominantly Triassic formations at a higher stratigraphic position than the Krizna nappe). Geothermal waters are bound to Triassic dolomites (mainly Upper Triassic Hauptdolomite) of the Choc and higher nappes. Furthermore geothermal reservoirs can be bound to Eggenburgian clastic sediments and to Karpatian sandstones and sands in the southern part of the Vienna Basin (Lab - Malacky block). The hydrogeothermal system is situated in a depth of 500 - 4500m and bears waters with a temperature of 40-140°C.

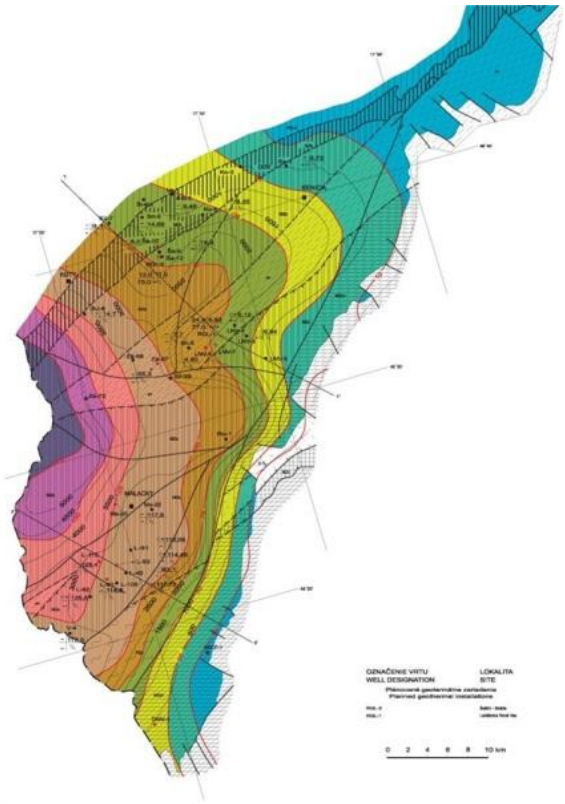

Figure 11: **Map of the pre-Tertiary basement containing the temperature distribution and the depth of the pre-Tertiary basement (taken from Franko, Remšík, Fendek, eds, 1995).**

(b) Danube Basin: Central depression

Central depression is fringed by the River Danube between Bratislava and Komarno in the southwest, by the Male Karpaty in the northwest, by Dobra Voda fault (Ludince line) in the northeast, and roughly by the River Nitra in the southeast. Several drill holes in the northwestern and south-eastern tracts of the depression have revealed that the Tertiary filling is directly followed by crystalline rocks (crystalline schists, granitoids). From the hydrogeological build-up of the Danube Basin it can be assumed that the Carpathian crystalline basement of the Danube basin does not contain relevant geothermal aquifers. However, suitable aquifers are bound to sands or sandstones of Pannonian, Pontian and Dacian age within the Tertiary basin fillings.

The highest heat flow densities have been recorded in the middle of the depression (q > 85-90mW/m^2) and do not correspond to lower temperatures (T < 45°C) nor thermal gradients. Whereas heat flow decreases towards the margins of the Danube basin, temperature increases. This irregularity is caused by a cold water body, which is bound to the uppermost hydro-geological unit showing a maximum thickness of 460m. The colder zone gradually perishes downward and the temperature field corresponds to the heat flow. Badenian volcanoclastics at depths of 5000 - 6000m may contain geothermal waters with aquifer temperature exceeding 200°C. They can be utilized by applying reinjection for reasons of sustainability. Because of its post-Sarmatian evolution, the Central depression has a bowl-like brachy-

synclinal shape (Priechodská, Z. - Vass, D. 1986). The hydrogeothermal characteristics of the depression are summarized in Franko, Remšík, Fendek, eds, 1995. The upper boundary of the geothermal water body is located at depths of 1000m below the surface and at the bottom it is confined by a fairly impervious substratum - an aquitard (clays) which plunges from the surrounding area towards the middle of the basin to a depth of up to 3400m below surface.

This hydrogeothermal system is likely to have interlayer leakage, inter-granular permeability and confined groundwater levels. It bears geothermal waters with registered temperatures between 42°C and 92°C warm, which are bound to sands and sandstones of Dacian, Pontian and Pannonian age. Figure 12 shows the temperatures and lithology at the depth of 5000m below surface at the western part of Danube basin (Franko, Remšík, Fendek, eds, 1995).

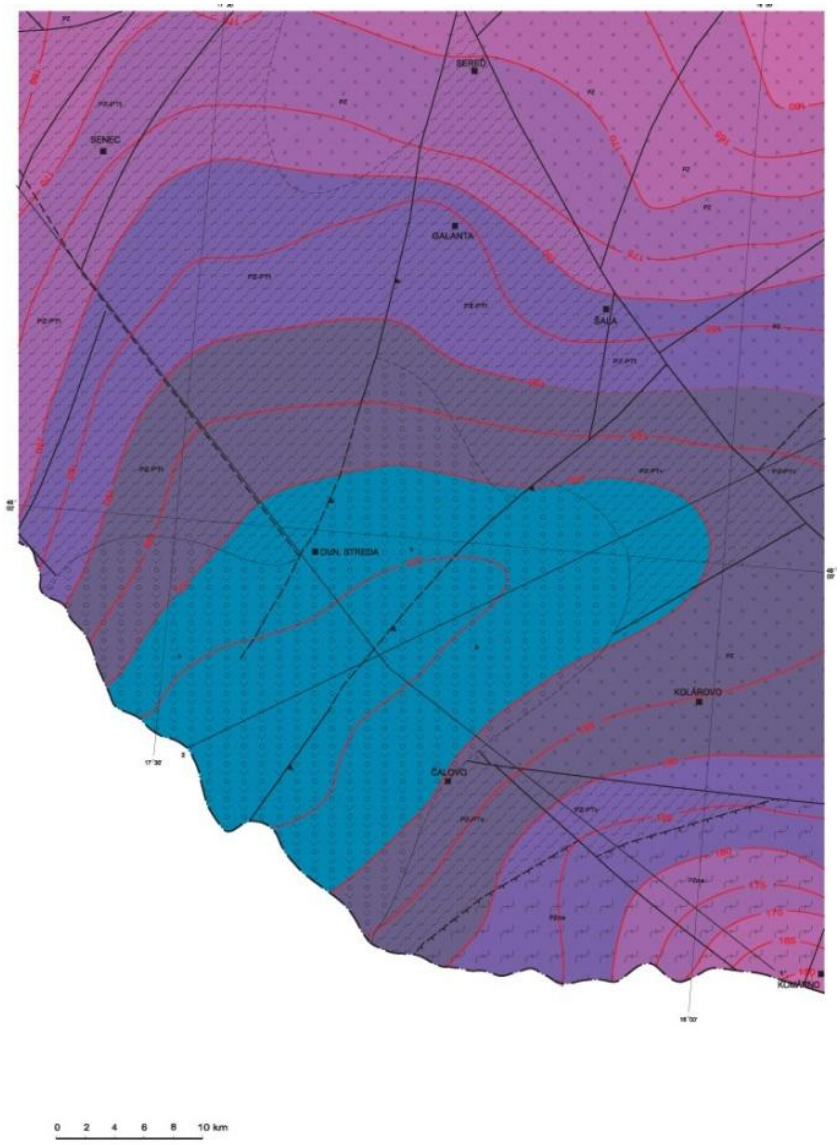

Figure 12: **Map of Danube basin – western part: Temperatures and lithology at the depth of 5000m below surface (taken from Franko, Remšík, Fendek, eds, 1995).**

(c) Komarno block

The Komarno block extends between Komarno and Sturovo. It is fringed by the River Danube in the south and by the east – west striking Hurbanovo fault in the north, which is separating this structure from the Veporic crystalline unit. The southern limit along the Danube is also tectonically derived and therefore the Komarno block can be assumed to be a sunken tract of the northern slope of the Gerecse and Pilis Mts. The surface of the pre-Tertiary substratum plunges towards the north from a depth of approximately 100m below surface near the Danube (wells Sb-1 and FGŠ-1) to as deep as 3000m below surface near the before mentioned Hurbanovo fault. The pre-Tertiary substratum of the Komarno block largely consists of Triassic dolomites and limestones showing a maximum thickness of up to 1000m. These dolomites are underlain by a very thick Lower Triassic shale formation. Palaeozoic units were revealed by drilling in the north-western section of the Komarno block. These include Permian conglomerates, sandstones, graywackes and shales as well as Devonian limestones and lydites. The Mesozoic and the underlying Palaeozoic formations of the Central Hungarian Mountains were probably overthrusted onto the crystalline rocks of the Veporic crystalline unit, which is directly covered by Tertiary units northwards of the Hurbanovo fault. However, the thrust plane sank along Hurbanovo fault and presumably reaches the pre-Tertiary surface in the north-western tract of the Komarno block. It is assumed that at a depth of 3000m below surface the Komarno block is dominated by Palaeozoic rocks and at depths of 6000m below surface by the Veporic crystalline unit.

Geothermal waters are bound to Triassic limestones and dolomites. From a hydrogeothermal point of view, the area is divided a high and marginal block (Remsik, A. - Franko, O. et aI. 1979; Franko, O. et. al. 1984; Remsik, O. et aI. 1992). Heat-flow densities suggest that the high block shows fairly low and the marginal block medium conditions. This difference is assumed to be caused by infiltrating cold karst waters.

The geothermal conditions at the high block are partly well known because of thermal springs at Sturovo and Patince showing outflow temperatures of 39°C and 26°C. The Komarno high block is confined by a 700 - 800m isobath of the Cretaceous carbonate substratum or by tectonic lines running close to this isobath. The structure has a fast water circulation and is considerably cooled (water temperature is varying from 20°C to 22°C at a depth of 600 to 800m below surface and varying between 24.5°C and 26.5°C at a depth of 1100 to 1300m below surface. At greater depths of 3000m below surface observed water temperature still remains at lowered levels of around 40°C. The hydraulic and thermal regime of geothermal waters in the high block is directly controlled by variations in the water level of the river Danube (Remsik, Franko et al 1979; Remsik, A. et al. 1992).

The Komarno high block is encircled by the marginal block in the west, north and east. The latter contains ground waters whose temperature exceeds 40°C (whilst the highest so far measured temperature is at a level of 68°C).

Figure 13 shows the pre-Tertiary basement in the western part of Danube basin and Komarno high and marginal block (Franko, Remšík, Fendek, eds, 1995).

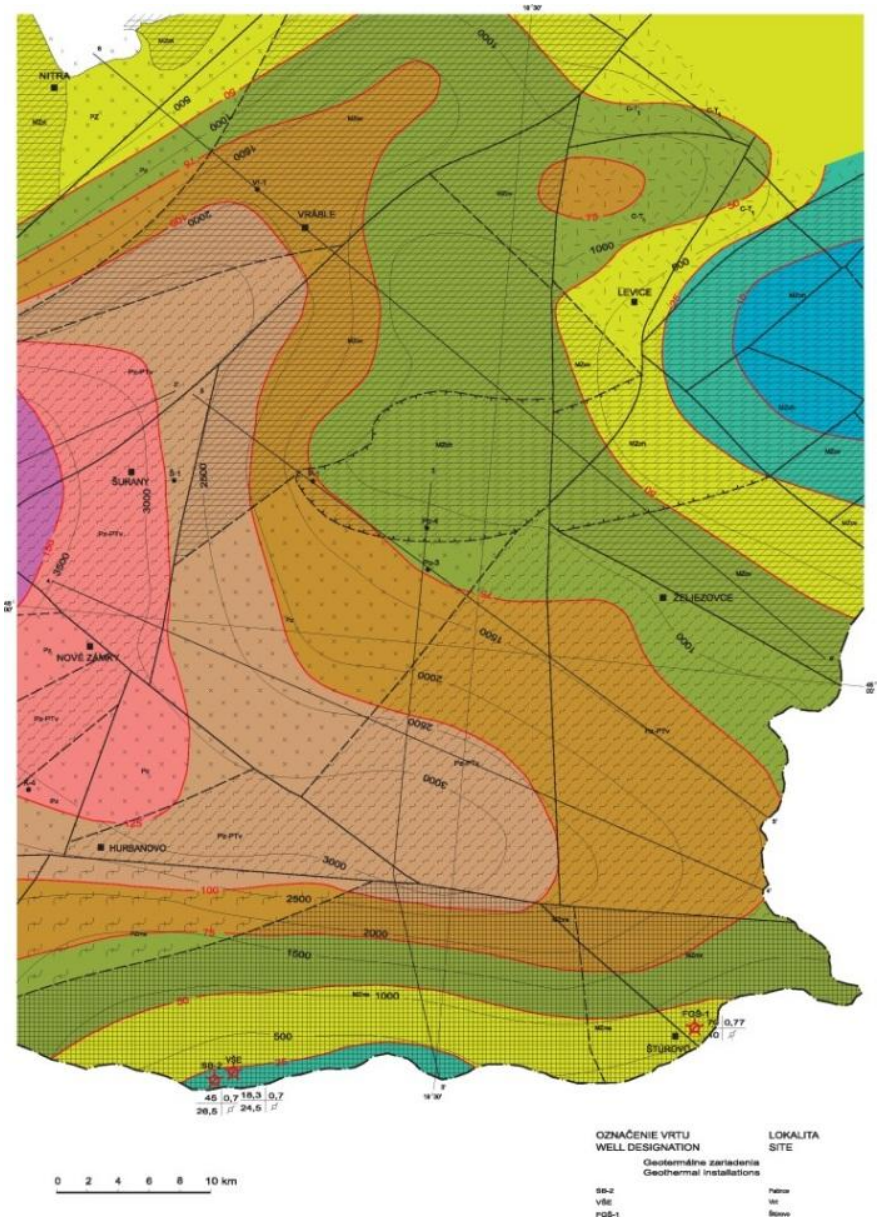

Figure 13: **Map of the pre-Tertiary basement in the western part of Danube basin and the Komarno high- and marginal blocks (taken from Franko, Remšík, Fendek, eds, 1995).**

An additional summary of the geothermal conditions within the Slovakian part of the Transenergy project area can be found at the Atlas of Geothermal Resources in Europe published in 2002 (Hurter and Haenel, 2002). In this work the area of the Danube basin was described by maps showing the distribution of temperature-, salinity-, thickness-, permeability- and piezometric levels as well as showing resources of geothermal regimes of Pontian and Pannonian to Pontian age (see also Figure 14 and Figure 15).

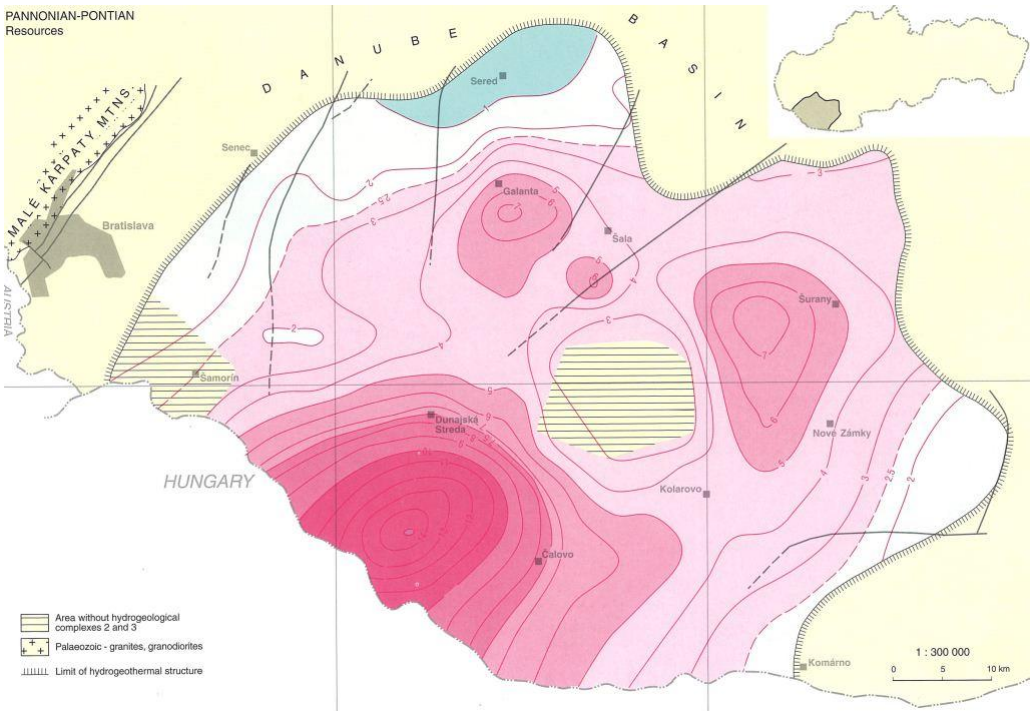

Figure 14: **Example map of the geothermal resources calculated in Pannonian-Pontian horizons in Danube Basin, compiled for Atlas of Geothermal Resources in Europe 2002 (taken from Hurter and Haenel, 2002).**

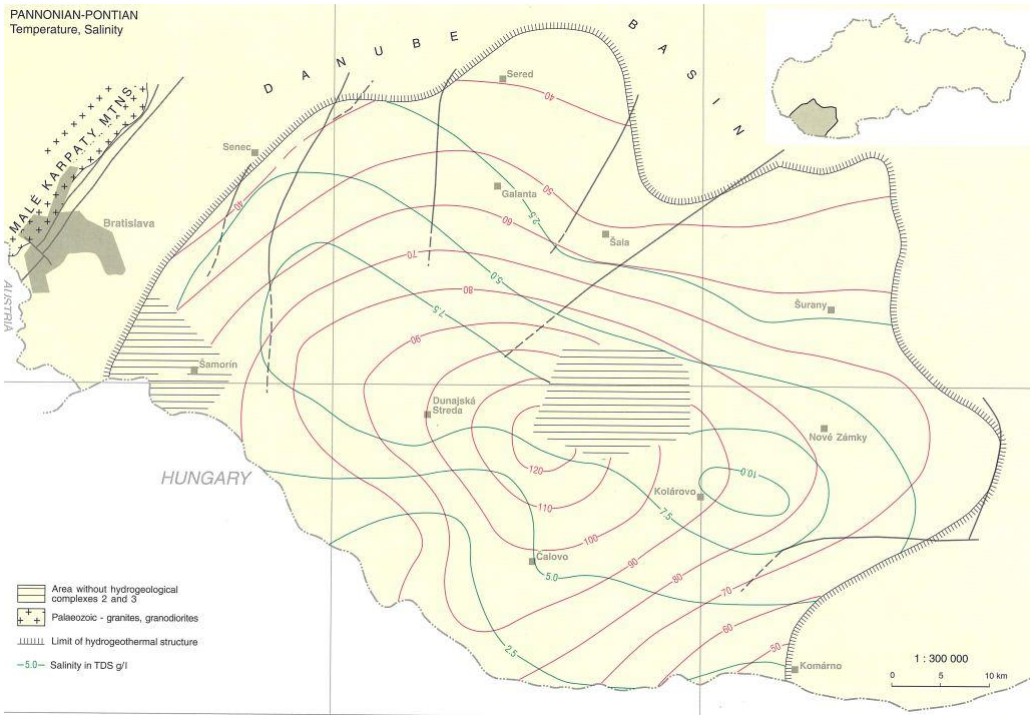

Figure 15: **Example map of the temperature and salinity in Pannonian-Pontian horizon in the Danube Basin compiled for Atlas of Geothermal Resources in Europe, 2002 (taken from Hurter and Haenel, 2002).**

1.3.5 Slovenia

The Slovenian part of the supra-regional area consists of the Mura-Zala basin in north-eastern Slovenia, which is situated in the south-western corner of the Pannonian basin. Due to the reduced crustal thickness (less than 30km east of Maribor), this area comprehends the greatest geothermal potential in Slovenia with respect to temperatures and heat flow density. Many users have already started direct heat use of geothermal energy in this region 2 - 3 decades ago. Recently new projects in Murska Sobota and Renkovci have been established. The planning of thermal water utilization in spas and greenhouses led to some local studies (in Murska Sobota, Moravske Toplice, Ptuj, Lendava). Temperature and surface heat flow density maps were compiled for the whole country in the previous studies, although the main focus is set on north-eastern Slovenia.

Figure 16 to Figure 18 show some of the already existing maps. These maps can also be found in the publication by Rajver & Ravnik (2002). In large parts of the Mura-Zala basin (except the Goričko region), east of the line Maribor-Ptuj, the geothermal potential is used by spas, thermal resorts and greenhouses.

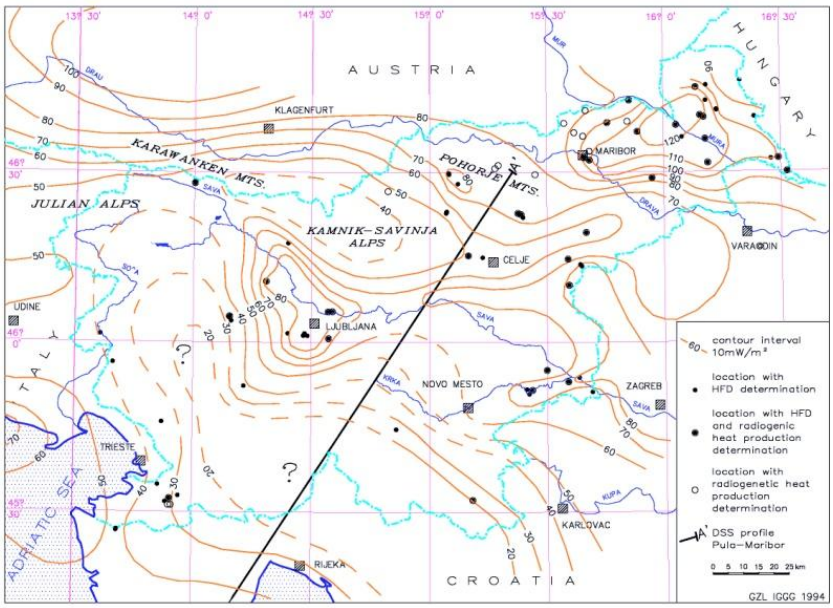

Figure 16: Heat Flow Density Map of Slovenia (Ravnik et al., 1995).

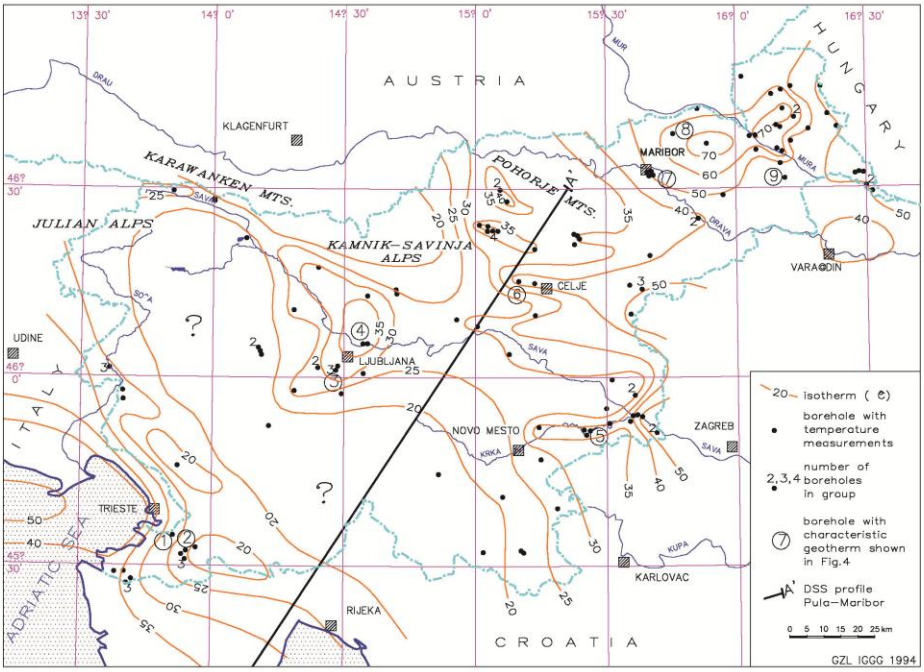

Figure 17: Temperature distribution at a depth of 1000m (Ravnik et al., 1995)

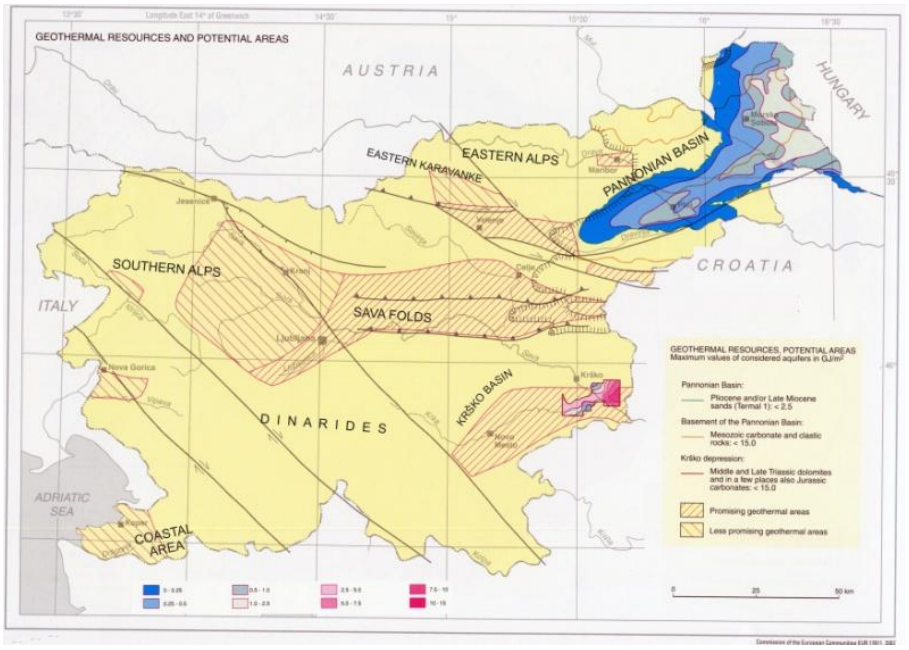

Figure 18: Geothermal resources and potential areas in Slovenia (Rajver et al., 2002)

The existing maps of heat flow density and temperature cover the whole country. However, they are more detailed and of better quality in north-eastern Slovenia due to a higher concentration of deep boreholes. The investigation area is characterized by increased geothermal gradients as wells as increasing surface heat flow density (SHFD).

At a depth of 1000m below surface, high temperature anomalies are discernible from Lenart to Moravske Toplice and around Lendava (expected formation temperature from 60°C to

70°C). Elsewhere in north-eastern Slovenia the subsurface temperatures are just a little above average (44°C to 55°C) at the above mentioned depth. The surface heat flow density reaches more than 100mW/m^2 eastwards of the town Maribor with an exception of the Ptuj area, probably due to lacking measurements and evaluation. The map showing the geothermal resources and potential areas (Figure 18) was prepared for the "Atlas of Geothermal Resources in Europe" (Hurter and Haenel, 2002). It illustrates the calculated Identified Resources for north-eastern Slovenia, where the Tertiary Mura formation represents the most promising reservoir.

The increased HFD values were determined especially on the Murska Sobota High between Lenart and Moravske Toplice and are attributed to the convection zones in the pre-Tertiary basement rocks. This is already confirmed at the exploration-production well in Benedikt, terminating at a depth of almost 1900m in the metamorphic, highly fractured dolomitic marbles with thermal water convection. This leads to an increased temperature gradient within the overlying tertiary beds and consequently to high HFD values (around 145mW/m^2). A similar situation with convection zones in the metamorphic pre-Tertiary rocks can be expected in the northeast, at Murska Sobota and Moravske Toplice at depths of about 1100 – 1500m as well as at Lendava – here at much greater depths (around 4000m). These assumptions could not be proven yet.

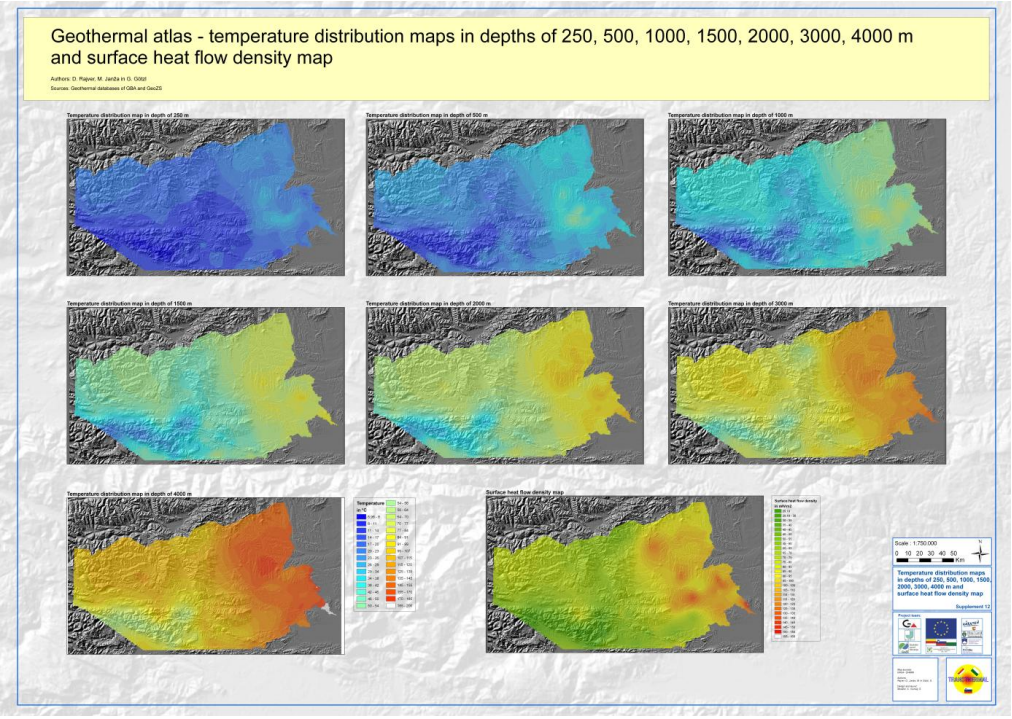

Figure 19: **From top left to bottom right: temperature distribution maps in depths of 250, 500, 1000, 1500, 2000, 3000, 4000m and a surface heat flow density map** (Rajver et al., 2008; Rajver & Goetzl, 2007)

Within the INTERREG IIIA project "Transthermal", several geothermal maps of the project area have been created (Figure 19). For the Slovenian part of the project area geothermal

data from about 300 boreholes have been analysed. Temperature maps indirectly show the geothermal gradients in the Tertiary sediments. Those are increased almost everywhere in north-eastern Slovenia (east of Maribor), especially between Lenart and Moravske Toplice, and reach values of up to 80mK/m on the Murska Sobota high. The geothermal gradient is, however, more reduced in the pre-Tertiary bedrock (carbonatic as well as metamorphic).

The HFD map also shows remarkably differing values in the north-eastern part (Mura-Zala basin) and in the rest of northern Slovenia, i.e. west of Maribor. For the entire Slovenian part of the Transthermal project area the average HFD value (± s.d.) is about 87 ± 34mW/m^2 (conclusion from data of 50 wells). However, for the Pannonian (Mura-Zala) part of the basin, the average HFD value (derived from 26 wells) is higher about 114 ± 22mW/m^2. This is a consequence of different lithospheric conditions in both areas (Goetzl & Lapanje (eds.) et al., 2008). Considering, as an example, singly the map of temperatures in a depth of 2000m, they are higher than 84°C practically everywhere east of the Maribor – Ptuj line. Here, the Benedikt anomaly is not discernible anymore - the thermal circulation causes high geothermal gradients only in the sedimentary cover. In Slovenia, the highest temperatures (above 100°C) at that certain depth are found at Veržej, across Murska Sobota towards Moravske Toplice and northeast from there, as well as in the wider Lendava area (Goetzl & Lapanje (eds.) et al., 2008). Elsewhere in north-eastern Slovenia, elevated temperatures at different depths appear also in the other smaller areas, i.e. SE of Lendava, between Maribor and Radenci, and along the border with Hungary. Further anomaly zones can be expected (for example north of Pečarovci and Šalovci), but have not yet been detected.

Advective heat transfer due to deep water circulation is capable of provoking locally confined anomalies to the geothermal regime down to depths of 1, 5 to 3km below the surface, depending on the existence of hydraulically conductive layers or fault-systems within crystalline bedrocks. The overall geothermal regime is in turn mainly controlled by the conductive heat exchange depending on the regional crustal thickness, leading to significant changes of geothermal conditions between the Mura-Zala basin and the other areas of northern Slovenia (Goetzl & Lapanje (eds.) et al., 2008).

2 Data background and workflow

2.1 Introduction

The geothermal regime of the supra-regional model is represented by means of temperature maps for several depths as well as by a surface heat flow density map. By using continuous thermal logs, bottom-hole-temperature (BHT) and drill-stem-test (DST) data obtained from wells, it is possible to estimate the geothermal regime. In addition to the in situ-data, outflowing water temperatures were included in the thermal processing. Because of the different data background in each country, the project partners did not work with the same types of data. In Austria, corrected BHT- and DST-data were used. In Slovenia mostly data from continuous thermal logs have been interpreted, as they are available in a very good quality. In Hungary, outflow temperatures were accessible in addition to BHT- and DST-data. The ap-

plied Slovakian datasets were derived from the Slovakian Geothermal Atlas (Franko, Remšik & Fendek, 1995).

Apart from required temperature data, parameters such as thermal conductivity and porosity had to be known for a determination of heat flow density. These data come from literature as well as old and new core measurements (see chapter 3.1.1).

In general the mapping of the geothermal regime is based on the following workflow:

1. Thermal Data Processing
2. Modelling of petrophysical data
3. Estimation of Heat Flow Density (in a borehole)
4. Estimation of Temperatures in various depths:
    a. 1000 m.b.s
    b. 2500 m.b.s
    c. 5000 m.b.s
    d. Top of pre-Tertiary basement
5. Estimation of Depth of different isothermal surfaces
    a. 50°C
    b. 100°C
    c. 150°C
6. Estimation of Specific Heat In Place and Specific Identified Resources
7. Interpolation and Visualization of Data from 4.-6
8. Modelling of the basal (background heat flow density)

2.2 Surface Heat Flow Density Map (HFD)

Overall, thermal data from 1243 wells were processed for the elaboration of the map. It was necessary to exclude 30 HFD values, because they were either unrealistically high (up to values of 1400mW/m^2) or had no specified location. The applied cut-off value for filtering of input data was set to 170mW/m^2. Furthermore four artificial datum points had to be added to the dataset in order to enhance the density of input data for interpolation. The majority of the HFD data was gathered in Hungary (731 values) and Austria (418 values). The remaining data was provided by Slovakia (57) and Slovenia (37).
Since the thermal logs in Slovenia (due to long shutdown times) are of good quality, the measured temperatures can be assumed as true formation temperature. Despite this, the Hungarian datasets have been divided into 9 different classes of quality, where >1< equals a very good and >9< an insufficient data quality. Furthermore the classification of the quality of Austrian data is based on differentiation between DST- and corrected BHT-values. In general temperature measurements during drill-stem-tests are more reliable because of the long shutdown time.

2.3 Temperature and Depth Contour Maps

Temperature Maps:

The compilation of temperature maps was performed at the depths of 1000m, 2500m and 5000m below surface (m.b.s).

The map at 1000 m.b.s was created using 6220 temperature values. The reason for this huge amount of values is the fact that the Slovakian partner has provided a GIS shape file with temperature values (as point information) extracted from contour lines of existing geothermal maps in addition to data from individual wells. Extracted points from contour lines were treated as data from wells in order to enhance the density of input data. The same procedure was applied for the other maps. The cut-off value for data filtering was set to 125°C. Only five values in total had to be excluded since they were unrealistically high (between 200 – 450°C).

The temperature map at a depth level of 2500 m.b.s. is basing on 6523 temperature values. Once again around 75 % of the available input data resulted from the Slovakian shape files. Again, an exclusion of data was unavoidable. The upper cut-off value was set to 250°C and the lower one to 20°C. Therefore, seven unrealistic temperature values with of up to 1000°C and lows of around 15°C had to be filtered out.

The temperature map at 5000 m.b.s was created using 6294 temperature values. The largest amount of these values originates again from the Slovakian dataset. This time, no exclusion of data was necessary, but nine artificial wells had to be added. This was essential for stabilization purposes of the interpolation at the border of the supra-regional model.

The temperature map at the top of the pre-Tertiary basement was compiled using 1850 temperature values. At locations where the basement is outcropping at the surface invariant temperature values of 10°C, which reflect the annual surface temperature at a first approach, were used for interpolation.

Depth Contour Maps of different isothermal surfaces:

Three Depth Contour maps of the 50°C, 100°C and 150°C isothermal surface were produced by 3D interpolation of temperature data from the temperature maps described above. The 3D interpolation was applied by using the numerical modelling software FEFLOW™.

2.4 Numerical Modelling (Background Heat Flow Density and Heat in Place)

2.4.1 Background Heat Flow Density

The dominant way of heat transport in the continental lithosphere is conduction. However, groundwater flow occurring in porous and fractured rocks in the upper part of the crust can modify the temperature field by convective heat transport. Depending on the flux of the groundwater flow the redistribution of heat can be significant resulting in strong temperature and heat flow density anomalies. Heat conduction can also result in thermal anomalies due

to variation of mantle heat flow density, heat production and thermal conductivity of rocks. Those thermal anomalies which cannot be explained by conduction are very likely caused by groundwater flow.

The background heat flow density is the heat flow density in sufficiently large depth, where the effect of near surface convective heat transport can be neglected. It is calculated assuming pure conductive heat transport and radiogenic heat production at the Earth's Crust. Based on project related datasets of (i) Surface Heat Flow Densities, (ii) interpolated subsurface temperatures and (iii) thermal rock parameters (see also Table) the background heat flow density was modelled for the entire lithosphere beneath the Transenergy project area. For that purpose assumptions for the build-up of the lithosphere were taken from literature sources and previous studies. The modelling was performed by using the numerical software package Comsol Multiphysics™. Further details can be found at chapter 3.

Comparing the distribution of the background heat flow with the observed surface heat flow allows outlining and characterizing geothermal anomalies driven by convection of thermal water.

2.4.2 Heat in Place

The parameters Specific Heat in Place and Specific Identified Resources represent the existing geothermal potential assuming that 100 % (Specific Heat in Place) or 33 % (Specific Identified Resources) of the available heat content at the subsurface can be extracted by cooling to a defined lower temperature level (reference temperature). These parameters limit the theoretically utilizable geothermal heat in a first approach ignoring the hydrogeological build-up of the subsurface. These two parameters can be estimated if the distribution of the following parameters in the subsurface is known: (i) specific heat capacity, (ii) bulk density, (iii) total porosity, and (iv) thickness of the investigated rock volume and (v) subsurface temperature.

The compilation of the parameters Specific Heat in Place and Specific Identified Resources was performed for four different cases:

i. in the Neogene sediments
ii. in the 50m upper part of pre-tertiary basement
iii. until a depth of 5km
iv. until a depth of 7km

The petrophysical input data (parameter: i to iii) were obtained from modelling and calibration by measurements on rock samples at the Austrian part of the supra-regional model (see also Table). At the other parts of the supra-regional area (Hungary, Slovakia and Slovenia) a simplified approach was applied by correlating petrophysical properties to the stratigraphical build-up, which consists of alternating clay and sand layers. The values of these parameters were obtained from literature and laboratory measurements (see chapter 3.1.1). For more details see also chapter 3.1.1.

The total thickness of the Neogene Sediments was derived from the geological model of the supra-regional area, whereas the thickness of the individual sedimentary horizons is based on literature research.

Assuming linear increase of temperature between the surface and depths of 1000m, 2500m and 5000m below surface, the temperature for a certain depth could be calculated. Below 5000m the temperature was extrapolated with the last gradient (between 2500 and 5000m). The surface temperature was assumed to be uniform (10°C). Furthermore, the temperature of re-injected water has to be known when calculating the Specific Identified Resources. The value was set to 25°C, so that a comparison of the Specific Identified Resources with previous studies (Franko et al., 1995, Hurter and Haenel, 2002) was possible.

3 Description of the applied methodologies and approaches

The following chapter treats the applied methodologies in order to elaborate the models and maps covering the entire project area. It intends to give a comprehensive understanding to the chosen approaches for:

- the preparation of petrophysical and thermal input data
- the geostatistical interpolation in order to elaborate the several maps
- the calculation of several geothermal potentials
- the applied 3D modelling for the estimation of the background heat flow density

This in turn shall enable a possible future adaption and update of the achieved results.

3.1 Preparation of input data

In general the applied input data are represented by petrophysical parameters and borehole related thermal data. Both datasets are related to different scales and approaches, which will be described in the subsequent subchapters.

3.1.1 Modelling of petrophysical data

In general heat transport is governed by the following material parameters:

a. Thermal conductivity
b. Specific heat capacity
c. Bulk porosity and density
d. Effective porosity
e. Radiogenic heat production

These formation characteristics were obtained for individual rock types from previous studies as well as from literature and exploration data. Since only values for individual rock types are known, generalized models for the pre-specified geological units at supra-regional scale (see Summary report of geological models, http://transenergy-eu.geologie.ac.at/) had to be defined.

As in Austria comprehensive laboratory measurements of thermal rock properties just commenced a couple of years ago and synthetic models of the geological units appearing in the subsurface of the Transenergy project area had to be calculated by means of weighted averaging according to the appearance of different rock types. The petrophysical parameters of individual rock types themselves had been taken from literature (e.g. Schoen, 1983). Afterwards the achieved petrophysical models were calibrated and evaluated by measured data gained from drilling-core analyses. The frequency of the individual rock types obtaining within a geological unit was used as a weighting factor for estimation of the material parameters.

For the remaining parts of the supra-regional area, a simplified correlation between petrophysical parameters and the stratigraphical build-up of the Tertiary basin fillings was conducted. This correlation is based on the alternation of shale and sand layers. As the variation of thermal properties at consolidated basement is much lower than in the basin fillings due to reduced porosity, simple models of weighted averages have been applied on the hard rocks of the pre-Tertiary basement.

a. <u>Thermal conductivity:</u>

As this material parameter provides information about the ability to transport heat, it is important for the interpretation and prediction of formation temperature. The thermal conductivity for estimation of the surface heat flow density was determined by following approaches:

In Austria, the mean thermal solid matrix conductivity for a geological unit was predicted in a first approach from the lithological composition of the layer:

$$\boldsymbol{\lambda_m} = (\prod \boldsymbol{\lambda_i^{c_i}})^{1/\sum c_i} \qquad \textbf{3-1}$$

The effective thermal conductivity represents the true formation characteristic, taking into account fluid-filled pore space and ambient temperature. According to Beck (1976), the effective parameter can be calculated by following equation:

$$\boldsymbol{\lambda_{eff}} = \prod \boldsymbol{\lambda_m^{(1-\phi)}} * \boldsymbol{\lambda_f^{\phi}} \qquad \textbf{3-2}$$

Furthermore, the parameter is affected by temperature. Empirical studies indicate that the effective thermal conductivity at a temperature around 200 °C is reduced by 30 % compared to the value at room temperature. For the estimation of the surface heat flow density a thermal correction, based on Sass et al. (1992), was unavoidable:

$$\boldsymbol{\lambda(T)} = \frac{\boldsymbol{\lambda(0)}}{\mathbf{1.007}+\boldsymbol{T_{form}}\cdot\left(\mathbf{0.0036}-\frac{\mathbf{0.0072}}{\boldsymbol{\lambda(0)}}\right)} \qquad \textbf{3-3}$$

The hypothetical thermal conductivity of the individual rock type at 0 °C [λ_0=λ(0)] can be derived from following equation:

$$\boldsymbol{\lambda_0} = \boldsymbol{\lambda}(\mathbf{25\ ^\circ C})\left[\mathbf{1.007} + \mathbf{25}\left(\mathbf{0.0037} - \frac{\mathbf{0.0074}}{\boldsymbol{\lambda}(\mathbf{25\ ^\circ C})}\right)\right] \qquad \textbf{3-4}$$

Table 6: **Thermal parameters of rocks used for the calculation of Specific HIP and Specific Identified Resources (see chapter 3.4).** Data of the Vienna and Styrian basin are from laboratory measurements made in the framework of TE project. Specific heats of clay and sand in other areas are from Kappelmeyer and Haenel (1974), bulk densities are from Szalay (1982).

Vienna basin									
	Specific heat (J/kg.K)			Bulk density (kg/m^3)			Porosity (%)		
Horizon	mean	min	max	mean	min	max	mean	min	max
Quaternary	758	758	758	1800	1800	1800	30	30	30
Upper Pannonian	782	754	807	1943	1900	2200	24	21	25
Lower Pannonian	782	754	807	1943	1900	2200	24	21	25
Sarmatian	767	763	769	1920	1900	1957	25	24	25
Badenian	1002	886	1176	2313	1963	2730	18	7	26
Lower Miocene	1062	957	1161	2450	2127	2680	13	6	20
pre-Tertiary basement	958	894	1121	2621	2200	2897	5	0	20
Styrian basin									
	Specific heat (J/kg.K)			Bulk density (kg/m^3)			Porosity (%)		
Horizon	mean	min	max	mean	min	max	mean	min	max
Quaternary	n.d.			n.d.			n.d.		
Upper Pannonian	787			2362	2189	2552	19	14	29
Lower Pannonian	787			2362	2189	2552	19	14	29
Sarmatian	774	774	774	n.d.			20	20	20
Badenian	803	769	829	2412	2270	2476	12	4	17
Lower Miocene	851	800	888	2546	2357	2728	6	5	8
pre-Tertiary basement	762	710	853	2709	2644	2799	3	0.3	18
Other areas (HU: Little Hungarian Plain, SK: Danube basin, SL: Drava basin)									
	Specific heat			Bulk density (kg/m^3)					

	(J/kg.K)								
Clay		950			2710				
Sand		920			2620				
pre-Tertiary base-ment		960			2620				

Table 7: **Thermal parameters of rocks used for the calculation of Background Heat Flow Density (see chapter 3.6).**

Vienna Basin								
	λ (W/m.K)			A (10^{-6} W/m^3)			c (J/kg.K)	ρ (kg/m^3)
Horizon	mean	min	max	mean	min	max		
Quaternary	3	3	3	n.d.			1282	2300
Upper Pannonian	3.1	2.8	4	1.3	1.3	1.3	1282	2300
Lower Pannonian	3.1	2.8	4	1.3	1.3	1.3	1282	2300
Sarmatian	3.2	3	3.3	n.d.			1282	2300
Badenian	3.6	3	4.1	1.2	1.1	1.3	1282	2300
Lower Miocene	3.4	2.1	4.1	0.7	0.7	0.7	1282	2300
Pre-Tertiary basement	3.4	1.9	5.6	1.1	0.6	2	1374	2800
Styrian Basin								
	λ (W/m.K)			A (10^{-6} W/m^3)			c (J/kg.K)	ρ (kg/m^3)
Horizon	mean	min	max	mean	min	max		
Quaternary	n.d.			n.d.				
Upper Pannonian	2.3	2	2.7	1.6	1.5	1.7	1282	2300
Lower Pannonian	2.3	2	2.7	1.6	1.5	1.7	1282	2300
Sarmatian	1.3	1.3	1.3	0.3	0.3	0.3	1282	2300
Badenian	2.5	2	2.8	0.7		1.3	1282	2300
Lower Miocene	3.3	2.2	5.2	1	0.3	1.4	1282	2300
Pre-Tertiary	3.4	2.4	4.4	1		1.8	1374	2800

basement								
Basement and Lithosphere		λ (W/m.K)		A (10^{-6} W/m^3)			c (J/kg.K)	ρ (kg/m^3)
		varies		1			1282	2300
crust		3		1			1374	2800
mantle		4		0			1554	3300

λ: thermal conductivity, A: volumetric heat production rate, c: specific heat, ρ: density

Data of the Vienna and Styrian basin are from laboratory measurements made in the framework of TE project. Thermal conductivity of sediments in the other areas comes from wells; HU: Dövényi (1994), SK: Franko et al. (1995), SL: Ravnik (1991), Ravnik et al. (1995), thermal conductivities of crust and mantle are from (Kappelmeyer and Haenel, 1974, Zoth and Haenel, 1988) densities are from (Parsons and Sclater, 1977). Specific is calculated in this study (see chapter 3).

The estimation of the thermal conductivity in Hungary was achieved using a different approach. The stratigraphy of Quaternary and Neogene sediments is simplified by using alternating layers of shale and sandstone (see chapter 2.4.2). For a given percentage of shale in a layer, the mean thermal conductivity of the layer was calculated by:

$$\frac{1}{\lambda_i} = \left(\frac{P_{sh}}{\lambda_{sh,i}} + \frac{100 - P_{sh}}{\lambda_{ss,i}}\right) / 100 \qquad \textbf{3-5}$$

The thermal conductivities of shale and sandstone in Equation 3.5 at a given depth were obtained using a thermal conductivity – depth functions shown in Figure 20. This correlation is based on 132 sandstone and 183 shale samples. The thermal conductivity of Neogene sediments depends on depth, lithology and to lesser extension on the sedimentation rate. The increase of thermal conductivity with depth is mainly due to decrease of porosity (because rock matrix is a better conductor, see Equation 3.2). A general calculation of the effective thermal conductivity was proposed by Vacquier (1984):

$$\lambda_{eff} = \lambda_m^{1-\phi} \cdot \lambda_f^{\phi} \qquad \textbf{3-6}$$

For other rock types, which are not dominated by either shale or sand, values from Table 8 were applied for calculating the surface heat flow density.

Temperature dependence of this parameter is taken into account using the empirical relationship established by Sekiguchi (1984):

$$\lambda(T) = 365.75 \cdot (\lambda(20°C) - 1.84) \cdot \left(\frac{1}{T} - \frac{1}{1473}\right) + 1.8 \qquad \textbf{3-7}$$

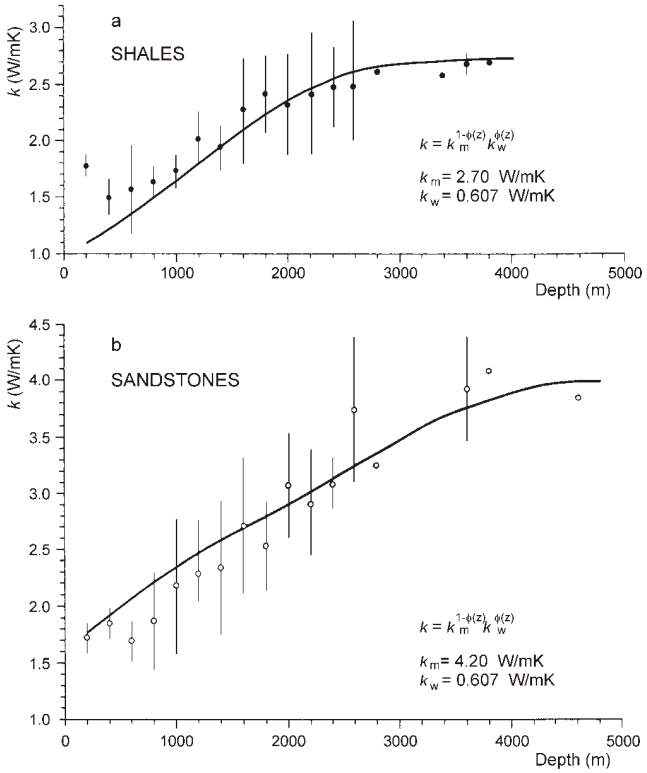

Figure 20: **Thermal conductivities of shales (a) and sandstones (b) measured on rock samples from boreholes (after Dövényi and Horváth, 1988).** Thermal conductivity-depth functions are calculated according to Equation 3.6 using the porosity-depth trends shown in Figure 21. The calculated trends are shown by thick lines. Conductivities refer to room temperature

Table 8: **Here the average thermal conductivity of pre-Neogene rocks and Miocene volcanites in Hungary after Dövényi et al. (1983) is shown**. The values refer to room temperature

Age	Rock type	No. of samples	λ [W/(m*K)]	σ
Miocene	andesite, andesite tuff	6	1.97	0.10
Eocene	andesite, andesite agglomerate	11	2.60	0.16
Cretaceous	trachydolerite	2	2.18	-
Jurassic	sandstone	16	3.69	0.92
	shale	28	2.83	0.89
	limestone	10	3.06	0.17
Triassic	schist	6	2.78	0.16
	shale	5	2.84	0.13
	limestone	14	2.69	0.07
	dolomite	18	4.41	0.36
Permian	sandstone	5	2.72	0.16
Palaeozoic	schist, breccia, quartzite gneiss	10	3.11	0.42

In Slovenia the estimation of surface heat flow density was obtained by using measured thermal conductivities. The values were corrected only for temperature influence. Figures from Zoth and Haenel (1988), showing temperature dependence of thermal conductivities for different rocks, were used for correction at depths > 2000 m.

b. *Specific heat capacity*

The specific heat capacity is an important material parameter, because it provides information about the ability to store heat. The specific heat capacity, which is used for determination of the Heat in Place, was estimated by following approach:

In case of the Austrian part, the specific heat capacity of the solid matrix for a geological unit was modelled from its lithological composition:

$$C_p = \sum C_{p,i} \cdot c_i \qquad \textbf{3-8}$$

The effective value for the specific heat capacity can be obtained by following equation:

$$C_{p,eff} = C_p \cdot (1 - \phi) + C_f \cdot \phi \qquad \textbf{3-9}$$

In the other parts of the supra-regional area (HU, SK and SL), the value of specific heat capacity for clay and sand was obtained from Kappelmeyer & Haenel (1974).

c. *Bulk porosity and density*

In Austria, the values of these two bulk parameters could be derived in general from existing borehole data (core samples and log interpretation) by simple averaging. In Hungary, the values were obtained from laboratory measurements (see Figure 21; after Szalay, 1982). In Neogene sediments, the density of shale and sandstone in great depth (> 4 km) is presumed as the density of pure rock, because porosity is very small (< 5 %). The same approach was used for the Slovenian and Slovakian part of the supra-regional area.

d. *Effective porosity*

The effective porosity for clay was set to zero and for sand assuming to be half of the total porosity. In case of the pre-Tertiary basement, a porosity of 3% (fissure porosity), based on Rajver et al. (2002) and Dövenyi et al. (2002), was used. For the Austrian part the estimation of the effective porosity was the same way as before (parameters c).

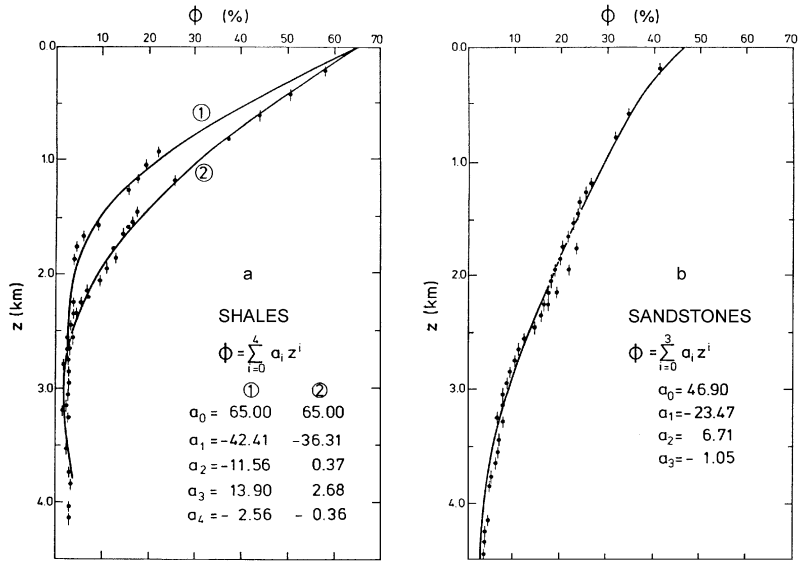

Figure 21: **Porosity-depth function for a) shale and b) sandstones in Hungary after Szalay (1982).** Solid circles indicate porosity values averaged over 100 m intervals.

e. *Radiogenic heat production*

As the radiogenic heat production rate only plays a minor role in the heat budget of the sedimentary basins it was neglected for calculating the Surface Heat Flow Density and the interpolation as well as extrapolation of borehole temperatures. Nevertheless the radiogenic heat production rate was taken into account in order to calculate the background heat flow density (see also chapter 3.6)

3.1.2 Thermal data processing

The temperature data, which are necessary for interpretation of the subsurface thermal regime in the project area, were provided mostly by BHT- and DST data at hydrocarbon wells. As borehole temperature has been of minor interest in the oil industry, a correction to obtain equilibrium temperature had to be applied to BHT-data. Considering that DST-data are more reliable than BHT-data (long shutdown time) and that they are good documented, the focus was only set on the evaluation of the data quality.

As far as known and under the condition that a BHT correction was applicable, all project partners used the same method. It is a line-source related graphical correction, also called “Horner plot” approach (Horner 1951; adapted by Fertl & Wichmann, 1977). The method requires several temperature measurements at the same depth at different times after the end of mud circulation. The undisturbed temperature is calculated by linear regression.

Additionally to this standard method, a numerical BHT correction (Götzl et al., 2010; cylindrical source) has been applied on Austrian data following a method by Leblanc et al. (1982),

where the undisturbed temperature is estimated inversely by least square optimization of thermal diffusivity.

Since Drill-Stem-Tests are very well documented, an exclusion of temperature data of poor quality was simple. The temperature measurements showing gas and drilling fluid approach in the probe were understood of poor quality and were therefore not considered at the further thermal processing.

3.2 1D modelling of the Surface Heat Flow Density (SHFD)

In addition to the subsurface temperature data, the surface heat flow density is an important parameter for interpretation of the heat content in the subsurface. The SFHD was determined by using two different approaches:

i. 1D Fourier inversion
ii. Interval method

Both methods follow a pure conductive approach based on Fourier's Law ignoring internal radiogenic heat sources. The 1D Fourier inversion (i) is based on the assumption that the overall SHFD along the entire profile of a borehole remains constant, so that changes in the geothermal gradient are only driven by changes in the conductivity of the geological layers in drilled section. This is only the case when heat transport by convection is absent and the thermal regime at a borehole is purely driven by heat conduction. The interval method (ii) allows changes in the HFD due to combined heat transport due to conduction and convection. Approach (i) offers the possibility to detect thermal anomalies within a borehole due to convection or erroneous data, but is in turn smoothing the resulting temperature profile. Approach (ii) does not smooth the resulting temperature profile, but is in turn prone to misleading interpretation due to the influence of erroneous input data. However, both methods are providing more or less the same SHFD values for an individual well. In the following both approaches are presented in a more detailed way:

The 1D Fourier Inversion has been applied on all Austrian boreholes which obtained interpretable information (DST and corrected BHT data). Based on Fourier's Law and a one-dimensional approach, the SHFD is limited to pure vertical direction:

$$q = \lambda \cdot \frac{\partial T}{\partial z} \qquad \textbf{3-10}$$

This equation can be transformed into an algorithm describing the temperature field of a layered half space (Götzl et al., 2010):

$$T_i = T_{i-1} + q \cdot \frac{m_i}{\lambda_{eff,i}} \qquad \textbf{3-11}$$

The surface heat flow density can be derived from Equation 3.11 by inversion, where an initially assumed heat flow density is iteratively varied until a sufficiently accurate adjustment between measured and calculated temperatures has been reached (Götzl et al., 2010). Furthermore, T-z profiles were derived with this algorithm for the boreholes.

The modified version of the same method has been applied to Hungarian data. The modification takes into account the difference in the quality of the temperature data. The heat flow density in a well is calculated at every depth, where the temperature is measured:

$$q_i = \frac{T_i - T_0}{\sum_{j=1}^{M} \frac{m_j}{\lambda_{eff,j}}} \qquad \textbf{3-12}$$

The mean heat flow density in a well is the weighted average of the HFD values obtained from Equation 3.12, where the weighting factors are determined by the quality class of the temperature data (see also chapter 2.2):

$$q_i = \frac{1}{\sum_{i=1}^{N} (9 - S_i)^2} \cdot \sum_{i=1}^{N} q_i (9 - S_i)^2 \qquad \textbf{3-13}$$

The Slovenian partners estimated the HFD values by applying the Interval method following Powell et al. (1988). The method was applied to wells, where thermal conductivity was measured on core samples. The T-z profiles (from continuous thermal logs) were divided into several depth intervals corresponding to lithological units or geological structure and values of thermal conductivity were attributed to those intervals. The overall surface heat flow density for a well represents the weighted average of obtained HFD values with respect to thickness of individual geological units or investigated interval lengths as weighting factors.

The origin of the Slovakian data is unknown as they were taken from the Geothermal Atlas of Slovakia (Franko, Remšik & Fendek, 1995).

3.3 Extrapolation of temperature within a borehole:

Based on measured data and the estimation of the SHFD borehole temperature values have been both interpolated and extrapolated to certain depth levels in order to elaborate the aimed temperature map series. According to Hurtig et al. (1992), it is possible to extrapolate the temperature linearly until a depth of +50% of the total length of a borehole. However, a constant temperature gradient at greater depths is not necessarily correct. Considering different drilling lengths of wells and mostly low penetration depths, an extrapolation of temperature data was necessary.

According to the quality of the derived results, all processed borehole temperatures have been divided into seven classes:

1. Measured data
2. Interpolated data
3. Extrapolation length between +50% and +100%
4. Extrapolation length between +100% and +200%
5. Extrapolation at artificial wells
6. Extrapolation length between +200% and +300%
7. Extrapolation length > 300%

The individual quality class of interpolated / extrapolated borehole temperatures was later regarded at the elaboration of temperature maps. Values of the quality classes 5 to 7 have only be used in case of insufficient density of input data at a specific area.

The following Table 9 shows the number and classification of the applied extrapolated data for the various temperature maps. It is obvious that an application of extrapolated data was required for some maps.

Table 9: Number and classification of extrapolated data for various temperature maps

Temperature map	Total amount of extrap. data	3rd class	4th class	6th class	7th class
1000 m.b.s	286	73	213	-	-
2500 m.b.s	758	280	478	-	-
5000 m.b.s	579	106	473		
Top Basement	370	164	58	21	127

3.4 Estimation of Heat-In-Place and Identified Resources

The parameter Heat in Place (HIP) describes the amount of thermal energy stored in the subsurface porous rocks including the water filling of pores. According to Muffler and Cataldi (1978) HIP is calculated by the following equation:

$$\Delta H_0 = (C_r(z)\rho_r(z)(1-\phi(z)) + C_w\rho_w\phi(z))(T(z)-T_0)\Delta z\Delta A \qquad \textbf{3-14}$$

If ΔH_0 is summarized to a certain thickness and area, then the total HIP in that volume can be obtained. Neglecting the area in Equation 3.14 leads to the heat stored in a rock column having unit area and termed as the Specific Heat in Place $H_{sp,0}$:

$$H_{sp,0} = \sum_{z=z_1}^{z=z_2} \Delta H_{sp,0} \qquad \textbf{3-15}$$

In general, z_1 and z_2 are top and bottom of a permeable formation, respectively, it is possible that z_1 is the surface (z_1=0) and z_2 is a fixed depth. As described in chapter 2.4.2, the compilation of the Specific Heat in Place was performed for several different cases.

Not all the heat stored in a fluid filled porous rock volume can be utilized in a technically way. Amongst others, constraining factors are given by hydraulic connection of water filled pores or by the low transport velocity of thermal conduction. The portion of heat, which can truly be utilized in a technical way, is described by the so called heat recovery factor. In this context a heat recovery factor of 1 means that the entire heat stored in a rock volume can be extracted. In opposite to this a heat recovery factor of 0 means, that no heat at all can be extracted from a rock volume. In general the heat recovery factor is a function of (i) the existing temperature levels, (ii) the temperature of the reinjected water, (iii) the hydraulic properties of the

investigated rock volumes and (iv) the applied geothermal utilization technique. The determination of the heat recovery factor is not trivial and is mostly executed by the help of empirical studies (e.g. site specific numerical parameter studies).

Nevertheless, in case of a doublet system consisting of a production and injection well, both filtered in the same reservoir, the recovery factor can be estimated in a very first approach following an approach by Hurter and Haenel (2002):

$$R = 0.33 \frac{T(z) - T_{inj}}{T(z) - T_0} \qquad \textbf{3-16}$$

According to Gringarten (1978), the recovery factor for a single well use (no reinjection) is equal to R = 0.1. The approach of Haenel and Hurter (2002) may be seen as an optimistic assumption outlining the maximum recoverable heat in place. In praxis heat recovery factors may vary in the range of <0.1 and 0.4.

The combination of the Specific Heat in Place and the heat recovery factor leads to the so called “Specific Identified Resources”, which is to be seen as the upper limit of the technically recoverable portion of heat stored in the subsurface:

$$H_{sp,1} = R \cdot H_{sp,0} \qquad \textbf{3-17}$$

In a first approach the heat recovery factor was obtained from Equation 3.16 and therefore neglecting the hydrogeological conditions at the subsurface in order to outline the magnitude of the maximum available heat stored in the underground for geothermal utilization. In the later course of the study Transenergy, especially at the pilot areas, a more sophisticated approach estimating the heat recovery factor will be applied.

The calculation of both parameters for the different cases was performed on the basis of 2D grids containing the input data.

3.5 Geo-statistical interpolation

Geo-statistical interpolation methods have been applied in order to elaborate the various map series including:

- Surface Heat Flow Densities
- Temperature distribution at different depth levels
- Depth distribution at different temperature levels
- Distribution of specific Heat in Place and Specific Identified Resources

In the following chapters the chosen raster interpolation algorithms, which have been applied using the software Package Surfer™, will be discussed.

3.5.1 Interpolation methods for Surface Heat Flow Density

Since different interpolation methods are available, a comparison and thus a selection of the most satisfying interpretation had to be made. The following approaches were compared in order to find the most suitable interpolation method:

- Inverse Distance to a Power (IDTAP)
- Kriging
- Minimum Curvature

In a first step, all three methods have been applied on the data set based on the same geometrical settings, which are shown in the subsequent Table 10).

Table 10: Grid line geometry for supra-regional scale data interpolation

	Minimum [km]	Maximum [km]	Spacing [km]	Number of Lines
X Direction	300	1000	1	701
Y Direction	5000	5500	1	501

Figure 22 shows the results of the applied different interpolation methods:

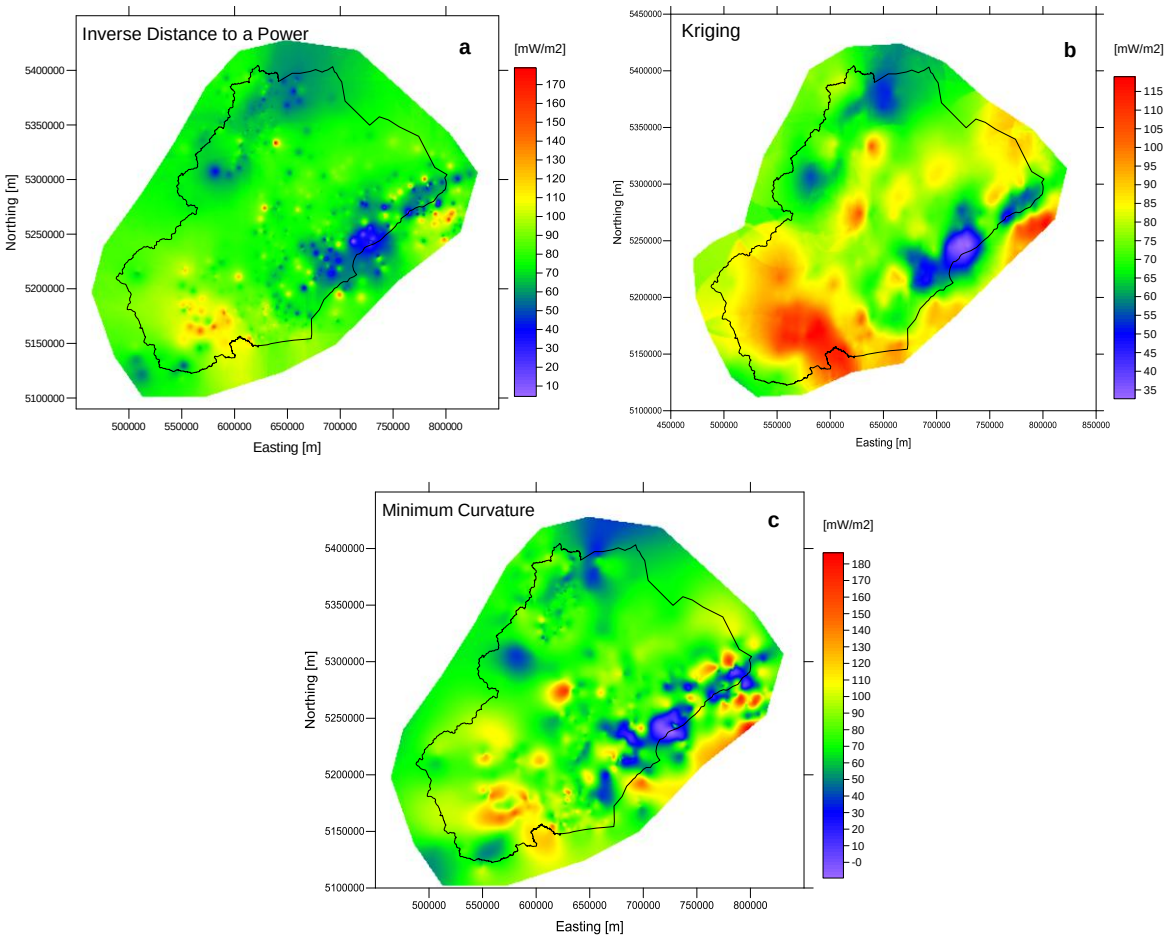

Figure 22: Surface Heat Flow Density map for supra-regional area from different interpolation methods; a: Inverse Distance to a Power, b: Kriging, c: Minimum Curvature.

The *Inverse Distance to a Power* (IDTAP) method is an averaging method and uses distance as weighting. It is fast but generates “bull’s-eye” patterns of concentric contours around individual datum points (see Figure 22 - a). By using an iterative approach the *Minimum Curvature* method attempts to fit a surface to all data values. It is a fast method, which generates

smooth surface, but it extrapolates values beyond the parameter range of the applied data set (see Figure 22 - c; negative values in purple). The *Kriging* method is one of the most flexible methods and uses trends in the map to extrapolate data (see Figure 22 – b), but it has the same disadvantage as *Minimum Curvature*.

Both the fact that the values exceed the heat flow density range by applying the *Minimum Curvature* method as well as the expected regional trends by using the *Kriging* method instead of isolated bull-eye shaped anomalies, as applied by the IDTAP method, led to the decision, that all 2D interpolation was achieved by using *Kriging*.

The second step was to change the statistical settings of the Kriging method (Variogram model & search options in order to minimize artificial patterns at the SHFD map: Due to numerous variogram models *Kriging* is a very flexible gridding method. The variogram characterizes the spatial variability of a dataset. A variogram analysis consists of the experimental variogram (black line with dots in Figure 23) estimated from the data and the variogram model fitted to the data (blue line Figure 23). The variogram model defines the spatial weights of the *Kriging*.

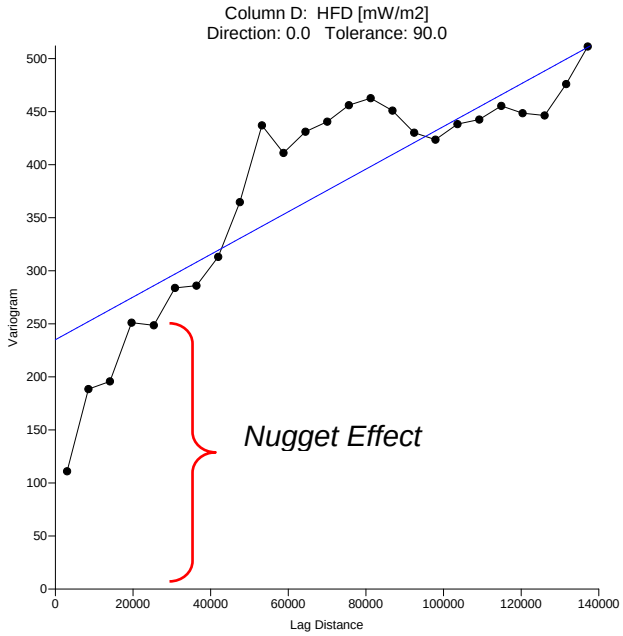

Figure 23: **Variogram of surface heat flow density data set (default settings).** Black line with dots: experimental variogram; blue line: variogram model (linear function with nugget effect)

According to Barnes (2002), the experimental variogram is estimated by averaging one-half the difference squared of the SFHD values over all pairs of observations with the specified separation and direction. The variogram model can be chosen from a set of mathematical functions, which describe spatial relationships. The appropriate model is chosen by fitting the variogram model to the experimental model. If the experimental variogram never levels out as in our case, the linear function is appropriate. Since the experimental model appears to intercept with the vertical axis not at zero, a so called *Nugget Effect* had to be applied. The *Nugget Effect* quantifies the short distance variability (i.e. spatial variations occurring at distance closer than the grid spacing). The variogram model was matched by changing the

Nugget Effect and the slope of the linear function. After choosing appropriate initial values for the *Nugget Effect* and the slope, a fine-tuning of the model was obtained by the option *Automatic Variogram Fitting*. The parameters were calculated by iterative LSQ-optimization (see Figure 24).

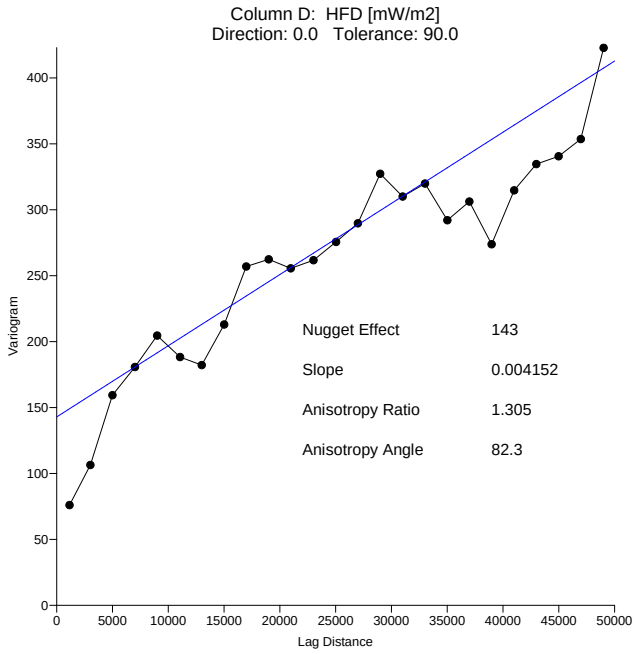

Figure 24: **Final variogram of surface heat flow density data set (default settings);** black line with dots: experimental variogram; blue line: variogram model (linear function)

The search option is a further possibility for modifications, because it controls which data are considered by the gridding operation when interpolating grid nodes, the maximum and minimum number of data and the radius in which to look for data. By trial and error these search parameters were determined for the surface heat flow density map (see Table 11).

Table 11: **Search options for surface heat flow density map**

Search radius	50 km
Number of search sectors	4
Maximum number of data in all sectors	64
Minimum number of data in all sector	2

The compiled surface heat flow density map with the above mentioned settings is shown in Figure 25.

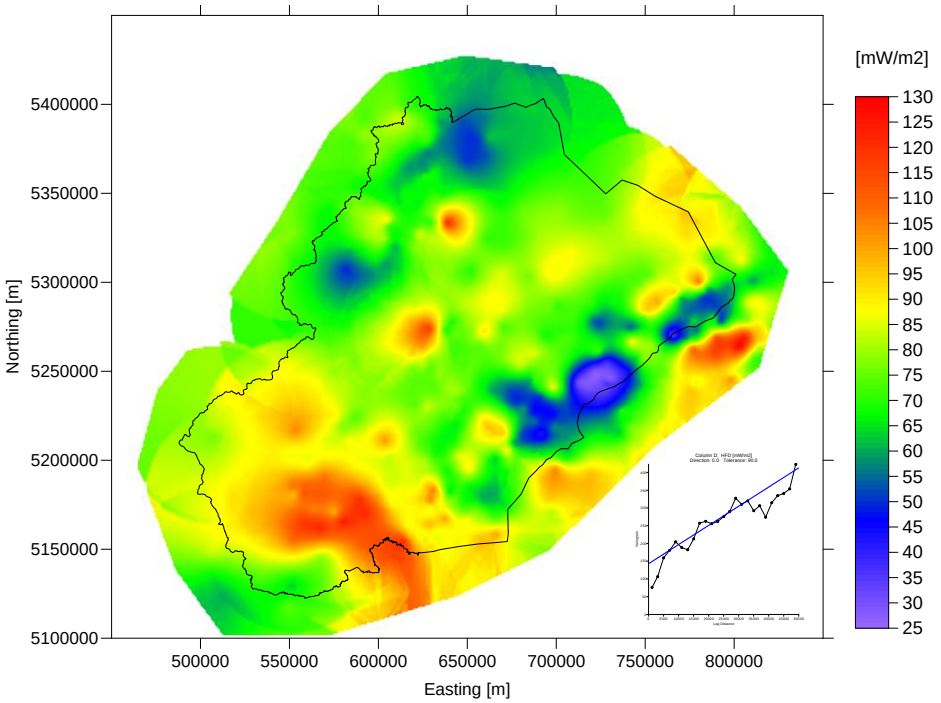

Figure 25: **Final version of the interpolated Surface Heat Flow Density map combined with the associated variogram**

3.5.2 Applied Interpolation methods for Temperature and Depth Maps

(a) Temperature Maps:

The applied 2D temperature interpolation procedures to the temperature data sets were quite similar to the one applied for the elaboration of the SHFD map. The gridding method *Kriging* was used for all temperature maps based the same geometrical settings (see Table 10). However, there was a problem with the associated variogram used for the SHFD maps (Gaussian model) for the maps at a depth of 1000 and 2500m below surface. It was found out by trial and error that a linear model was best fitting in order to create reasonable temperature maps (Figure 26 and Figure 27).

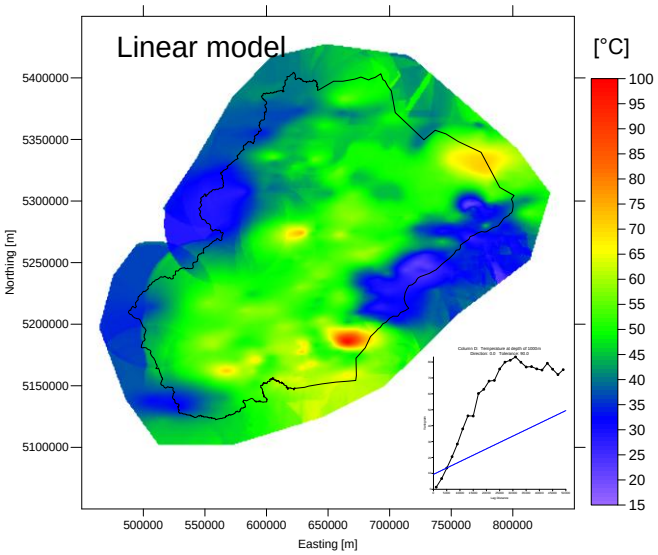

Figure 26: **Optimized temperature map at a depth of 1000m below surface applying a linear variogram model (optimization by auto fitting).**

Table 12: **Search options for temperature at 1000 m.b.s**

Search radius	50km
Number of search sectors	4
Maximum number of data in all sectors	64
Minimum number of data in all sector	1
Variogram model	Linear
Slope	0.000792
Anisotropy Ratio	2
Anisotropy Angle	5.18
Nugget Effect	9.4

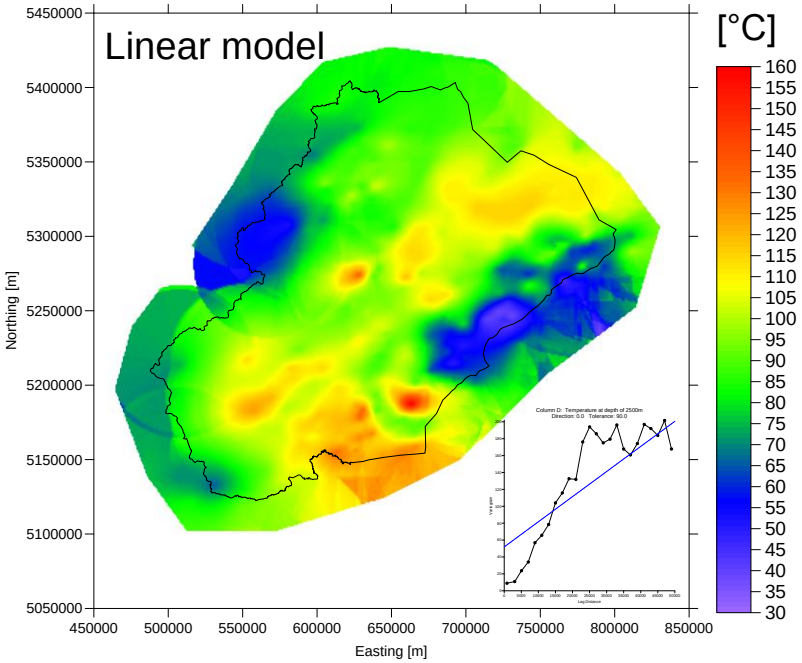

Figure 27: **Optimized temperature map at a depth of 2500m below surface (m.b.s.) applying a linear variogram model (optimization by auto fitting).**

Table 13: **Search options for temperature at 2500 m.b.s**

Search radius	50km
Number of search sectors	4
Maximum number of data in all sectors	64
Minimum number of data in all sector	1
Variogram model	Linear

Slope	0.002817
Anisotropy Ratio	1.4
Anisotropy Angle	20
Nugget Effect	51.94

In case of the temperature map at 5000 m.b.s., the interpolation was performed without any difficulties. The shape of the experimental model was almost linearly. Thus, a linear variogram model was used for interpolation. In Figure 28 the temperature map at 5000 m.b.s. and the associated variogram is plotted.

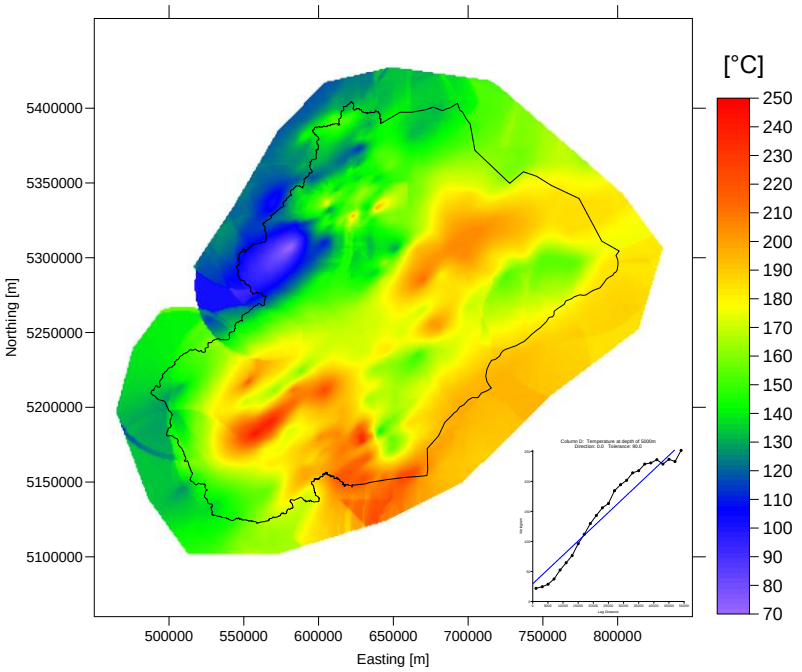

Figure 28: **Optimized temperature map at a depth of 5000m below surface (m.b.s.) applying a linear variogram model (optimization by auto fitting).**

In Table 14 the important settings for interpolation are specified.

Table 14: **Search options for temperature at 5000 m.b.s**

Search radius	50km
Number of search sectors	4
Maximum number of data in all sectors	64
Minimum number of data in all sector	1
Variogram model	Linear
Slope	0.003163

Anisotropy Ratio	2
Anisotropy Angle	40.3
Nugget Effect	29.5

For compilation of the temperature map at the top of pretertiary basement the same gridding method (*Kriging*) was applied (see Figure 29).

Since the experimental model for this temperature map didn't level out the linear model was used for interpolation purpose. The settings of the temperature interpolation are shown in Table 15.

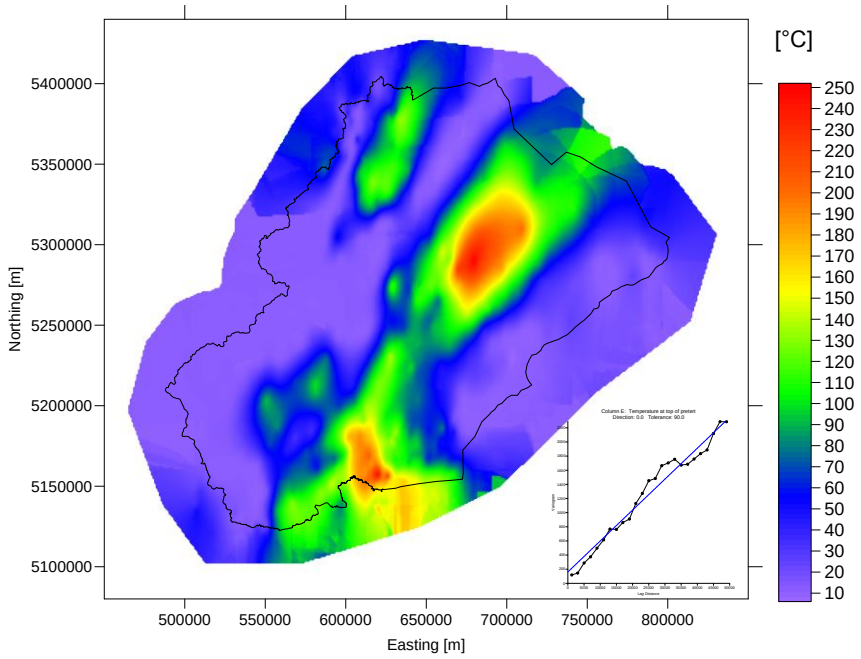

Figure 29: **Optimized temperature map at the surface of the pre-Tertiary basement applying a linear variogram model (optimization by auto fitting).**

Table 15: **Search options for temperature at top of pre-Tertiary basement**

Search radius	50km
Number of search sectors	4
Maximum number of data in all sectors	64
Minimum number of data in all sector	1
Variogram model	Linear
Slope	0.003163
Anisotropy Ratio	2
Anisotropy Angle	40.3
Nugget Effect	29.5

(b) *Depth Maps of different temperature levels*:

Depth maps of three different temperature levels, (50 °C, 100 °C and 150 °C) have been compiled for the whole supra-regional area. Since isothermal maps were only available for the Hungarian part, the depth information has to be interpolated from the previous generated temperature maps.

The finite element simulation software package FEFLOW™ was used for 3D temperature interpolation. Steady state finite element methods can be used for interpolation by applying dirichlet or first kind ("fixed temperature") boundary condition only and setting the material properties homogeneous and isotropic. Through that approach the heat equation is simplified and collapses to Laplace's equation $\Delta T = 0$. The solution of this equation is independent of any material parameter and represents a 3D interpolation based on the heat equation. This procedure was carried out for the whole supraregional area to assure consistence.

3.5.3 Interpolation methods for Heat-In-Place and Specific Identified Resources

The calculation of Specific Heat in Place and Specific Identified Resources was basing on the previously elaborated interpolated subsurface temperatures at depths of 1km, 2.5 and 5 km below surface (see chapter 3.5.2) as well as on interpolated petrophysical data. For the creation of potential maps the same interpolation routines as applied for the temperature maps (see chapter 3.5.2) have been applied.

3.6 Estimation of background heat flow densities (Lenkey L. & Raáb D.)

The following chapter treats the estimation of the background heat flow densities based on pure conductive 3D thermal modelling. Although the background HFD will not be displayed in terms of individual maps, the achieved results will help later to outline and classify existing thermal convection zones caused by circulating thermal water. Therefore the following chapter gives a detailed overview about the applied methodologies and workflows.

This chapter was compiled by Lenkey, L. and Raáb, D. on behalf of the Geological Institute of Hungary.

3.6.1 Introduction

We calculated the three-dimensional temperature distribution in the lithosphere under the area of the TE project assuming conductive heat transport using the finite element modelling software Comsol Multiphysics. We made a steady-state model and two transient models; one of them takes into account the stretching of the lithosphere during Middle Miocene, and the other additionally takes into account the thermal effect of the Neogene and Quaternary sedimentation.

We compared the modelled surface heat flow density and temperatures in 1 and 2.5 km depths with surface heat flow density map (Figure 25) and temperature maps (Figure 26and Figure 27) based on observations. We also compared the modelled temperatures with temperatures measured in wells. We assume that the best fit model describes the conductive temperature field in the lithosphere in the study area. In the best model we calculated the

heat flow density at the Mohorovicic discontinuity. It can be used as thermal boundary condition prescribed at the bottom in the thermal models of the pilot areas, in which groundwater flow and coupled heat transport will be modelled.

3.6.2 Description of the chosen modelling approach

(a) Physical settings

Assuming conduction the distribution of temperature in solid materials is governed by the following equation (e.g. Carslaw and Jaeger, 1959):

$$c\rho\frac{\partial T}{\partial t} = \frac{\partial}{\partial x}(\lambda\frac{\partial T}{\partial x}) + \frac{\partial}{\partial y}(\lambda\frac{\partial T}{\partial y}) + \frac{\partial}{\partial z}(\lambda\frac{\partial T}{\partial z}) + A \qquad \textbf{3-18}$$

Where T is temperature, c is specific heat, ρ is density, t is time, λ is thermal conduction, and A is volumetric heat production rate. c, ρ, λ and A can vary in space. If the temperature does not change with time the thermal field is called to be in a steady-state condition. In that case the left side of the equation is equal to zero.

We solved equation 3.18 applying the finite element method using Comsol Multiphysics™ in three dimensions. The average length of an edge of a tetrahedral element in the model was 2 km.

(b) Geometrical settings

The model was built in UTM33 coordinate system and it includes three layers with individual material properties (Figure 30). These layers constitute:

(i) sedimentary rocks,
(ii) crust,
(iii) lithospheric mantle

They are bordered and divided by the following horizons: (a) surface, (b) the depth of the pre-Tertiary basement, (c) the Mohorovicic discontinuity, and (d) the bottom of the lithosphere (see Figure 31). In case of the steady-state model the bottom of the lithosphere corresponds to the observed lithosphere shown in Figure 31d. In case of the transient models the bottom horizon of the lithosphere was set at a depth of 125km, except in those areas where the observed thickness is larger than 125km. In those areas the observed lithospheric thickness (see Figure 31d) was used. The reason therefore is the stretching model of the lithosphere (McKenzie, 1978), which was used to obtain the initial temperature distribution in the lithosphere of the transient models. These three layers were filled up with material properties.

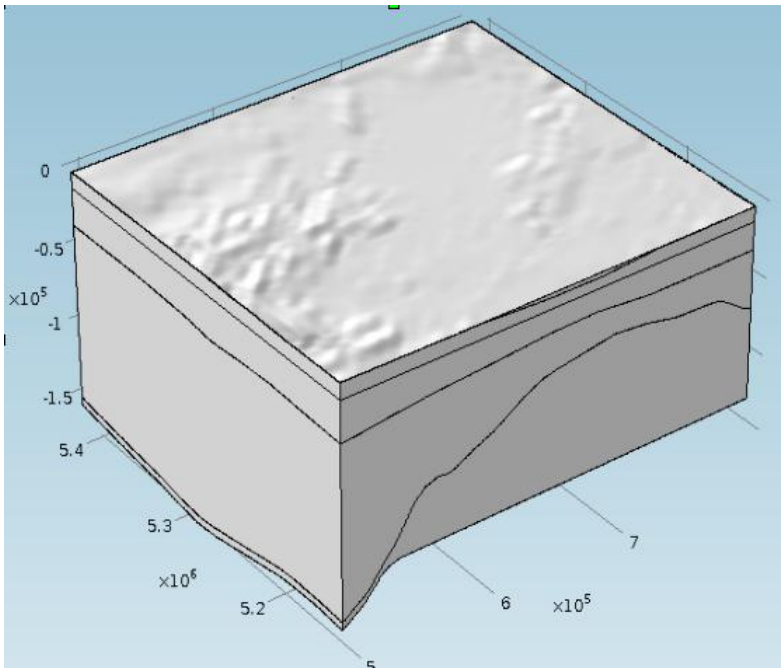

Figure 30: **Geometrical model applied for the estimation of the background heat flow density.**

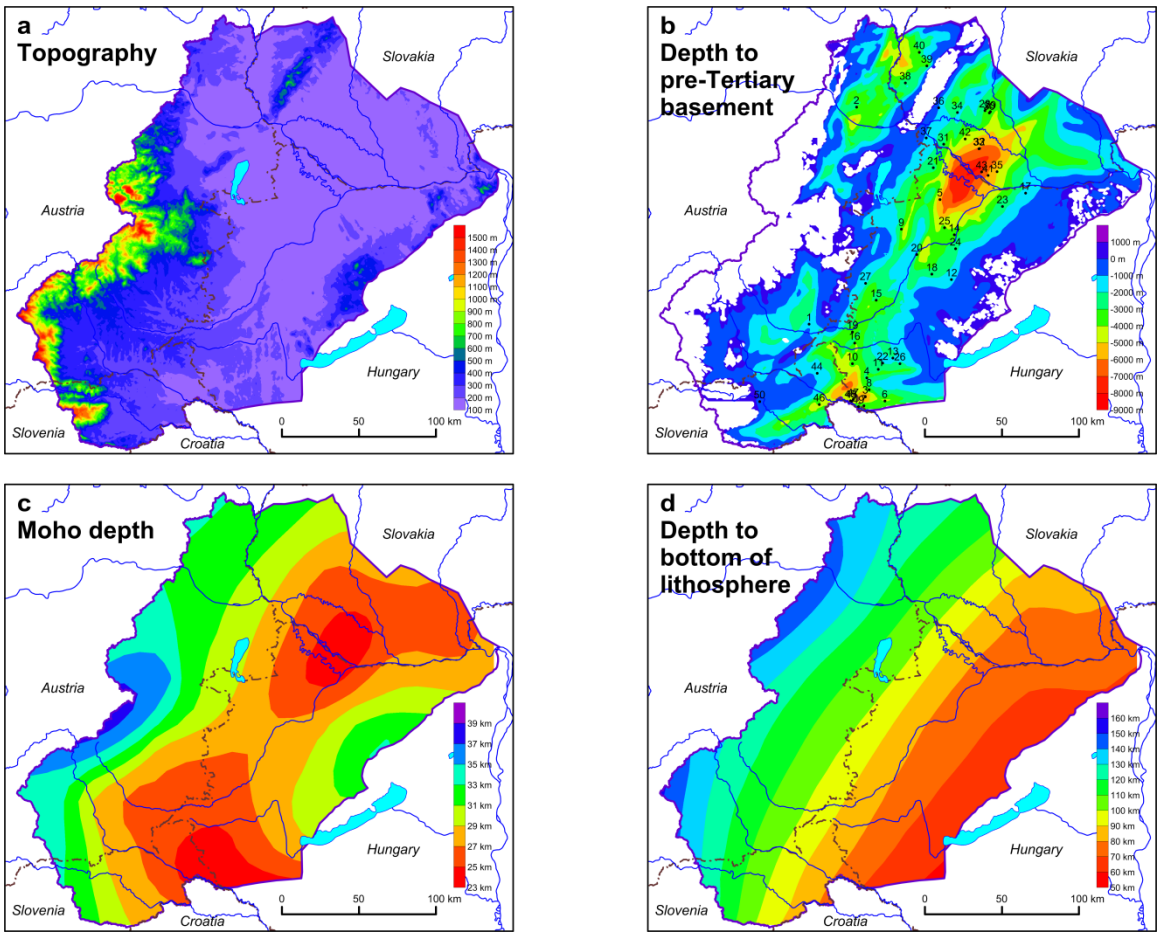

Figure 31: **The horizons which bound and separate the layers comprising the model.** a) Surface topography, b) Depth to the pre-Tertiary basement, c) Depth to the bottom of the crust (Lenkey, 1999), d) Depth to the bottom of the lithosphere (Lenkey, 1999).

(c) Thermal parameters of rocks

Considering equation 3.18 the most important material parameters are the thermal conductivity and heat production of rocks. Specific heat and density only play a role in transient models. We assumed that except for the sediments the crust is homogeneous. We made this assumption, because we do not know in detail the spatial extent of the different types of rocks in the crust, e.g. the thickness of Triassic carbonates in the Transdanubian Central Range (TCR) is known only in a few wells. On the other hand the difference between the thermal conductivities of crystalline, metamorphic rocks and limestones is less than the contrast in thermal conductivities of the sediments and their basement. Thus, in spite of the simplification of a homogeneous crust, the model takes into account the first order features in the thermal conductivities. Most of the temperature measurements and thus heat flow density estimates were carried out in the sedimentary basins. Therefore, the model results can be fitted in these areas and the model remains less constrained in the areas of the outcrop of the pre-Tertiary basement.

Thermal conductivity of crust and mantle were taken from Kappelmeyer and Haenel (1974) and Zoth and Haenel (1988) (see also Table 7). The thermal conductivity of sediments varies both horizontally and vertically, due to variations in their composition (e.g. shales, marls, sand, and sandstones) and compaction. In the model we used the same thermal conductivities of sediments, which were applied in the heat flow density estimates in the Transenergy project. In the Vienna and Styrian basins we assigned the values given in Table 7. As the material parameters are given for different age horizons, we had to further subdivide the Neogene sediments. We estimated the thickness of the sediments with different ages using stratigraphic sections by Kovač et al. (2004) for the Vienna Basin and by Goldbrunner (2000) for the Styrian basin. In the rest of the study area we chose wells, in which we knew, or we calculated the thermal conductivity of sediments.

In Hungary the thermal conductivity of sediments was taken from the Geothermal Database of Hungary (Dövényi, 1994).

In the Slovakian wells we calculated the thermal conductivity in the following way. In the “Atlas of the geothermal energy of Slovakia” (Franko et al., 1995) temperatures in wells are presented for 500m intervals, and the heat flow density is also given for the same wells. We calculated the temperature gradients for 500m intervals. By assuming a constant heat flow density we determined the thermal conductivities from the Fourier equation.

Finally, we chose those Slovenian wells, in which thermal conductivity of sediments were published (Ravnik, 1991, Ravnik et al., 1995).

In the 3D model the thermal conductivity of each element must be prescribed. The thermal conductivity of the sediments in a given place was calculated by horizontal and vertical extrapolation using the values in the wells or the values given in 3D grids in the Vienna and Styrian basins. The extrapolation was done by the modelling software Comsol Multiphysics™.

The volumetric heat production rate in the crust and sediments was set to 1μW/m^3. This value in the sediments is supported by measurements (Table 7). However, in the crust the radiogenic heat production rate is somehow arbitrary. Granites show higher (2-3μW/m^3, Rybach and Cermak, 1982) and lower crustal granulites lower (0.2-0.5μW/m^3, Rybach and Buntebarth, 1984) heat production rates. In general, it was assumed that heat production decreases with depth. Due to limited information about the crustal structure in the study area we chose an average crustal heat production rate. We checked our choice of thermal parameters by calculating the steady-state geotherms in the continental lithosphere by applying equation 3.18.

In case of an average continental crustal thickness of 35km, and a lithospheric thickness of 125km with an assumed temperature of 1300°C at its bottom, and 10°C at the surface of the model, 1μW/m^3 heat production rate together with the crustal and mantle thermal conductivities (Table 7) result in surface heat flow density of 63mW/m^2, which is close to the average continental value of 57mW/m^2 (Sclater et al., 1980). Therefore, we accepted the heat production rate in the crust and the thermal conductivities of the crust and mantle. The steady-state geotherm calculated with the above conditions and parameters are presented in Figure 32.

The rock density of crust and mantle material corresponds to the average values (Parsons and Sclater, 1977). We calculated the specific heat of rocks from the definition of the thermal diffusivity (κ): $\kappa = \lambda / c\rho$. Thermal diffusivity was kept constant in the whole lithosphere (8.23 x 10^{-7} m^2/s, after Royden and Keen, 1980), so the specific heat was determined from the given density and thermal conductivity of rocks.

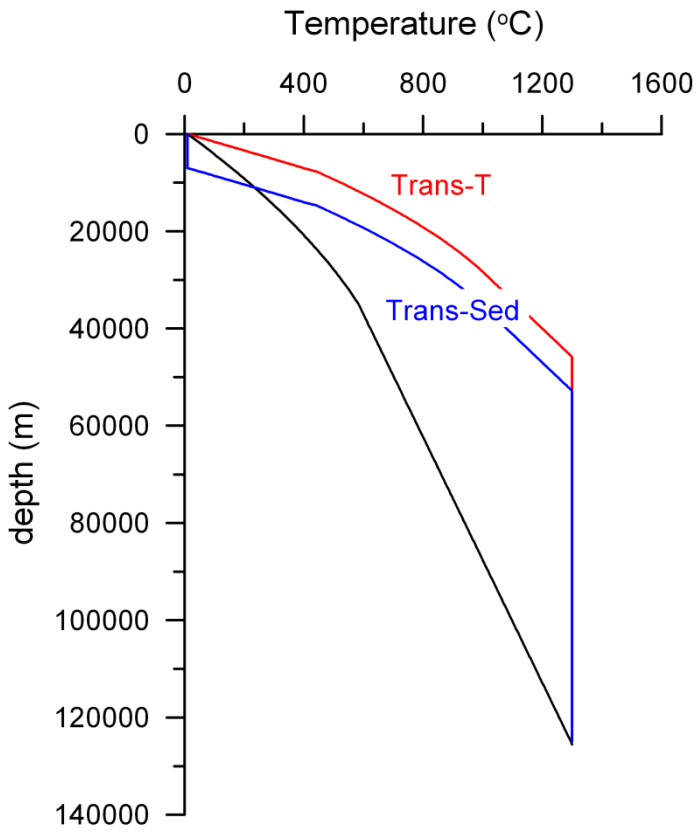

Figure 32: **Geotherms in the lithosphere.** Black line: steady state temperature, which exists in a 125 km thick lithosphere, with35 km thick crust. Values of the thermal parameters are shown in Table 8.

Red line: initial geotherm (t=0 time) calculated from the steady state geotherm by stretching the lithosphere (Trans-T model). Blue line: initial geotherm (t=0 time) calculated from the initial geotherm of the Trans-T model by placing 7 km thick sedimentary pile with temperature of 10 °C on the top of the crust (Trans-Sed model).

(d) Initial and boundary conditions

For simplicity reasons the surface temperature was kept constant at 10°C. In case of steady-state model the temperature at the bottom of the lithosphere was also constant 1300°C. In case of transient models the above conditions were applied at locations, where the depth of the bottom of the lithosphere is larger than 125km. Where the lithosphere is thinner than 125km, there 1300°C was prescribed at 125km depth (see geometry of the model, chapter 3.6.2 b). The vertical boundary planes of the model were insulating.

In case of transient heat transport processes the solution of equation 3.18 also depends on the initial temperature distribution. The most important geological processes resulting in transient thermal field are a) the change of the surface temperature due to palaeo-climatic temperature variations, b) volcanism, c) tectonic events, d) sedimentation and erosion.

a) The Pannonian Basin palaeo-climatic effects mainly influence the subsurface temperature at depths above 500m below surface (Demetrescu et al., 2001). In most cases we compared temperatures measured deeper than 1km with the calculated model temperatures, therefore we neglected the palaeo-climatic effects.
b) The effusive material from volcanic activity does not have effect on the subsurface temperature. It is mostly the magma chamber, which warms up the host rock. Several model calculations showed that a normal size magma chamber cooled down in less than 1 Ma year in the absence of additional magma supply (Raáb, 2011). As volcanic activity in the Styrian basin and the Little Hungarian Plain decayed more than 1 Ma (Pécskay et al., 1995). Therefore we did not take volcanism into account for the transient conductive models.
c) The strongest effect on the subsurface temperature derives from tectonic events. The Pannonian basin was formed during the Early-Middle Miocene by lithospheric stretching as it is evidenced by the thin lithosphere and crust, normal faults bounding the sediment filled depressions, and high heat flow density (Royden et al., 1983a, Royden and Horváth, 1988). It was shown by numerous studies that the observed subsidence rate of the basement and the heat flow density in the Pannonian basin can be reproduced applying Royden and Keen's (1980) non-uniform lithospheric stretching model (Royden et al., 1983b, Royden and Dövényi, 1988, Lankreijer et al., 1995, Sachsenhofer et al., 1997, Lenkey, 1999).

   According to the stretching model instantaneous stretching of the lithosphere leads to high initial geothermal gradient, and thus high initial heat flow density (Figure 32). Following stretching the high temperature in the lithosphere slowly decreases and the original HFD is approached after a time period of about 100 Ma (McKenzie, 1978). We modelled the transient thermal effect of stretching using the crustal and mantle stretching factors derived by Lenkey (1999). We compressed the steady-state geo-

therm in the lithosphere according to the stretching factors, and thus we received the initial temperature-depth function (Figure 32). We repeated the above process in a grid with 5km spacing. In those places, where stretching did not occur we kept the steady-state geotherm calculated with the geometries given in Figure 31.

We assumed that the stretching of the lithosphere was instantaneous, and it have occurred 17.5 Ma ago. This moment was the starting time of the transient calculations.

The stretching factors were calibrated to reproduce the present day basement depth and sedimentation corrected heat flow density smoothed by a low pass filter with 100 km cut-off wavelength (Lenkey, 1999). We wanted to obtain the same cooling rate of the initial thermal anomaly in the lithosphere in our model than in the stretching model, therefore we applied the same thermal diffusivity ($\kappa=8.23*10^{-7}m^2/s$, see in the above section) as Lenkey (1999) after Royden and Keen (1980).

The stretching model and the obtained results are referd in the following as Trans-T.

d) Sedimentation reduces the subsurface temperature as the newly deposited sediments have “cold” surface temperature and it therefore takes time until the sediments are heated up (e.g. Lucazeau and Le Douaran, 1985). Erosion has the opposite effect on the temperature. In the model area sediments were accumulated over several kilometres thickness in the basin areas during the Neogene and Quaternary, and erosion in the peripheral areas has been active since Late Miocene-Pliocene times. According to Lenkey (1999) mainly sedimentation affected the temperature field and the heat flow density regime. We applied a simple model in calculating the thermal effect of sedimentation. We assumed that all sediments had been deposited before the start of the calculation, and they had initial temperature of 10°C (Figure 32). Below the sediments the temperature-depth function was obtained by shifting downward the initial geotherm of the stretched lithosphere with the thickness of sediments.
The model which takes into account the sedimentation and the stretching is referres in the following as Trans-Sed.

4 Results

4.1 Surface Heat Flow Density Map

The Surface Heat flow Density (SHFD) represents the overall heat flow density including conductive as well as advective heat transport at the uppermost part of the subsurface. It was calculated from observed borehole temperatures for individual wells. The SHFD is directly correlating with the geothermal conditions. That means an elevated SHFD is accompanied by a high geothermal gradient. Therefore the elaborated map, which can also be found at **Enclosure 1,** allows differing between regions with favourable and less favourable geothermal conditions. However, it does not directly outline or estimate existing hydrogeothermal reservoirs or plays. For that reason a SHFD can be seen as the first step towards the

evaluation of the geothermal resources in a specific region. Nevertheless, the following options for further calculations and interpretation can be gained from the elaborated map:

- Geothermal boundary conditions for local to regional scale geothermal models at the pilot areas.
- Evaluation of the entire amount of heat flowing into the project area for thermal balancing.
- Identification of areas affected by the circulation of subsurface waters.

The elaborated map is based on around 1200 input data in the range of <5 to >185mW/m² (see also Figure 33). The average calculated SHFD at the Transenergy project area is represented by 77.69±21.50mW/m², which is above the continental average. The distribution of calculated SHFD values shows a clear maximum at the class of 65 to 70mW/m², which is accompanied by an asymmetric slope with a slighter decrease towards values of enhanced SHFD.

A 3 – colour scheme was applied to the SHFD map showing a colour range from dark blue (low values) to white (average) and dark red (high) values in order to easily outline areas of favourable and less favourable geothermal conditions (Figure 34). The pattern of the interpolated SHFD map show clear enhanced conditions at the south-western part of the project area covering parts of the Styrian- and Mura – Zala Basin. In opposite to this lowered geothermal conditions can be found at the margin of Eastern Alps (north-western part of the project area) and the Transdanubian Range (eastern part of the project area). At both regions crustal thickening in combination with massive inflow of cold meteoric water can be seen as major reason for the lowered geothermal conditions.

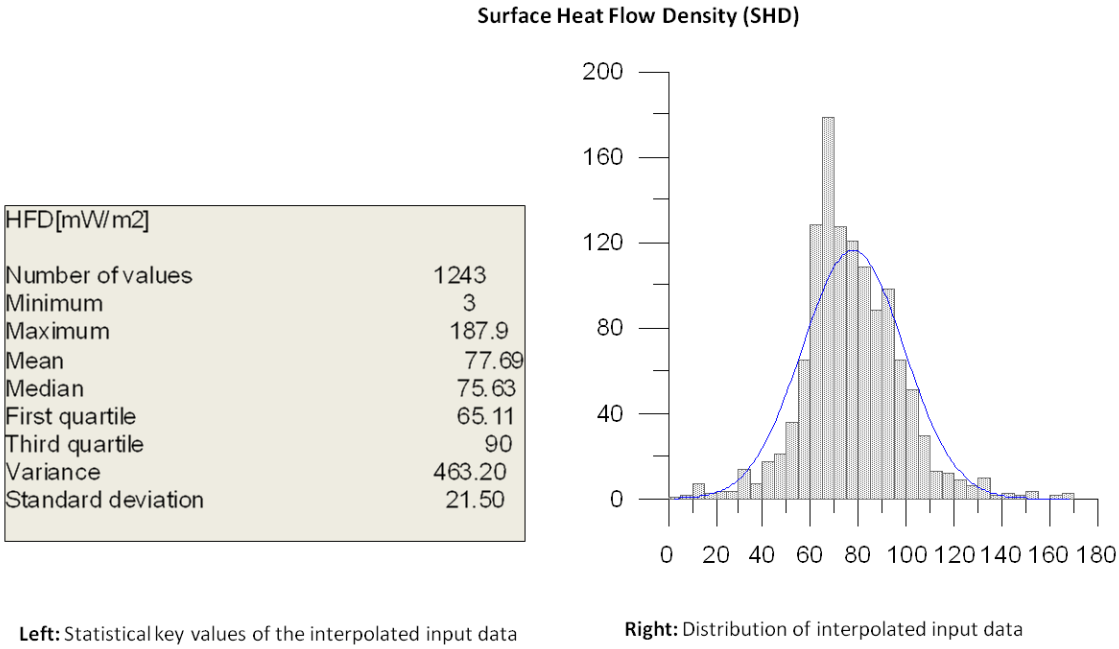

Left: Statistical key values of the interpolated input data

Right: Distribution of interpolated input data

Figure 33: Statistical overview on the applied input data in order to elaborate the SHFD map.

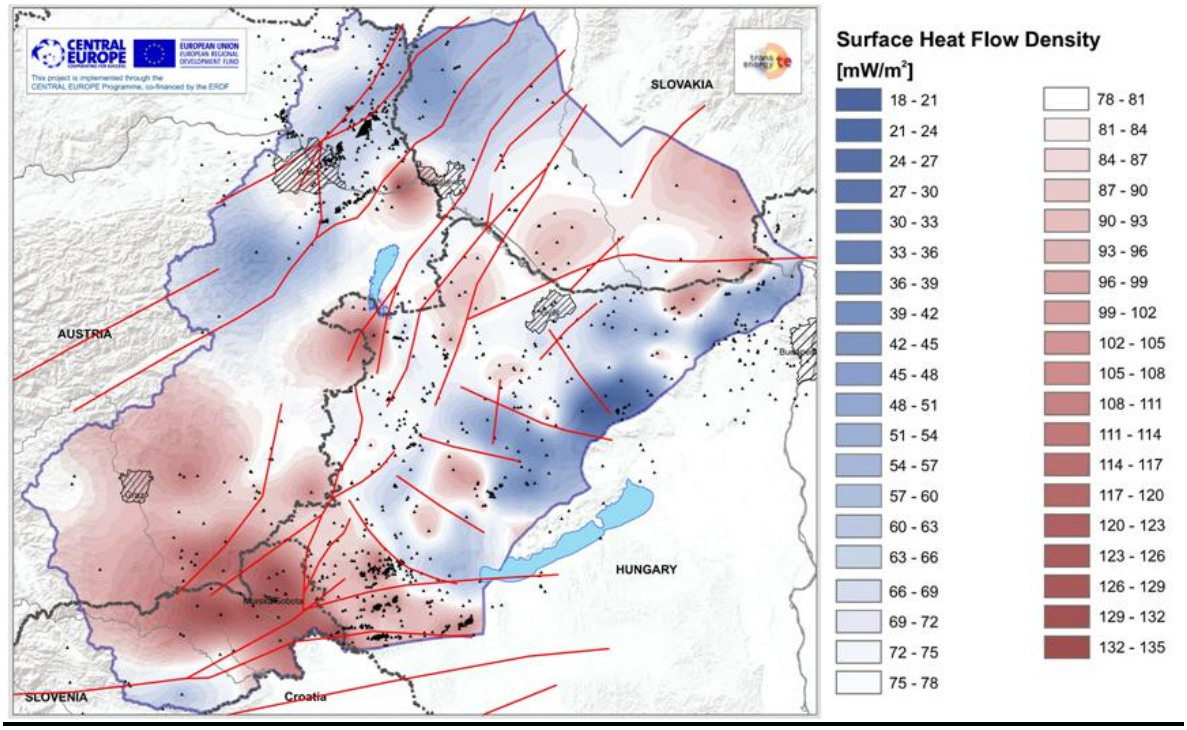

Figure 34: Surface Heat Flow Density map of the entire project area

Several local to regional scale geothermal anomalies are superimposed to the regional – supra-regional scale pattern of the SHFD values. Most of these low scale anomalies are caused by the circulation of subsurface water. Despite of the influence of circulating subsurface waters, a regional scale attenuation of the geothermal conditions in the central and northern parts of the Vienna Basin (north-western part of the project area) is assumed to be linked to non-steady-state conditions due to fast sedimentation in the Vienna Basin in combination with enhanced crustal thickness.

4.2 Temperature Map series

The temperature map series shows the distribution of subsurface temperatures at depth levels of 1000, 2500 and 5000m below surface in order to give an overview on the expectable rock temperatures in certain regions. They have been compiled from individually interpolated and extrapolated borehole temperatures. A statistical overview of the interpolated input data can be found in Figure 35, while the maps themselves are shown in Figure 36 and Figure 37.

Furthermore the expected temperature at the top of the pre-Tertiary basement have been interpolated from the temperature map series in order to give an overview about the expectable maximum subsurface temperatures at the Tertiary basin fillings, which constitute a relevant hydrogeothermal reservoir at many regions within the project area (e.g. western Pannonian Basin).

The entire temperature map series can also be found in **Enclosures 2a – 2d**.

At a depth of 1000m below surface (m.b.s) the observed average rock temperature corresponds to 49.4±9.4°C. Significant positive temperature anomalies are linked to local to regional scale ascent and discharge areas of hot subsurface waters, as for example to be observed in a significant anomaly at Héviz westwards of lake Balaton. In opposite to this cool areas predominately correspond to the descent and infiltration paths of cold meteoric waters. Such patterns indicate the estimated boundaries of confined hydrodynamic flow systems including recharge and discharge areas. It can be summarized, that the patterns of the subsurface temperatures at depths up to 1000 meters below surface are more likely to correspond to surface near hydrodynamic systems than to large scale crustal structures.

The distribution of temperature at a depth of 2500 m.b.s shows an average value of 100.8±13.1°C. The comparison with the mean value at a depth of 1000 m.b.s. results in an average geothermal gradient for the project area of 3.4°C/100m, which is again slightly above the global average. The pattern of the subsurface temperatures at this depth are already influenced by large scale crustal structures, as enhanced conditions with temperature levels of above 130°C can be observed at parts of the Styrian and Mura – Zala Basin (see also chapter 4.1).

Temperature at a depth of 1000 meters below surface (m.b.s)

Temperature at 1000 m.b.s	
Number of values	6220
Minimum	12.6
Maximum	122.8
Mean	49.4
Median	50
First quartile	45
Third quartile	55
Variance	88
Standard deviation	9.4

Left: Statistical key values of the interpolated input data

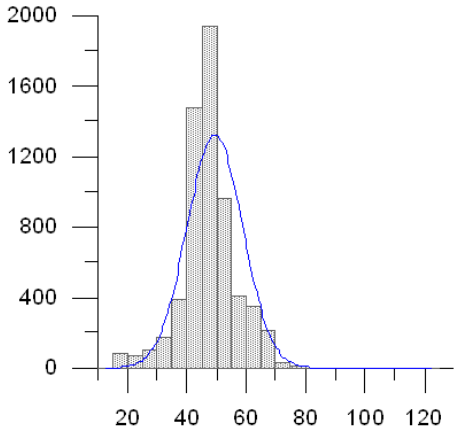

Right: Distribution of interpolated input data

Temperature at a depth of 2500 meters below surface (m.b.s)

Temperature at 2500 m.b.s	
Number of values	6523
Minimum	20.5
Maximum	289.5
Mean	100.8
Median	100
First quartile	95
Third quartile	110
Variance	171.3
Standard deviation	13.1

Left: Statistical key values of the interpolated input data

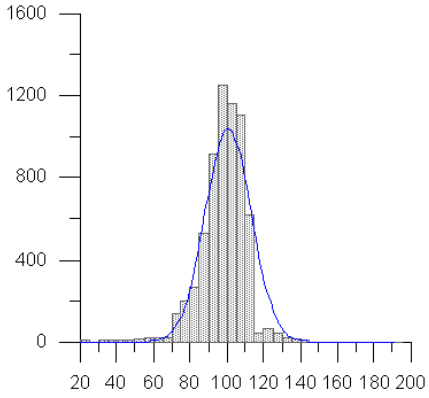

Right: Distribution of interpolated input data

Temperature at a depth of 5000 meters below surface (m.b.s)

Temperature at 5000 m.b.s.	
Number of values	6294
Minimum	57.90
Maximum	321.80
Mean	178.90
Median	180
First quartile	170
Third quartile	190
Variance	340.70
Standard deviation	18.50

Left: Statistical key values of the interpolated input data

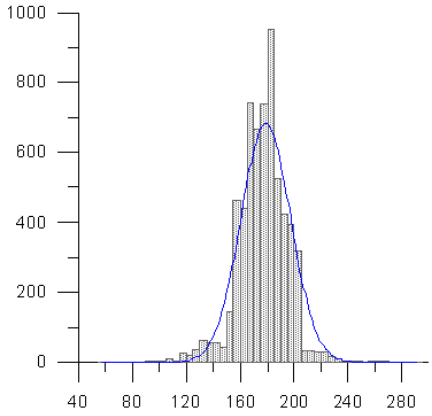

Right: Distribution of interpolated input data

Figure 35: **Statistical overview on the input data applied on the elaboration of the map series showing the temperature distribution at a depth of 1000, 2500 and 5000m below surface**

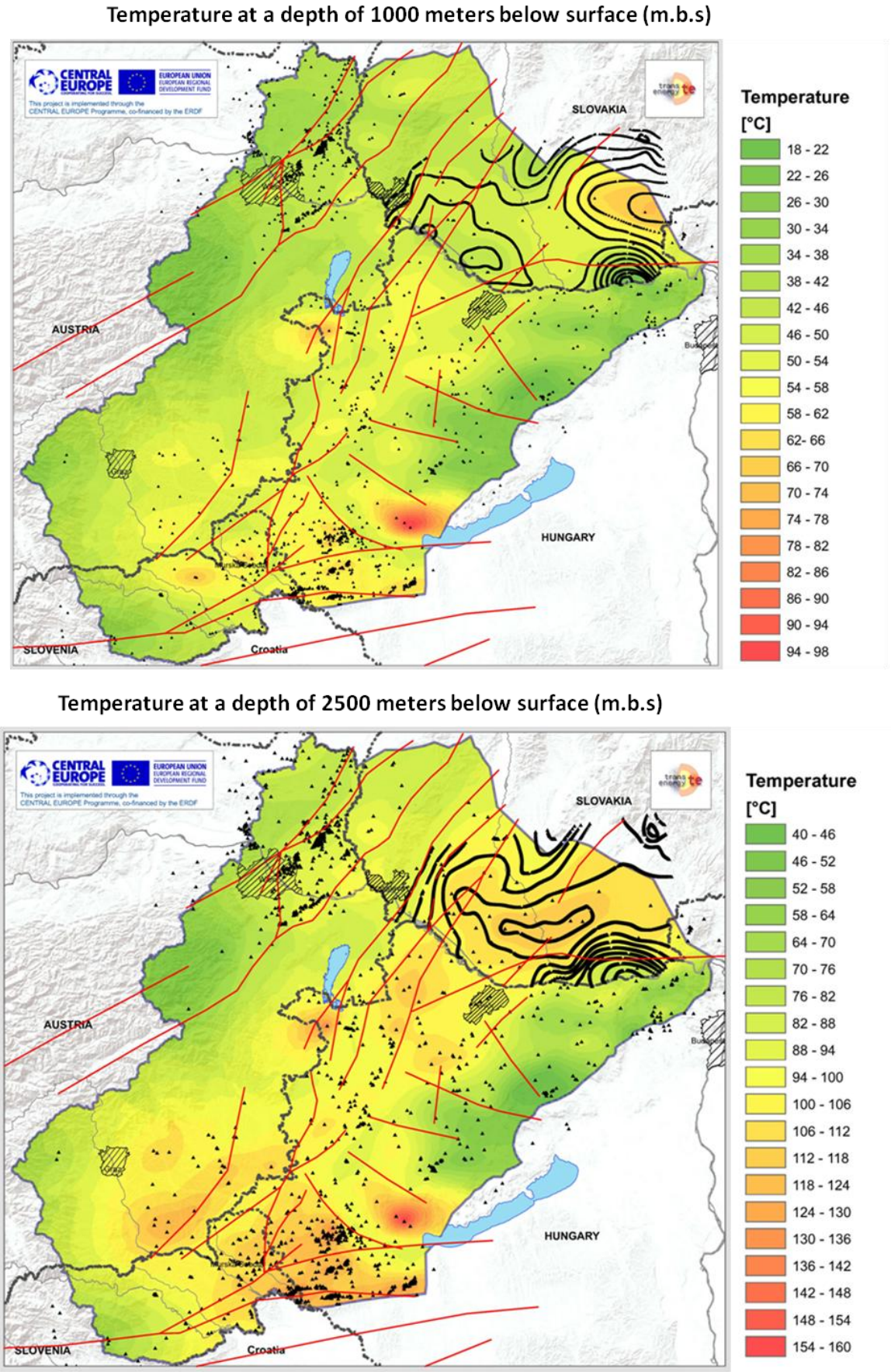

Figure 36: **Distribution of subsurface temperatures at depth levels of 1000m and 2500m below surface.**

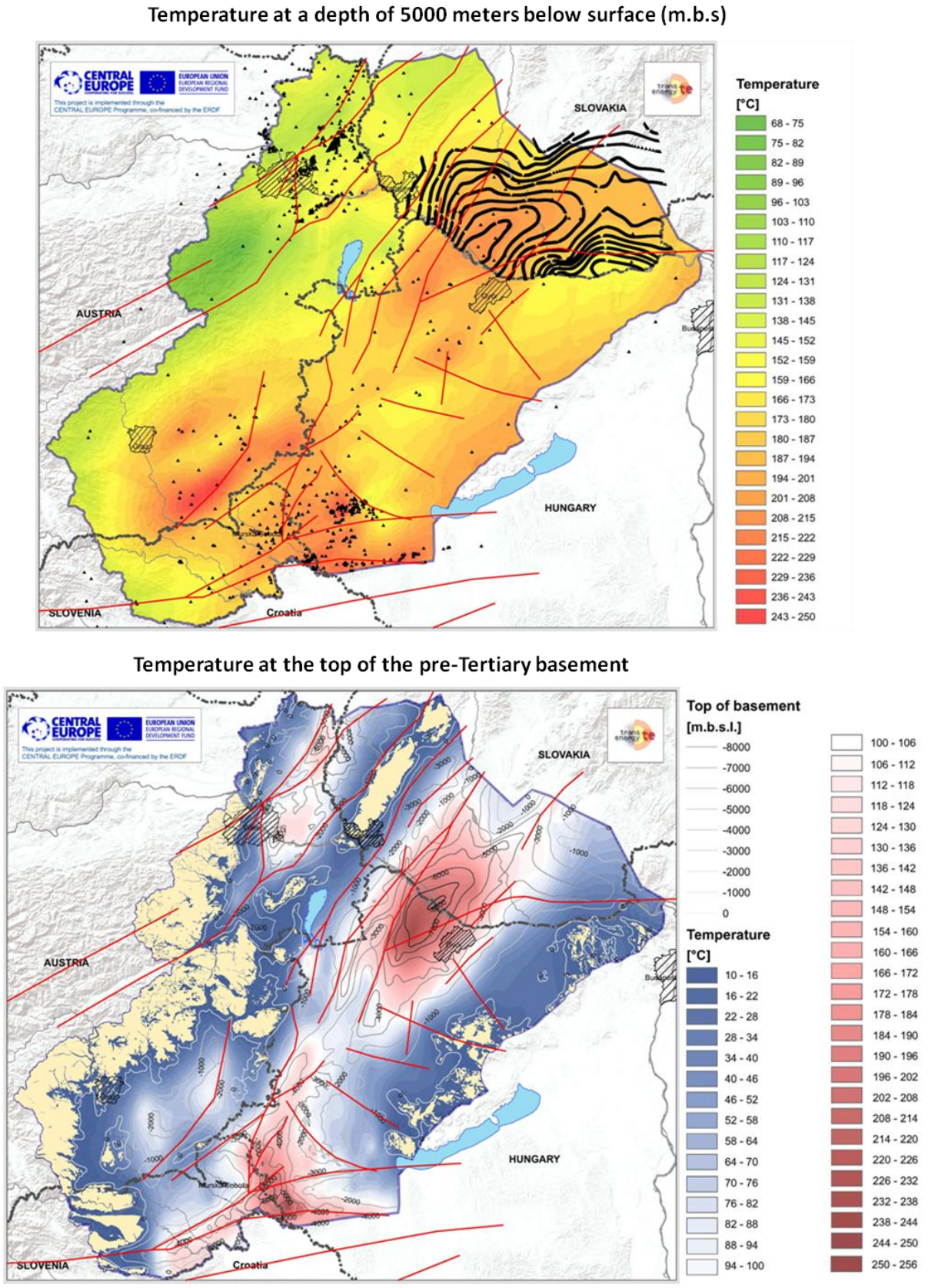

Figure 37: Distribution of temperature at a depth of 5000m below surface and at the top of the pre-Tertiary basement.

At a depth level of 5000m below surface the mean interpolated or extrapolated formation temperature is corresponding to 178.9±18.5°C, which in turn leads to an average geothermal

gradient of 3.12°C/100m between the depth intervals of 2500 and 5000m. Except for the margin of the Eastern Alps in the western and northwestern part of the project area, the interpolated temperature maps now strongly correlates with large scale crustal structures. At the margin of the Eastern Alps there are deeply infiltrating fresh water circulation systems known, which still lead to an attenuation of the subsurface temperature regime. However, it has to be kept in mind, that at the depth level of 5000m below surface most apllied data are gained from extrapolation and therefore probably afflicted with a significant range of uncertainity.

The temperature map of the pre-Tertiary surface (see Figure 37) was compiled from individually prepared borehole related input data. The map itself is combined with outcropping areas of the pre-Tertiary basement rocks and depth contours of the basement within the basins in order to enable an easy interpretation of the map. Once again a 3 – color scheme was applied, where dark blue to white colors reflect subsurface temperatures below 100°C and white to dark red colors in turn outline areas above 100°C. The 100°C isotherm was chosen with repsect to the generation of electric power by applying geothermal methods. The resulting patterns of course strongly reflect the depth of the pre-Tertiary basement. Regions with expected maximum temperatures at the basin filling above 100°C are only to be expected at (i) the central and northern part of the Vienna Basin, (ii) the eastern Styrian Basin, (iii) parts of the Mura – Zala Basin and (iv) the Danube Basin. The latter region is supposed to serve the highest temperatures within the basin fillings in the project area with expected maximum temperatures of more than 220°C eastwards of the city of Györ.

4.3 Contour map series of specific isotherms

Based on the previously elaborated temperature maps, depth contour of the (i) 50°C, (ii) 100°C and (iii) 150°C isotherm have been calculated by using FEFLOW™. This map series intend to give an overview about the minimum depths of reservoir in order to guarantee a certain reservoir temperature for energetic geothermal utilization. The isotherm of 50°C (i) was assumed to be a critical value for low temperature applications (e.g. balneological use combined with green house or facility heating). The 100°C isotherm (ii) is seen as a critical value for electric power generation based on binary circle technology (e.g. ORC process), as well as the 150°C isotherm (iii), which constitutes the boundary to direct electric power generation based on steam turbines. All maps are shown in the subsequent Figure 38 to Figure 40 and can also be found in **Enclosure 3a to 3c**.

The depth of the 50°C isotherm (Figure 38) between 600 meters at discharge areas of hot thermal waters (e.g. Heviz, Oberlaa – Vienna) and 2700 meters at the infiltration zones of fresh surface waters (Eastern Alps, Bakony Mountains). It has to be pointed out, that this variation of depths coincides with range of investments for drilling of more than €1.5 Mio. In general the depth of the 50°C isotherm is situated around 1000 to 1200m.

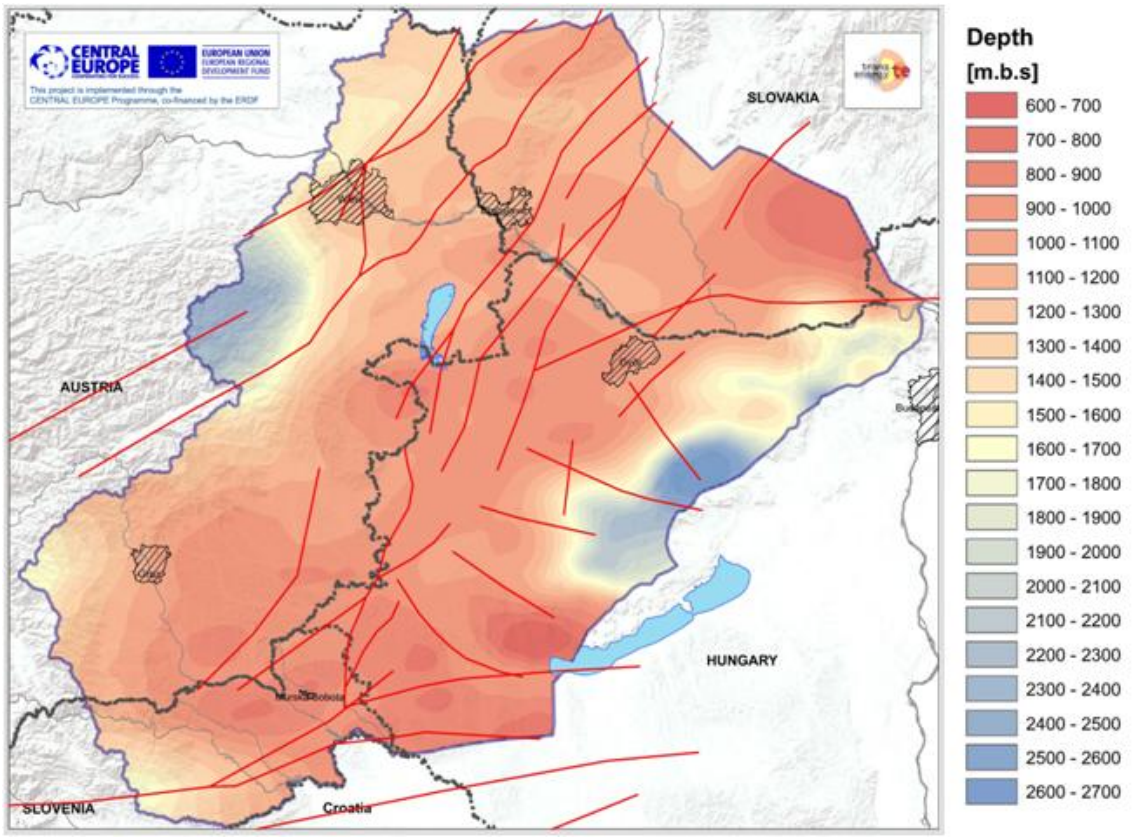

Figure 38: **Depth contour map of the 50°C isotherm.**

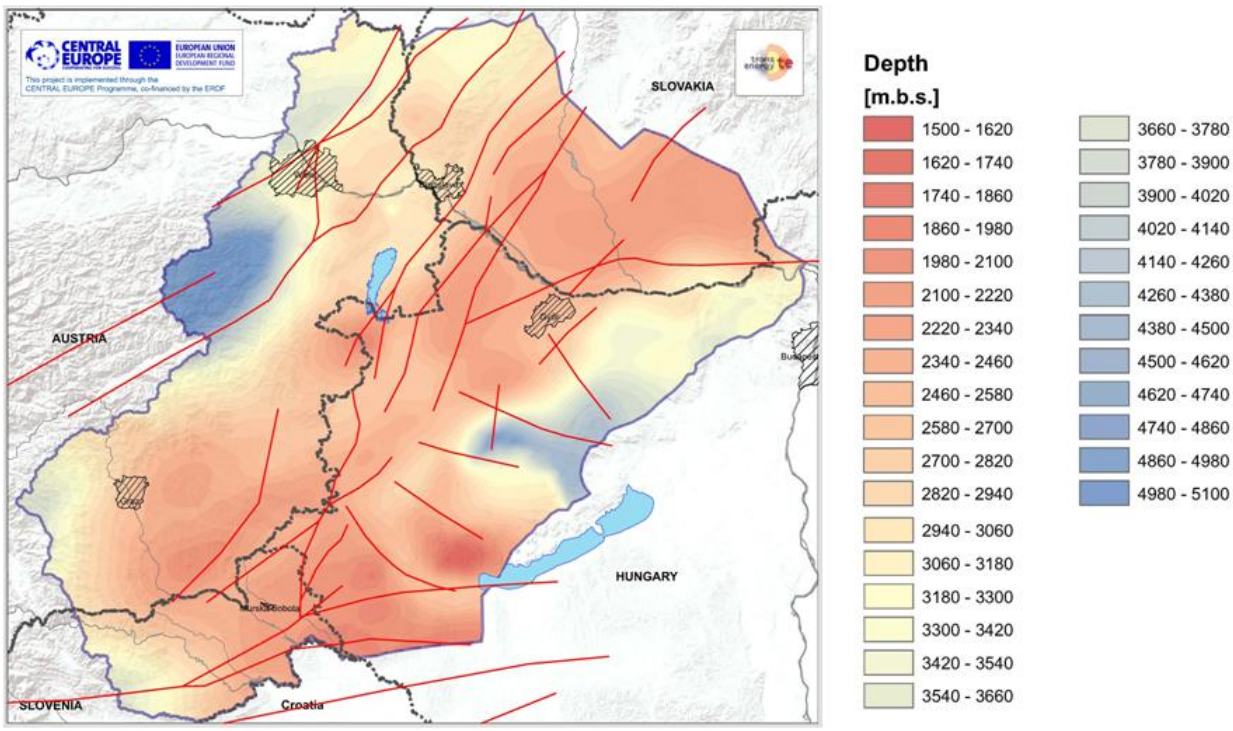

Figure 39: **Depth contour map of the 100°C isotherm.**

The depth of the 100°C isotherm varies between the range of 1500m below surface (Lake Heviz and other parts of the Zala Basin) and 5100m (deep infiltration zones at Eastern Alps and Bakony Mountains). The mean utilization depths are expected at around 2250 to 2500m below surface. The pattern of the calculated depth contours is still quite similar to the ones of the 50°C isotherm. They clearly point out deep circulating infiltration zones of hydrodynamic systems.

In opposite to this, the pattern of the 150°C isotherm is more corresponding to crustal structures, showing favourable utilization depths at southwest – northeast heading zone covering the eastern Styrian-, the entire Mura Zala Basin as well as the central and north-eastern parts of the Danube Basin. Referring to the interpolated contours minimum reservoir depths in order to reach rock temperatures of 150°C exist around 2700 to 2800m, while the average depths are to be expected around 4000 to 4200m below surface.

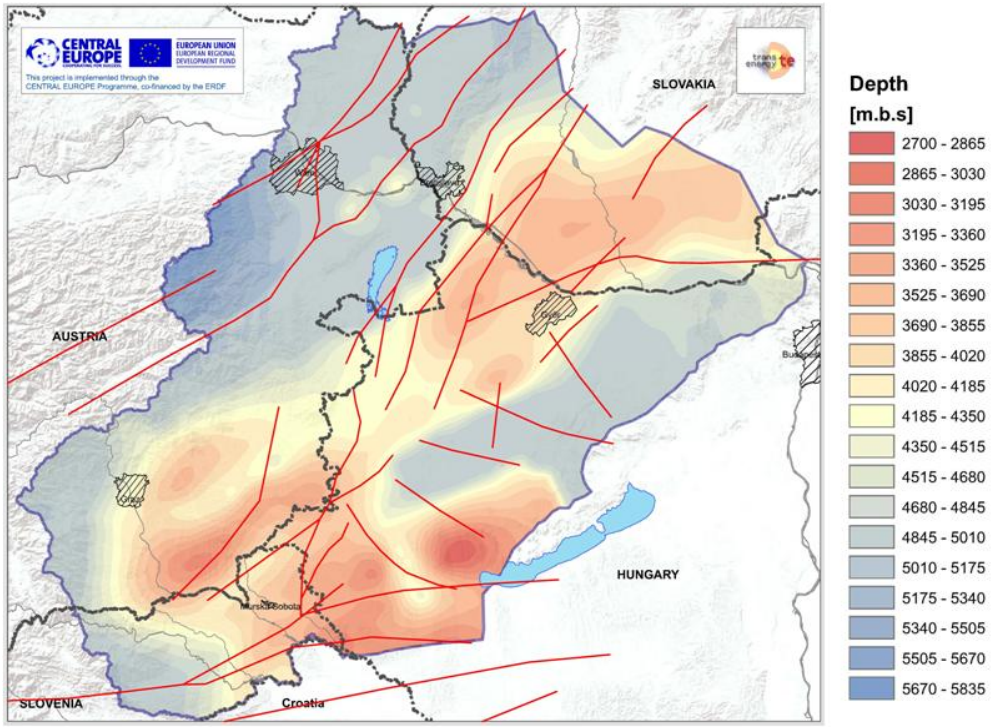

Figure 40: Depth contour map of the 150°C isotherm.

4.4 Geothermal Potential Map series

The geothermal potential map series contains the parameter “Specific Heat in Place” and “Specific Identified Resources”. Although the latter parameter contains the term “resources”, both parameters have to be understood as theoretical potentials limiting the theoretically available heat content in the subsurface for geothermal utilization, as they are more or less neglecting existing geothermal plays. Nevertheless, they are able to provide crucial information about favourable and non-favourable regions with respect to the geothermal regime of the subsurface.

The following maps were generated:

- Specific Heat in Place for Neogene sediments
- Specific Heat in Place for 50m upper part of the pre-Tertiary basement
- Specific Heat in Place from surface until 5000 m.b.s
- Specific Heat in Place from surface until 7000 m.b.s
- Specific Identified Resources for Neogene sediments
- Specific Identified Resources for 50m upper part of the pre-Tertiary basement
- Specific Identified Resources from surface until 5000 m.b.s
- Specific Identified Resources from surface until 7000 m.b.s

All elaborated maps are presented in the subsequent figures from Figure 41 to Figure 43 and can also be found at **Enclosure 4a to 4h**.

The Specific Heat in Place at the sedimentary basin fillings is strongly corresponding to areas of great depths of the basement, which are in turn offering high subsurface temperatures. The highest values at a level of up to 2400GJ/m² can be found at the central part of the Danube Basin westwards of the city of Györ, as in this region the sedimentary basin fillings reach maximum thicknesses of more than 7000 meters. Another hot spot can be found at the trans-boundary region between Hungary and Slovenia within the Mura – Zala Basin. At other relevant basin regions, such as the central Vienna Basin or the Styrian Basin the calculated Specific Heat in Place reaches only half of the level of the previous mentioned regions.

The Specific Heat in Place at the uppermost 50m of the pre-Tertiary basement can be understood as the theoretical potential of petrothermal utilization as potential hydrogeothermal plays are neglected in this assessment. In this context stored subsurface heat may be extracted by fracturing and artificial circulation of fresh surface water using geothermal doublet or multiple techniques. Due to the reduced thickness of the investigated rock column (50 meters versus up to several kilometers at the sedimentary basin fillings) the calculated Specific Heat in Place reaches levels of only 2% of the heat stored in the sedimentary basin fillings. Nevertheless, the pattern of the calculated Specific Heat in Place strongly follows the pattern observed at the sedimentary fillings, showing strong positive anomalies near the city of Györ and the trans-boundary region of Hungary and Slovenia. .

Specific Heat in Place (H_0) at sedimentary basin fillings

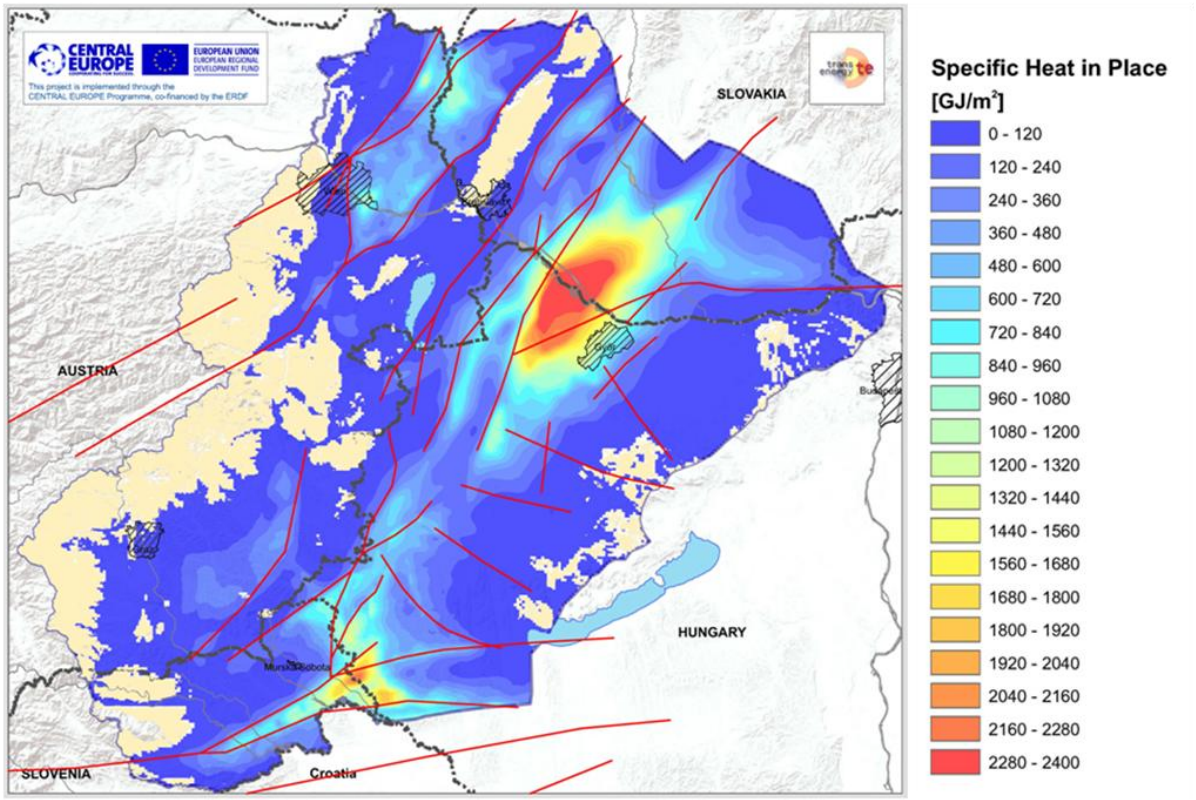

Specific Heat in Place (H_0) at the uppermost 50 meters of the pre-Tertiary basement

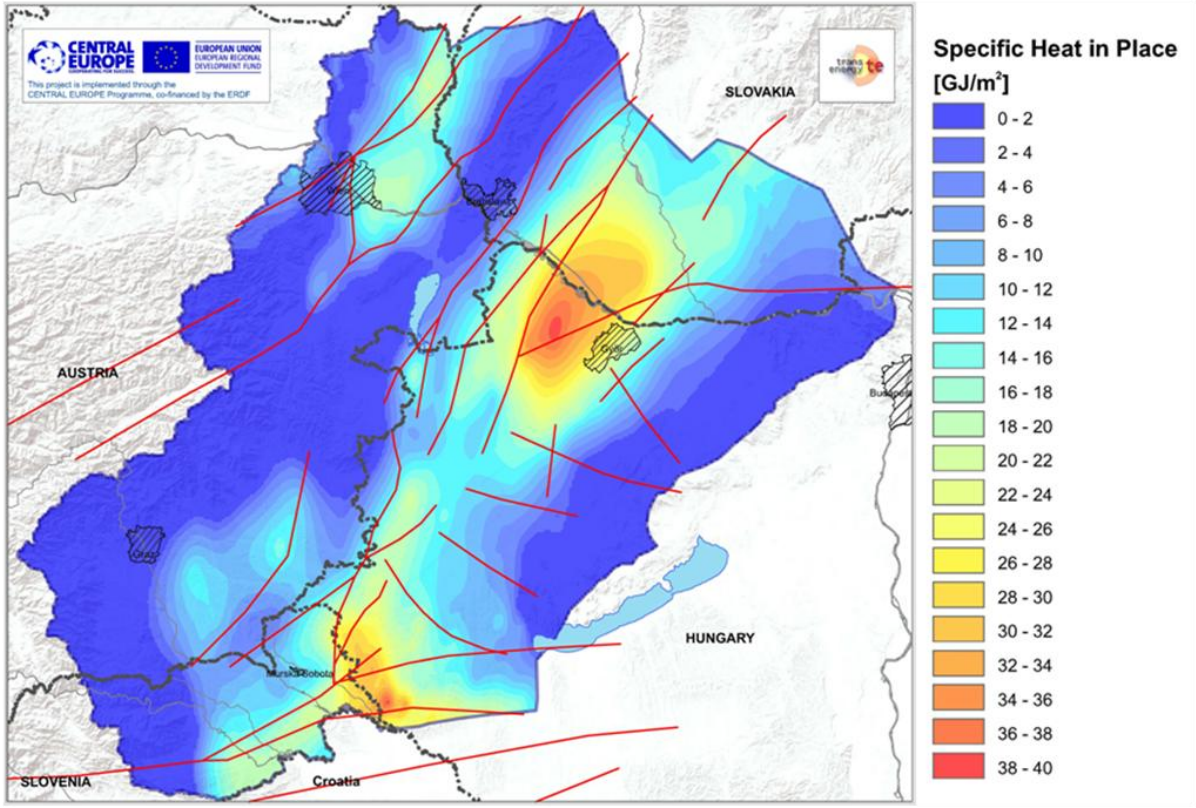

Figure 41: **Specific Heat in Place in sedimentary basin fillings (above) and the uppermost 50m of the pre-Tertiary basement (below).**

Specific Heat in Place (H_0) at uppermost 5km of the Earth's Crust

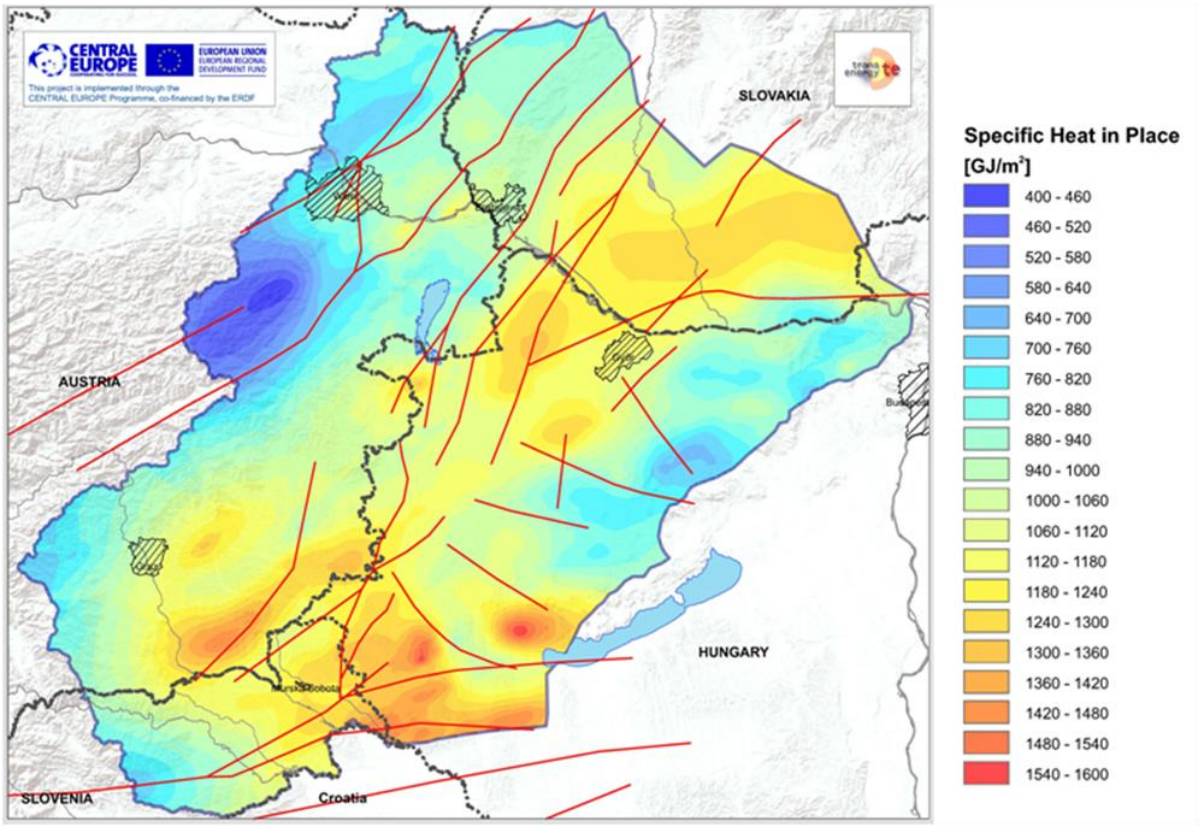

Specific Heat in Place (H_0) at uppermost 7km of the Earth's Crust

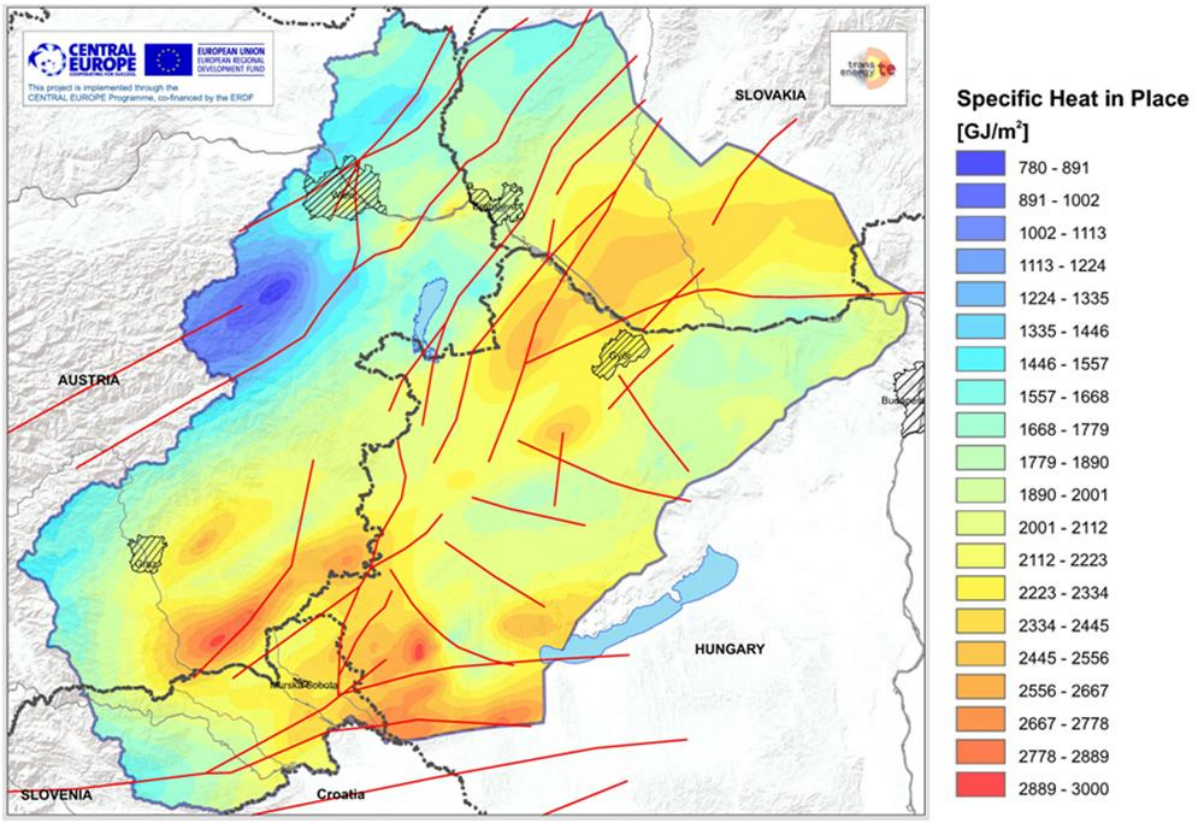

Figure 42: **Specific Heat in Place in uppermost 5km (above) and the uppermost 7km of the Earth's Crust (below).**

Both results, the Specific Heat in Place of the uppermost 5km and 7km of the Earth's Crust show similar patterns, which are strongly governed by the temperature regime of the subsurface and to a minor extend to the geological build-up of the investigated rock column. The calculated Specific Heat in Place values vary between the range of 400GJ/m² to 1600GJ/m² for the uppermost 5km of the subsurface and between 800GJ/m² and 3000GJ/m² at the uppermost 7km of the Earth's Crust. Both maps imply enhanced heat content along a southwest to northeast heading central zone of the project area.

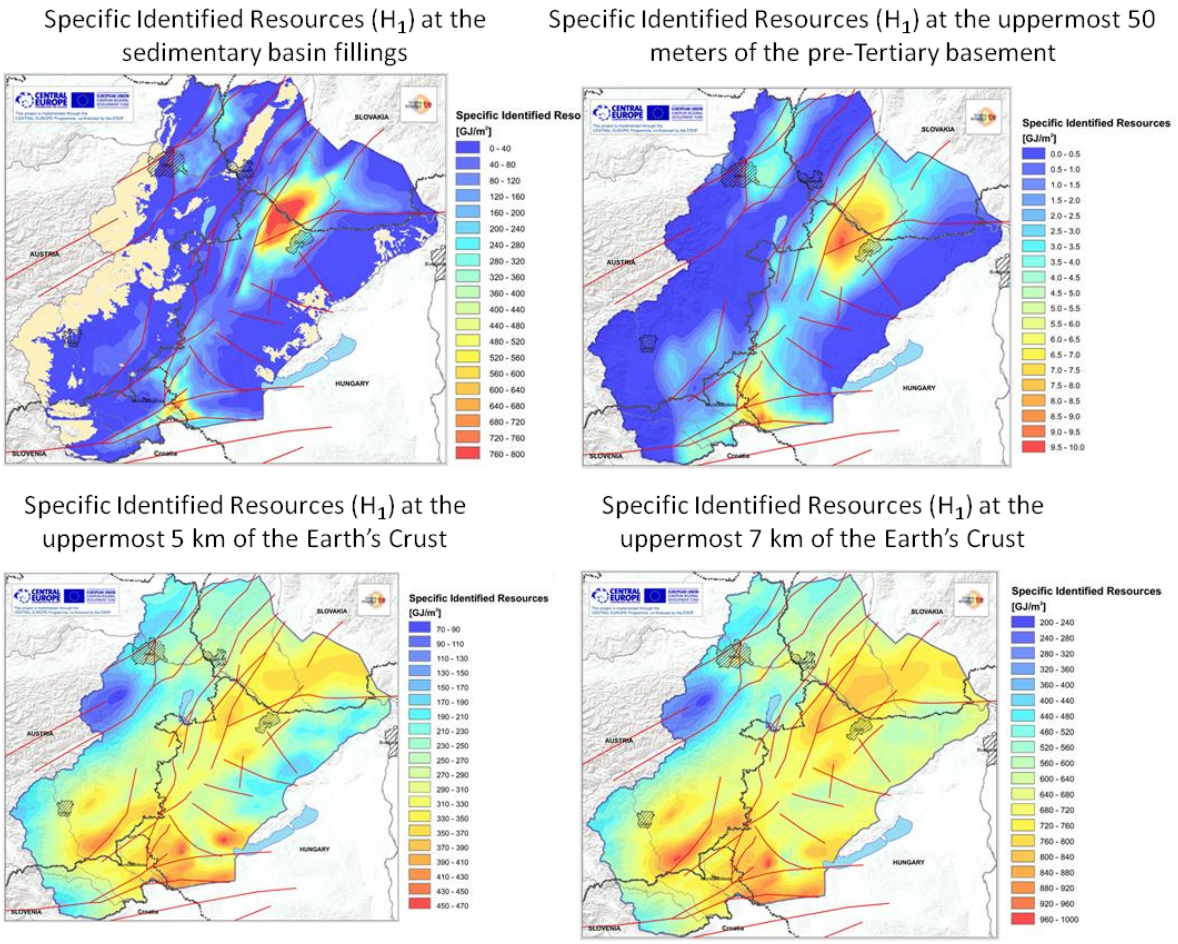

Figure 43: Specific Identified Resource map series

The pattern of the various maps showing the Specific Identified Resources are identical to the maps showing the Specific Heat in Place, as this parameter is directly derived from the Specific Heat in Place by applying a heat recovery factor, which is proportional to the temperature, and show that approximately 33% of the entire stored heat can be utilized.

4.5 Distribution of Background Heat Flow Density (Lenkey L. & Raáb D.)

We present the results in the forms of temperature-depth curves along control wells, temperature maps in 1km and 2.5km depths and heat flow density maps. The model is best constrained along those wells, where the thermal conductivity of sediments is known. We chose a few wells out of them, in which temperature measurements were made. The modelled and ob-

served temperatures along these control wells are shown in the subsequent

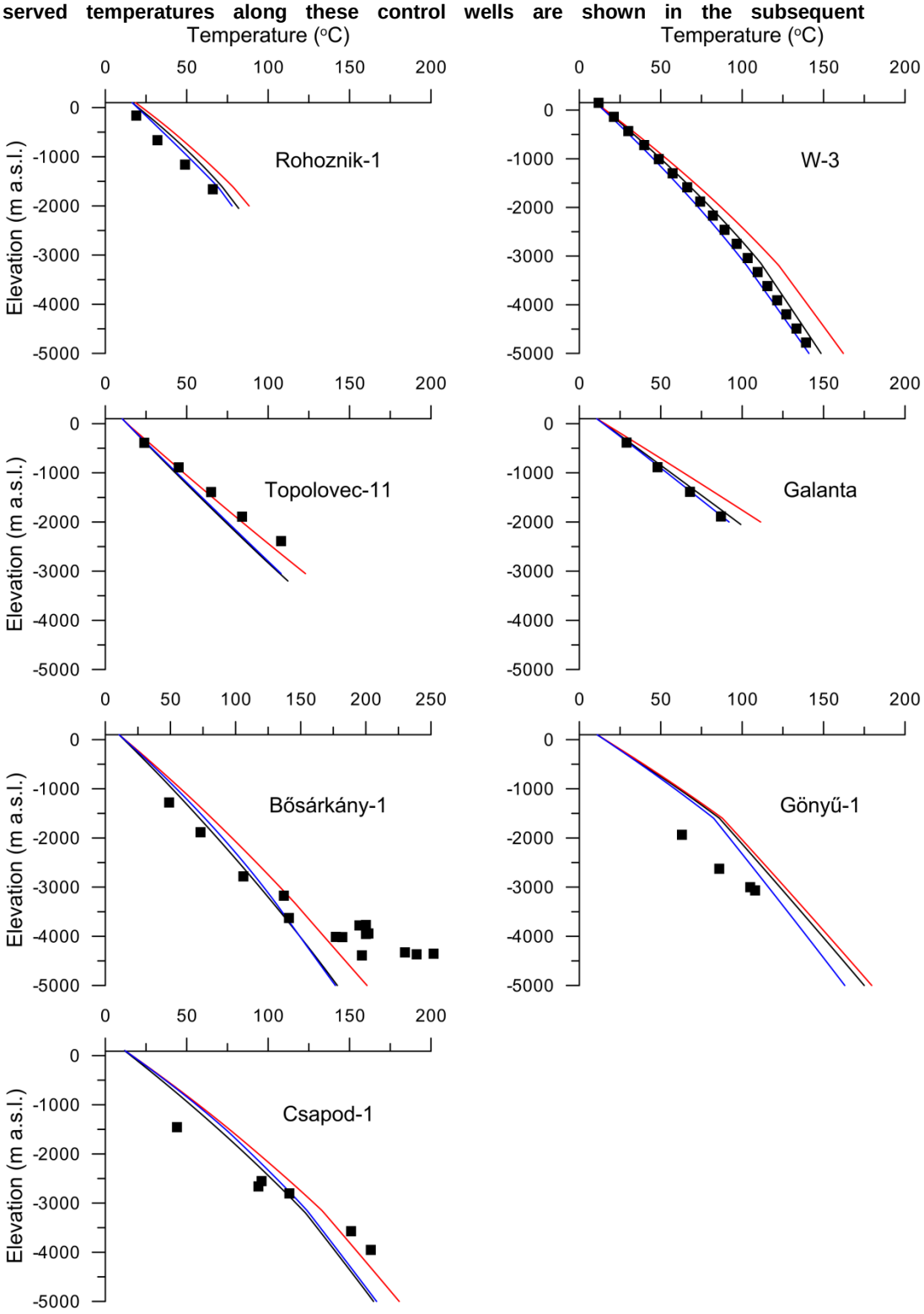

Figure 44 and Figure 45.

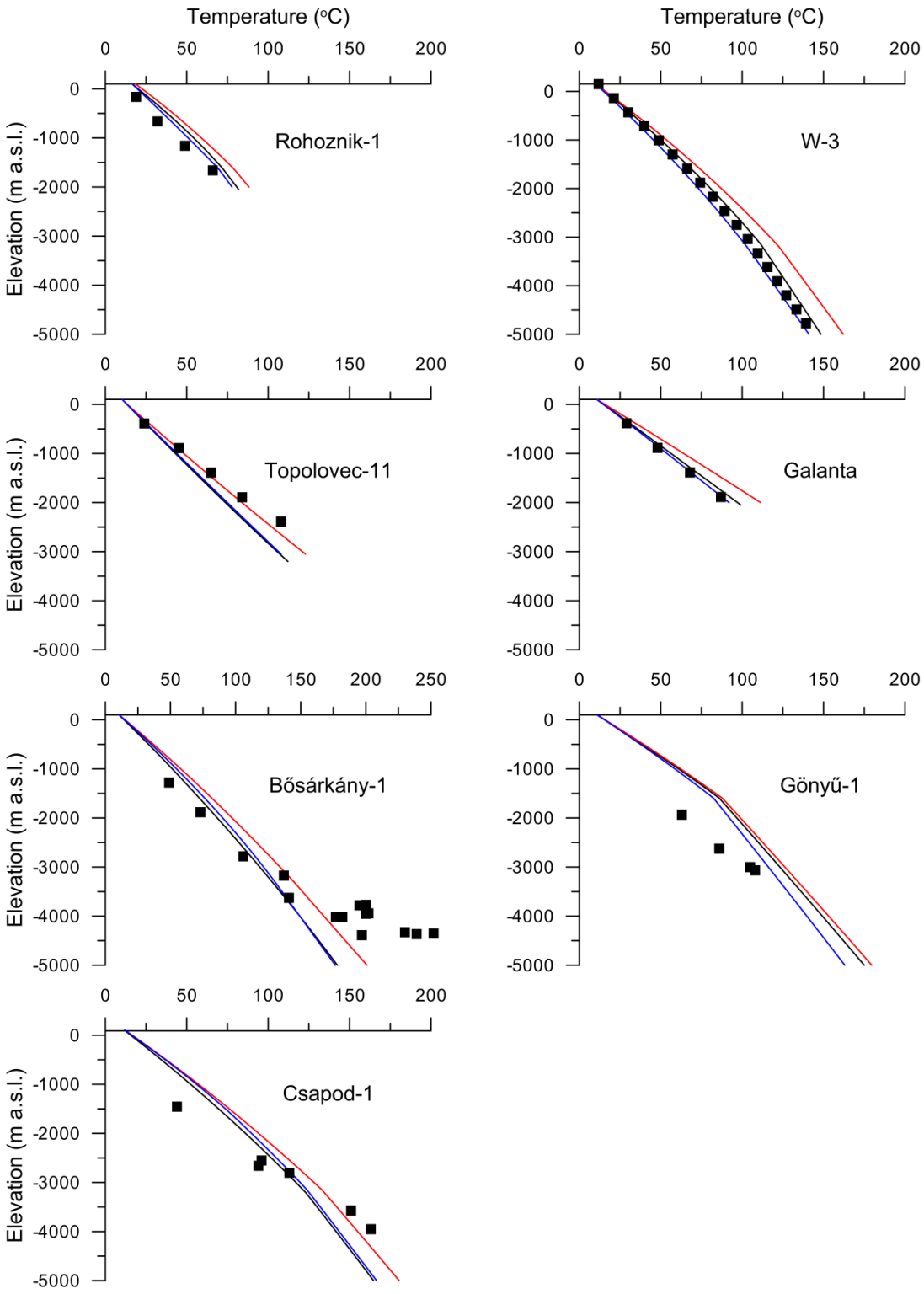

Figure 44: **Observed and modelled temperatures in control wells in the northern part of the area.** Black squares: observed temperatures, black line: steady-state temperature, red line: temperature in the Trans-T model calculated from the initial geotherm after 17.5 Ma, blue line: temperature in the Trans-Sed model calculated from the initial geotherm after 17.5 Ma. Thermal parameters are given in Table 7, the boundary conditions are described in the text.

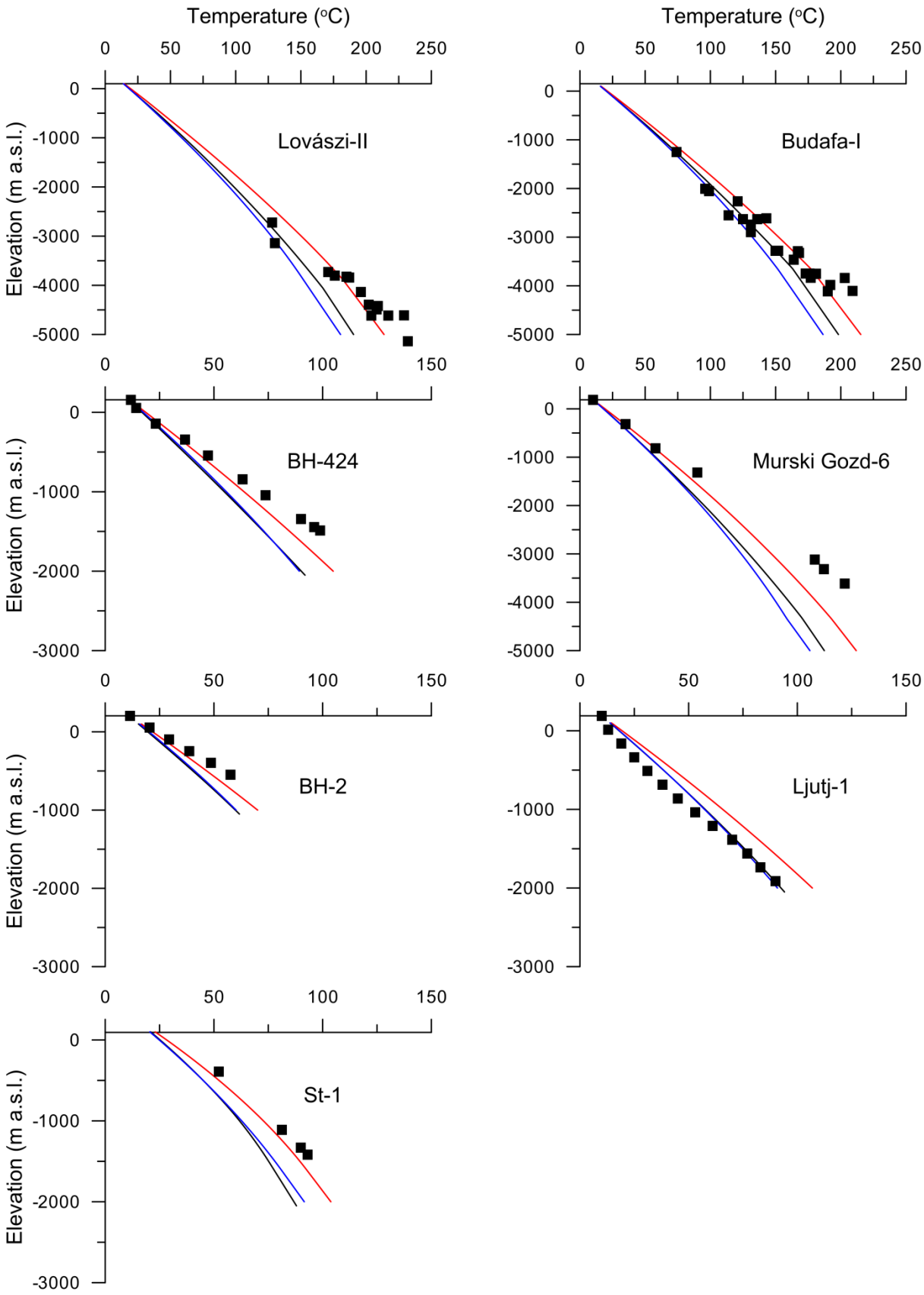

Figure 45: **Observed and calculated temperatures in control wells in the southern part of the area.** For detailed explanations see Figure 44

Table 16: Input and calibration wells used for the calculation of the Background Heatflow Density.
k… Thermal conductivity; T… borehole temperature.

Austria			
No.	**Well name**	**Abbrev.**	**Data type**
1	Styrian basin	St-1	T
2	Vienna basin	V-3	T
Hungary			
No.	**Well name**	**Abbrev.**	**Data type**
3	Lovászi-II		*k*, T
4	Bárszentmihályfalva-1		*k*
5	Bősárkány-1		*k*, T
6	Budafa-I		*k*, T
7	Újfalu-I		*k*
8	Ortaháza-Ny1		*k*
9	Csapod-1		*k*, T
10	Csesztreg-I		*k*
11	Szilvágy-33		*k*
12	Dabrony-1		*k*
13	Nagylengyel-II		*k*
14	Tét-5		*k*
15	Egyházasdaróc-1		*k*
16	Őriszentpéter-2		*k*
17	Gönyü-1		*k*, T
18	Celldömölk-ENy1		*k*
19	Iváncz-1		*k*
20	Mihályi-28		*k*
21	Mosonszolnok-1		*k*
22	Nagylengyel-74		*k*
23	Pér-1		*k*
24	Vaszar-DNy1		*k*
25	Pásztori-1		*k*

26	Bak-5		*k*
27	Szombathely-II		*k*
Slovakia			
No.	**Well name**	**Abbrev.**	**Data type**
28	Galanta	FGG-1	*k*, T
29	Galanta	FGG-2	*k*
30	Galanta	FGG-3	*k*
31	Cilistoc	FGC-1	*k*
32	Dunajska Streda	DS-1	*k*
33	Dunajska Streda	DS-2	*k*
34	Králova pri Senci	VMK-1	*k*
35	Calovo	C-1	*k*
36	Chorvátsko Grob	FGB-1	*k*
37	Rusovce	HGB-1	*k*
38	Láb	L-90	*k*
39	Rohoznik	R-1	*k*, T
40	Závod	ZA-57	*k*
41	Ciliska Radvan	CR-1	*k*
42	Horná Poton	FGHP-1	*k*
43	Topolovec	VTP-11	*k*, T
Slovenia			
No.	**Well name**	**Abbrev.**	**Data type**
44		BH-2	T
45		BH-424	T
46	Ljutj-1		*k*, T
47	Petisovci-7/88	Pg-7/88	*k*
48	Petisovci-1/91	Pec-1/91	*k*
49	Murski Gozd-6	Mg-6	*k*, T
50	Maribori-1/90	Mb-1690	*k*

The stretching model (Trans-T) predicts the highest and the combined stretching-sedimentation model (Trans-Sed) predicts the lowest temperatures. The steady-state model is either equal to the Trans-Sed model (mainly in the northern part of the area), or is between the two transient models (some wells in the southern part). In the northern part of the Vienna basin and Danube basin the steady-state model and the Trans-Sed model fit to the observations, and the Trans-T model overestimates the temperature. In the central and southern part of the Danube basin-Little Hungarian Plain the Trans-T model is the best, the steady-state model and the Trans-Sed model underestimate the temperature. In the Bősárkány-1 well the deeper temperatures are higher than they would be in case of extrapolating the temperature from shallower depths. As the deeper temperatures are more reliable, thus either the shallower values are false, or groundwater flow is occurring in the porous sediments in the upper part of the well. At the location of Gönyü-1 well groundwater flow takes part in the carbonatic basement. That explains why all models predict higher temperatures than the observed ones. In the Styrian basin and in SW Hungary the Trans-T model fits to the observations. In Slovenia, except the Ljutj-1 well, the models underestimate the temperature, but still the Trans-T model is closest to the observations. In the Ljutj-1 well the Trans-Sed and the steady-state models fit to the observed temperatures. However, the temperature gradient in the Ljutj-1 well seems to increase with depth, therefore we suspect, that there is downward groundwater flow near the well.

The Trans-Sed model is either equal to the steady-state model or it misfits to the observation, therefore we rejected this model. In the following we present temperature maps and heat flow density maps for the steady-state and Trans-T models.

The elaborated steady-state pure conductive 3D model was compared to the temperature maps at depths of 1000m below surface and 2500m below surface as well as to the surface heat flow density maps (see Figure 46 to Figure 48).

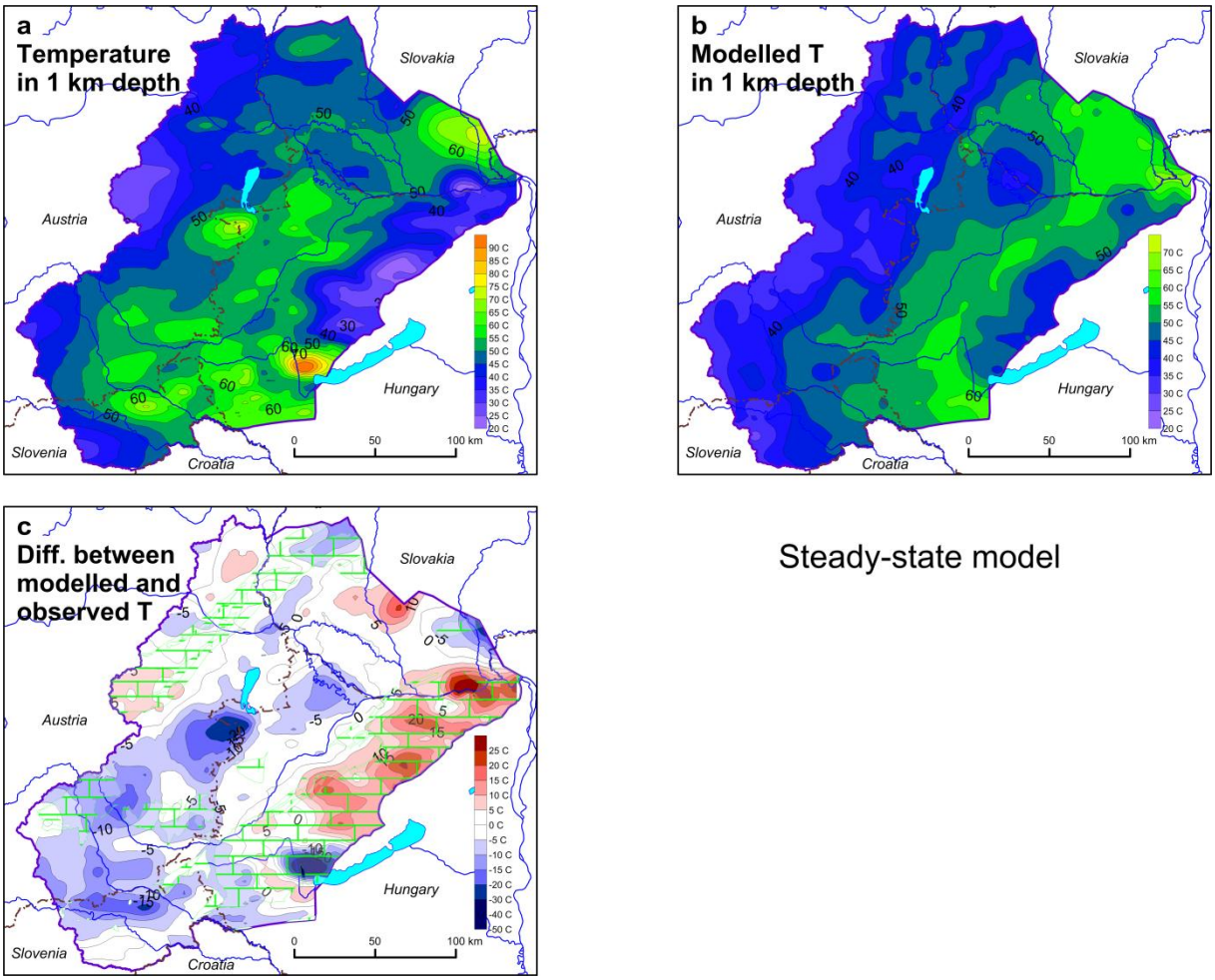

Figure 46: **Observed and modelled temperatures in 1 km depth and their difference.** Temperatures were calculated assuming steady state condition. a) observed temperature, b) modelled temperature, c) temperature difference = modelled minus observed temperature. In red areas the model temperature is higher, in blue areas the model temperature is lower than the observed one. Green hatches indicate carbonates.

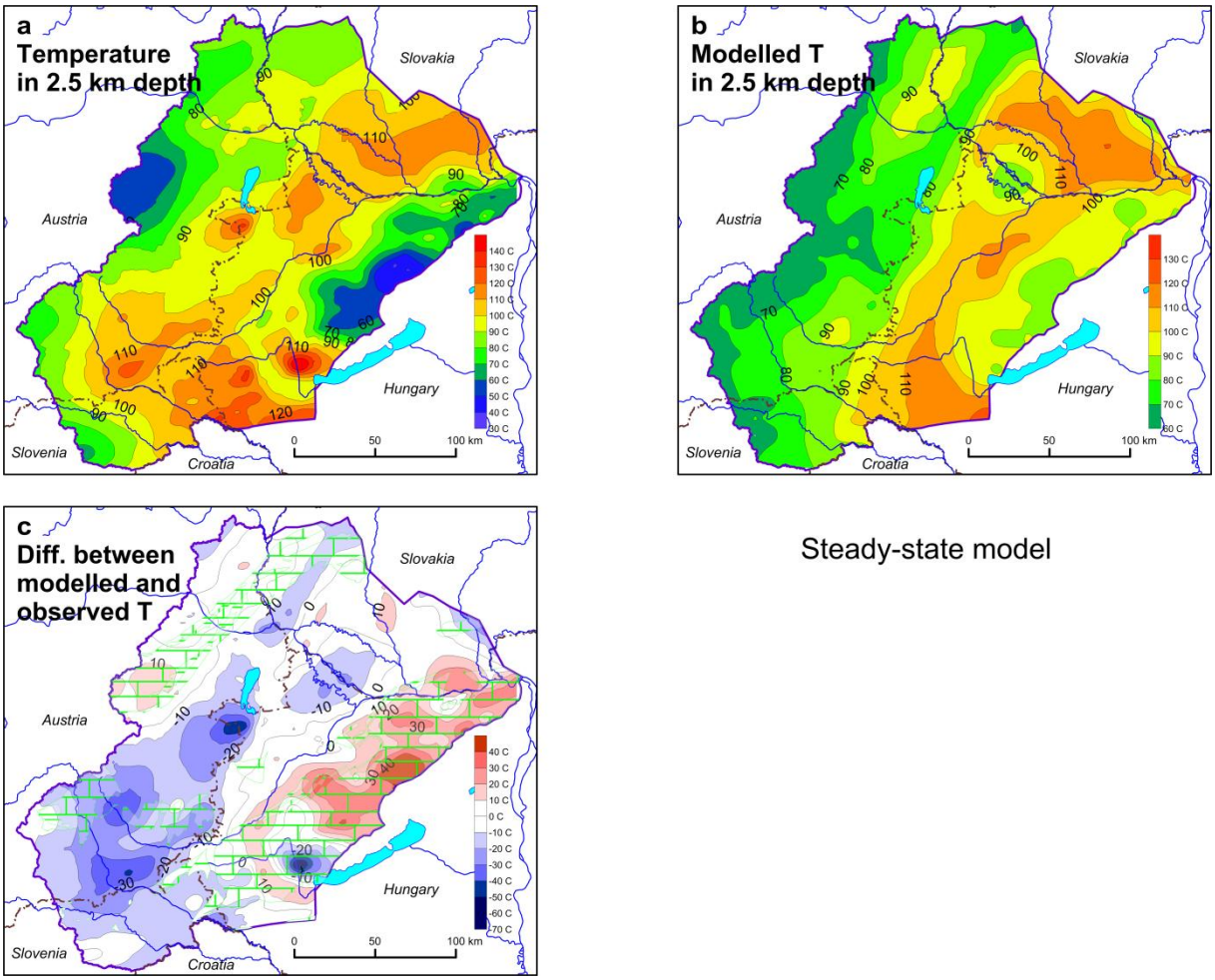

Figure 47: **Observed and modelled temperatures in 2.5 km depth and their difference.** Temperatures were calculated assuming steady state condition and using geometry given in Fig. 2. a) observed temperature, b) modelled temperature, c) temperature difference = modelled minus observed temperature. In red areas the model temperature is higher, in blue areas the model temperature is lower than the observed one. Green hatches indicate carbonates.

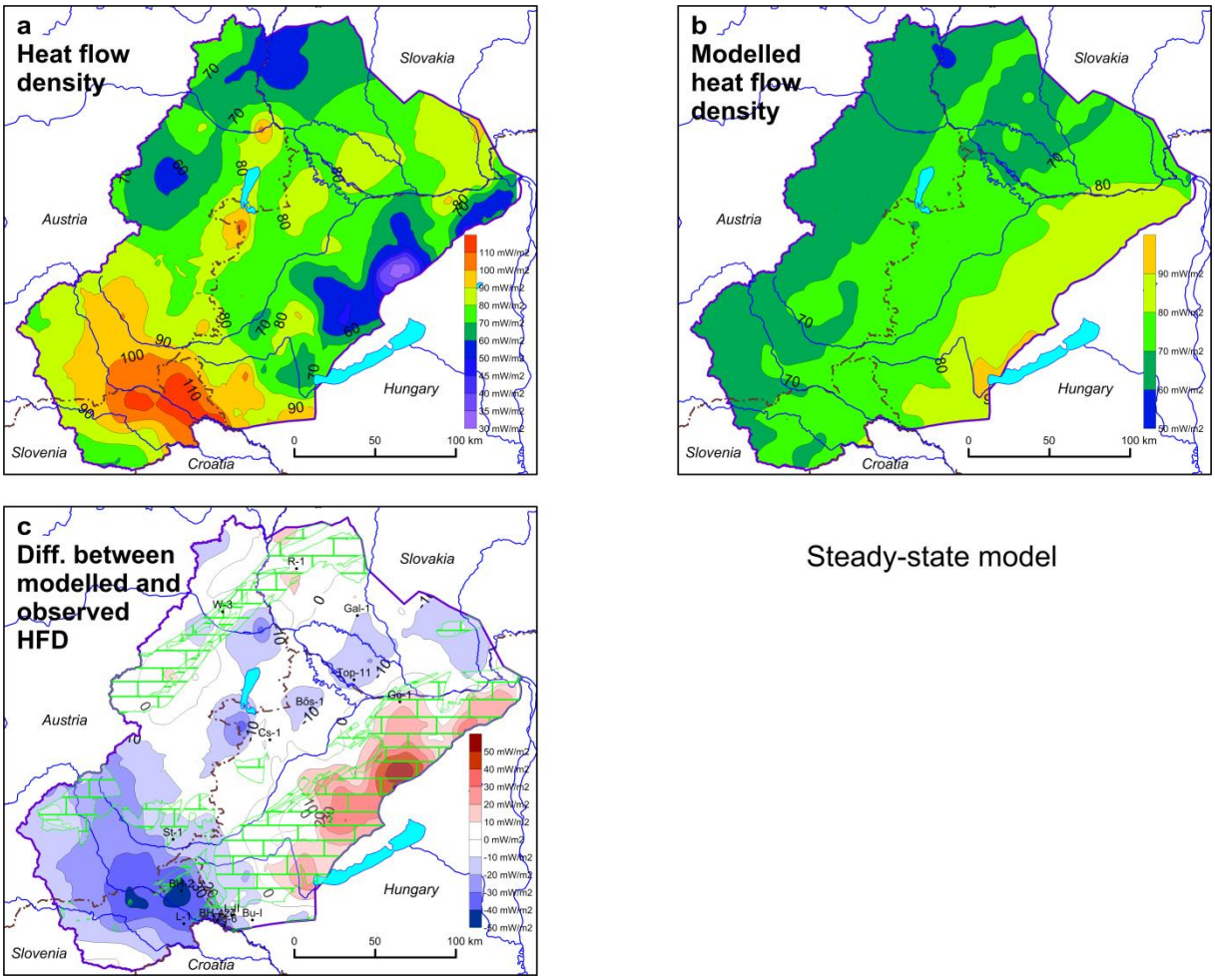

Figure 48: **Observed and modelled heat flow densities and their difference.** Heat flow density was calculated assuming steady state condition. a) observed heat flow density, b) modelled heat flow density, c) difference in heat flow density = modelled minus observed values. In red areas the model HFD is higher, in blue areas the model HFD is lower than the observed one. Green hatches indicate carbonates. Black dots indicate the location of control wells.

We can interpret the modelled heat flow density (Figure 48 - b) easiest. As the thickness of the lithosphere decreases from NW towards SE (Figure 31d), and the temperature at the base of the lithosphere is fixed, the geothermal gradient in the lithosphere, and thus the heat flow density increases towards SE. This trend is slightly perturbed by the variation of the crustal thickness and thermal conductivity. In those places where the crust is thinner, less heat is produced. Sediments have lower thermal conductivity than the crust, thus heat flow density is slightly diverted towards the basement flanks. When these two effects are superposed, like in the Little Hungarian Plain-Danube basin, the heat flow density is a little bit reduced relative to the surrounding areas. This reduced heat flow density is the reason of the low predicted temperature in the centre of Little Hungarian Plain relative to the surroundings (see Figure 46 and Figure 47). There is an apparent contradiction between the modelled temperature and heat flow density in the SE part of the study area. The heat flow density is constant or slightly increases towards SE, but the temperature decreases. This is due to the fact, that towards SE the thickness of sediments reduces, therefore the average thermal

conductivity increases, which in turn leads to a reduction of the geothermal gradient according to the Fourier Law of thermal conduction.

The difference between the modelled and observed quantities is presented in part -c- of Figure 46 to Figure 48. Positive values align with modelled data higher than the observed one, negative values have the opposite meaning.

In the Transdanubian Central Range and the SE part of the Little Hungarian Plain the modelled heat flow density and temperatures are higher than the observed ones. In these areas there is intensive downward karstic water flow in the carbonatic rocks comprising the basement, which results in lower temperatures. There is similar situation in the Vienna basin, but there the thermal anomaly is smaller. In other areas the steady-state model in general predicts lower temperatures and heat flow density than it is observed (blue patches in part -c- of Figure 46 to Figure 48).

There are two really locally confined, but significant temperature anomalies, where the observed temperature is higher than the modelled one: In the SW corner of the Lake Balaton and S to the Fertő-tó/Neusiedlersee. These are discharge areas with upwelling warm groundwater. In other places, like in the SW part of the study area and in the Little Hungarian Plain the predicted low temperatures and heat flow density are difficult to explain. These are either discharge areas too, or the heat flow density from the mantle is higher. We think that the second choice is more likely.

The heat flow density in the steady-state model strongly depends on the lithospheric thickness. However, lithospheric thickness data are not available from the Styrian basin and the Zala-Mura-Drava basins, where the misfit is largest between the observations and the model results. The lithospheric thickness in this area is based on interpolation from distant data. Additionally, we know that the steady-state condition in the area is not fulfilled. This was the reason to apply the stretching model. As the stretching factors are based on the heat flow density we expected a better fitting to the observed data. The results of the Trans-T model are shown in Figure 49 to Figure 51.

In case of the temperatures and heat flow density the fit between the observed and modelled data improved significantly. In the SW area the observed heat flow and temperatures are still higher than the predicted ones, but the difference is reduced to range, which can be explained either by convection or local conduction phenomena. We note that in the SW area the modelled heat flow density misfits to the observations, but the model temperatures fit to the observations. One way to resolve this contradiction is if we assume that maybe we used lower thermal conductivities in the modelling than those ones, which were used in the heat flow density estimates. On the other hand, there are indications that upward groundwater flow occurs along faults in the area (Kraljic et al., 2005).

The thermal anomalies of the karstic areas (TCR, Vienna basin) are present in this model too. In the central area the model fits to the observations. There is a new misfit in this model compared to the steady-state model: the transient model predicts higher temperatures in the NE part of the Danube basin. However, this misfit may also indicate that downward groundwater flow occurs in the porous sediments, which outcrop at the feet of the Western Carpa-

thians. At this stage it is not possible to decide if this is an “overshooting” of the model or groundwater flow can explain the thermal field.

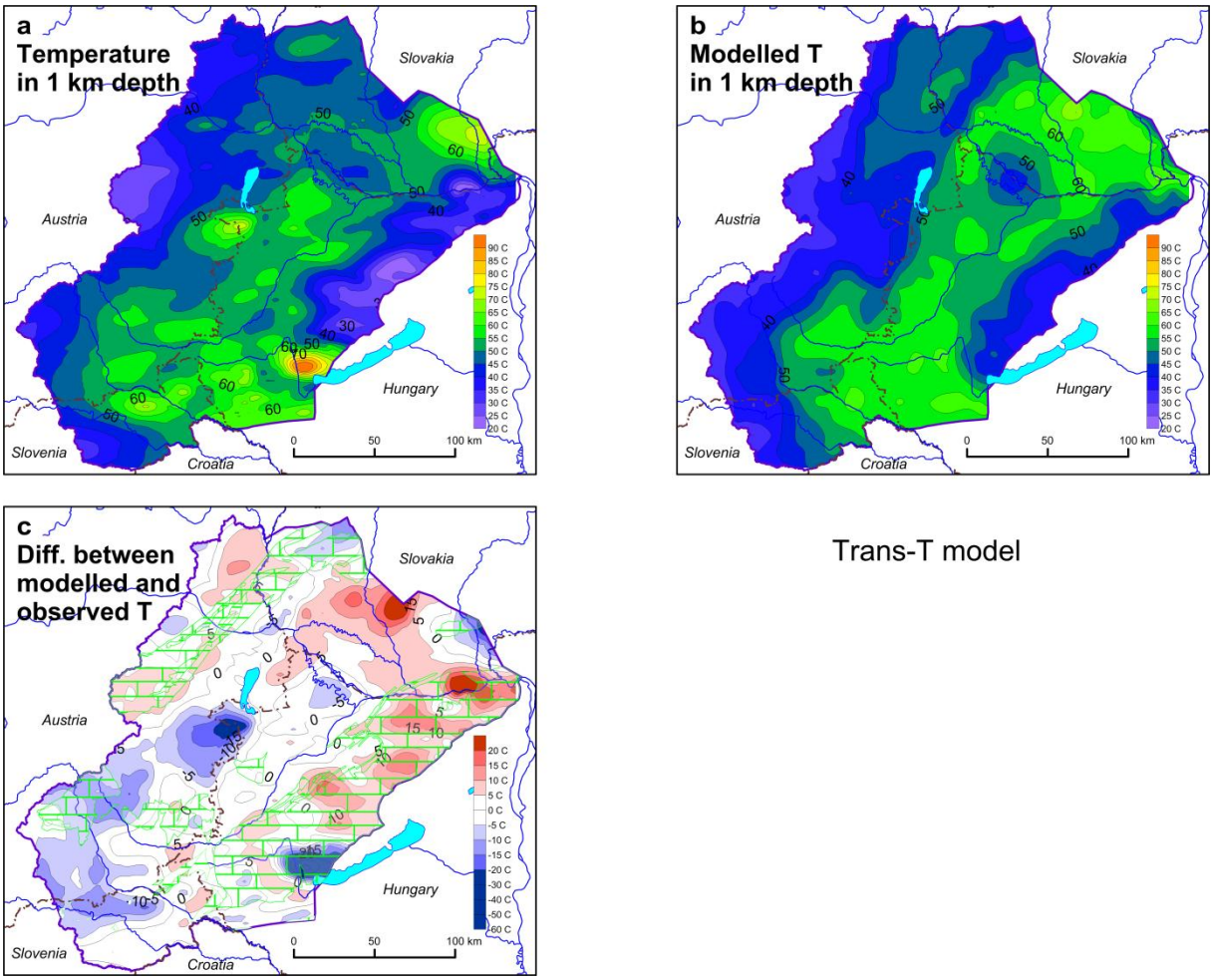

Figure 49: **Observed and modelled temperatures at a depth of 1 km and their difference.** Temperatures were calculated from the Trans-T model. a) observed temperature, b) modelled temperature, c) temperature difference = modelled minus observed temperature. In red areas the model temperature is higher, in blue areas the model temperature is lower than the observed one. Green hatches indicate carbonates.

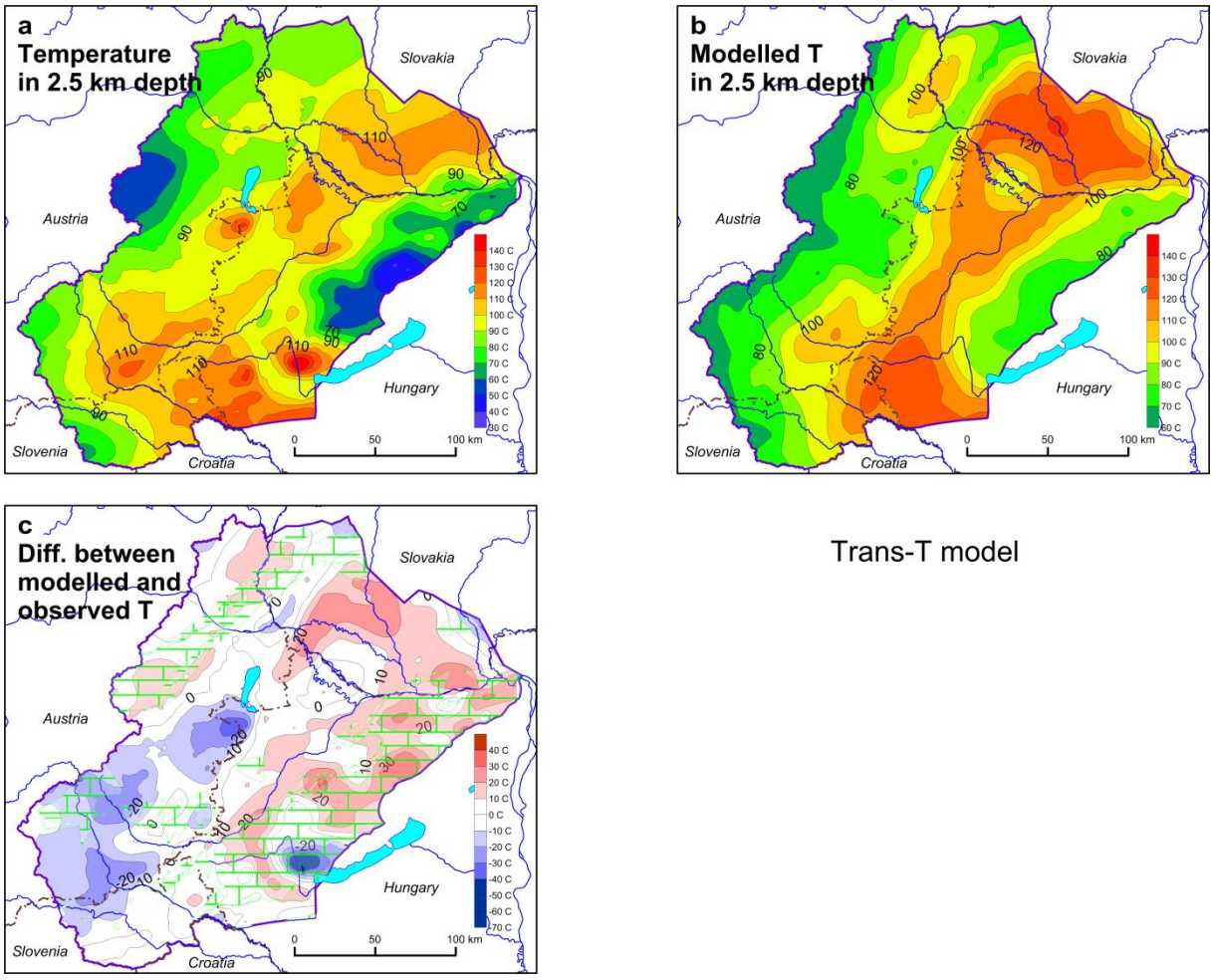

Figure 50: **Observed and modelled temperatures in 2.5 km depth and their difference.** Temperatures were calculated from the Trans-T model. a) observed temperature, b) modelled temperature, c) temperature difference = modelled minus observed temperature. In red areas the model temperature is higher, in blue areas the model temperature is lower than the observed one. Green hatches indicate carbonates.

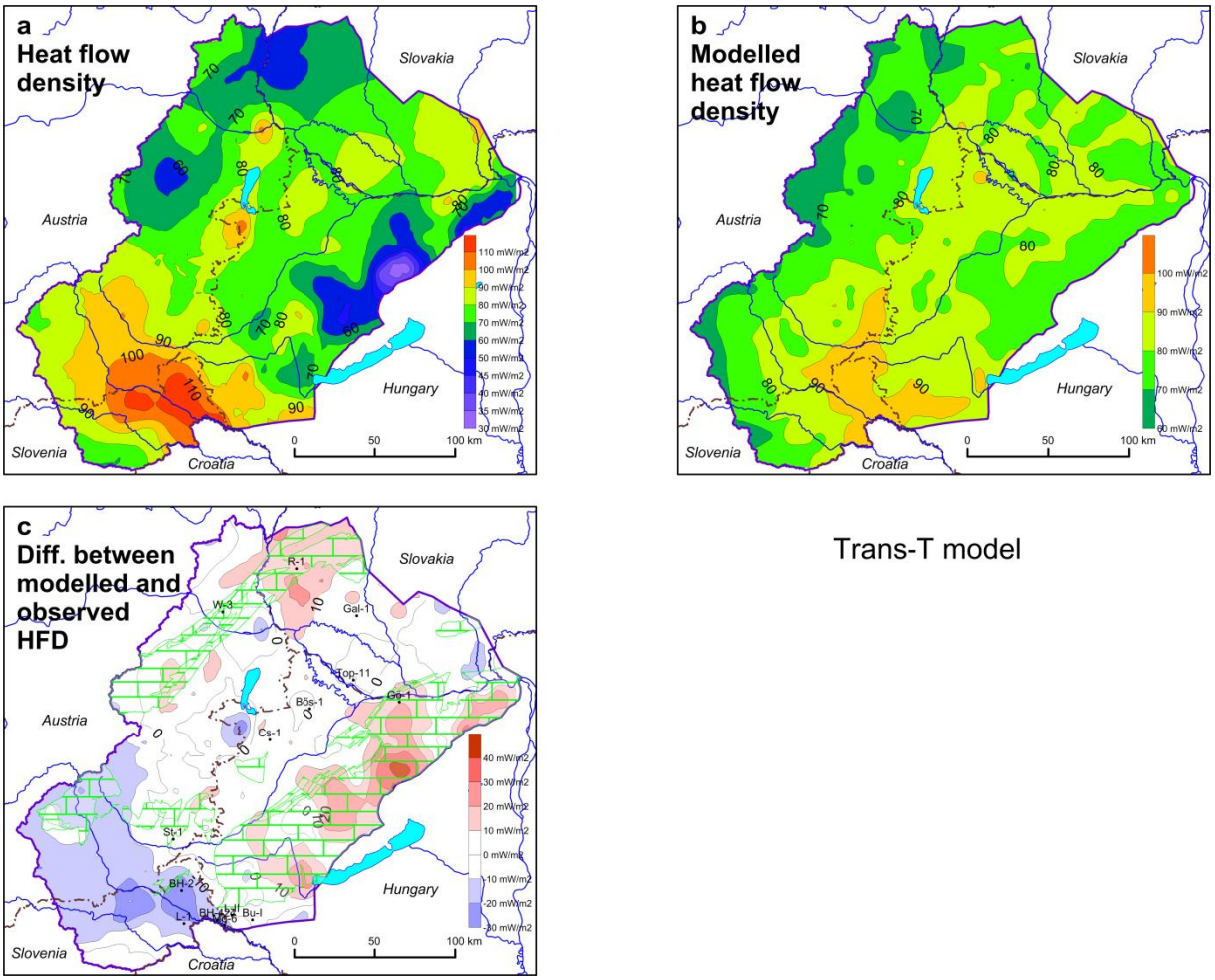

Figure 51: **Observed and modelled heat flow densities and their difference.** Heat flow density was calculated from the Trans-T model. a) observed heat flow density, b) modelled heat flow density, c) difference in heat flow density = modelled minus observed values. In red areas the model HFD is higher, in blue areas the model HFD is lower than the observed one. Green hatches indicate carbonates. Black dots indicate the location of control wells.

5 Summary and Conclusions

In the following chapter all main results will be summarized and interpreted with respect to the aims of the project Transenergy.

5.1 Surface Heat Flow Density and temperature maps

The surface heat flow density (Enclosure 1) and temperature maps (Enclosure 2a-2d) indicate that in some parts of the supra-regional area positive geothermal anomalies occur in the subsurface. Therefore the elaborated maps represent a first step towards the evaluation of the geothermal resources in specific regions.

The south-western part of the project area covering the parts of the Styrian and Mura – Zala Basin is a region with favourable geothermal conditions (> 120mW/m^2). The increased HFD values (in the Mura – Zala Basin) are related to the convection zones in the pre-Tertiary

basement rocks and to various geological conditions like e.g. reduced lithospheric thickness and tectonic evolution. This conclusion has already been confirmed by exploration and production wells in Slovenia and Austria.

Additionally several local to regional scale geothermal anomalies are depicted on the elaborated maps. The positive geothermal anomalies in the southern part of Vienna ("Oberlaaer High") and between Bratislava and Vienna (Bad Deutsch-Altenburg) are likewise related to naturally ascending thermal water (hydrodynamic systems), which supposedly are not interconnected.

At the central part of the Danube basin westwards of the city Györ and the western part of the Danube Basin in Slovakia high HFD values can be observed. This is probably a result of increased heat flow density from the mantle due to thinner lithosphere. In the region of Komarno and Sturovo (SK, eastern part of the project area) the depicted positive geothermal anomalies are correlated with circulating systems.

The different temperature maps give an overview on the expectable rock temperatures in certain regions. The observed positive anomalies in 1000m below surface correspond to shallow hydrodynamic systems, whereas deeper subsurface temperature distributions are mainly influenced by large scale crustal structures.

As a result of the compiled map series, areas with favourable geothermal conditions could be outlined. Within the pilot areas, further detailed studies of these outlined regions will be performed.

5.2 Potential Map Series

The Specific Identified Resources maps imply that a huge amount of heat is stored in the subsurface. The derived potential is enough to cover the heat demand of the countries participating in the TE project for many hundreds of years. However, only the heat stored in porous, permeable rocks can be utilized economically by production of hot water or steam, and these rocks comprise only a small fraction of the total volume of rocks.

Although the calculation of parameters describing the geothermal potential at a certain area, such as "Specific Heat in Place" and "Specific Identified Resources", is only accompanied of mathematical uncertainty of approximately ±25%, the interpretation of these values towards the realistic amount of energy, which can be technically extracted is very unconfident, as the Heat Recovery Factor is not exactly known. Nevertheless a geothermal balancing of the entire Transenergy project areas has been executed in order to demonstrate the great range of variation accompanied to the interpretation of parameters describing the geothermal potential. This balance covers the following parameters:

- Already installed hydrogeothermal capacities for energetic utilization
- Natural heat recovery based on the observed SHFD
- Identified Resources at the uppermost 50 meters of the pre-Tertiary basement
- Identified Resources at the sedimentary fillings.

The calculated balances are shown in the subsequent Table 17 and Figure 52.

Table 17: Overview on calculated geothermal balances for the entire project area

Estimated installed capacity (excluding balneology)	**0.097**	**GW**
Natural het recovers (based on SHFD)	**27**	**GW**
„Identified resources„ (sedimentary basin fillings)*	**9000**	**GW**
„Identified resources“ (top 50 meter basement)*	**193**	**GW**

* Referring to an operational period of 100 years

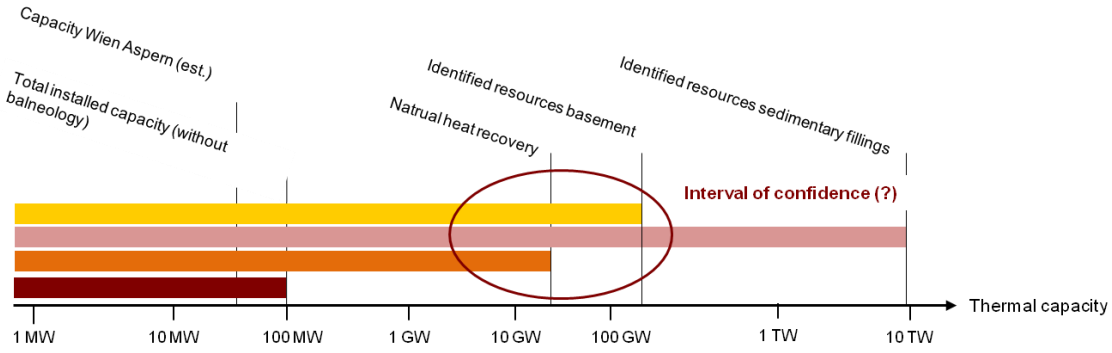

Figure 52: Overview on the different ranges of the estimated geothermal potentials in the Transenergy project area. For comparison reasons an actually developed hydrogeothermal heating plat at the city of Vienna (Aspern) with a planned thermal capacity of 40 MW is also shown on the capacity bar. The red ellipse outlines the estimated interval of confidence of the inferred geothermal resources including both, hydrogeothermal and petrothermal utilization.

Table 17 and Figure 52 clearly show, that the range of variance accompanied to the interpretation of the parameter Identified Resources is covering the range of several thousands of Gigawatts and therefore not suitable for a detailed resource management. However, a relevant parameter for thermal balancing is given by the Natural heat recovery, which was calculated by spatial integration of the observed SHFD over the entire project area. The Natural heat recovery is limiting the extractable amount of heat with respect to a sustainable use[3] – that means the amount of extracted heat is covered by the terrestrial heat flow. With respect to the Natural heat recovery (27 GW) only 0.37% of the available geothermal heat flux is already used for energetic utilization (already installed capacity 97 MW).

Of course in this balance existing geothermal plays and reservoirs are not taken into account. Therefore, as a next interpretative working step, outlines and attributes of known geothermal reservoirs will be combined with the elaborated geothermal potential maps in order to derive more precise parameters in terms of “Inferred Resources” and “Identified Re-

[3] In case the total energy extraction at a defined area exceeds the natural heat recovery a continuous cooling of the affected subsurface volume will take place. For that reason the thermal recovery of that volume in order to reach initial temperature levels will take much longer than the period of utilization.

sources", which are in accordance with the Canadian Geothermal Code for Public Reporting (Deibert & Toohey, 2010).

5.3 Background Heat Flow Density (Lenkey L. & Raáb D.)

The transient model Trans-T, in which the Middle Miocene lithospheric stretching determines the initial geotherm, results in reasonable fitting to the observed temperatures and heat flow density. The modelled heat flow density increases from NW towards the centre of the area and southward, which is in agreement with the long wavelength variation of the observed heat flow density. The observed and modelled heat flow densities and temperatures are different significantly in those areas, where groundwater flow is occurring. Thus, the model results are in accordance with the *a priori* hydrological information. Specifying the initial geotherm is analogous with prescribing the mantle heat flow density.

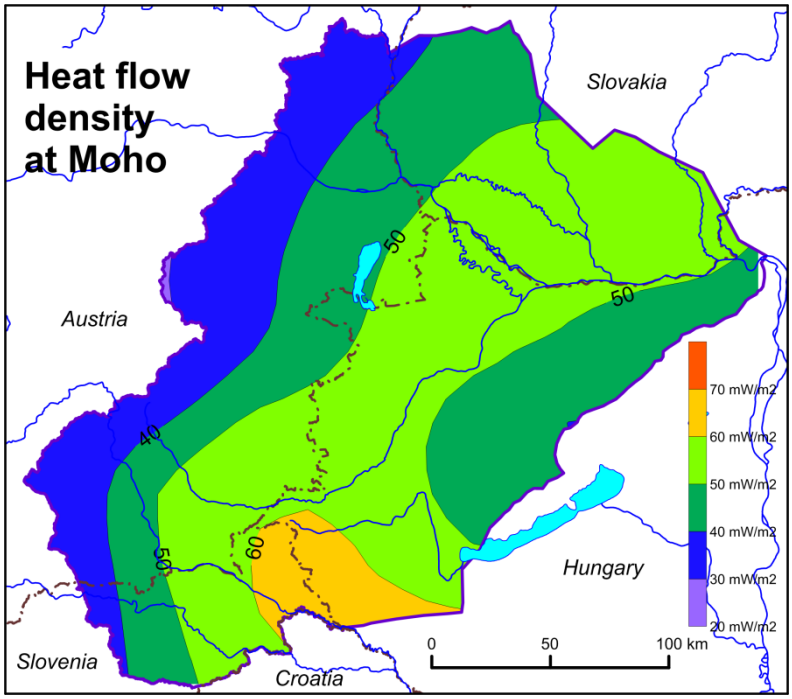

Figure 53: **Heat flow density from the mantle at the base of the crust calculated from the Trans-T model.**

As the Trans-T model results fits to the observed temperatures and HFD very good, it has simple material properties, and it is based on reasonable geological and physical considerations, we consider it as the best model in the moment.

The model results can be further improved by coupled groundwater and heat transport modelling, which will be carried out in the pilot areas. The aim of these models is to determine the natural groundwater flux and calculate its thermal effect. The mantle heat flow density at the Moho discontinuity (Figure 51), or heat flow density, or temperature in large depth (e.g. in 10 or 20 km) derived from the Trans-T model can be used as thermal boundary condition prescribed in the bottom of those models. If the thermal anomalies in the pilot areas can be obtained with this boundary condition than the Trans-T model is good, otherwise it must be revised.

5.4 Final Remark

The joint interpolation and modelling of harmonized geothermal data led to a compilation of geothermal maps in scale of 1:500.000, which cover the entire Western Pannonian Basin and its adjacent areas for the first time. The quality and significance of the elaborated heat flow density and temperature maps reflect the data situation of 2010. By applying easily applicable, well documented approaches the existing maps can be updated in future without great effort.

The elaborated potential maps and balances only allow taking a first look on the available geothermal resources and actual degree of exploitation at the project area, irrespective to known or estimated geothermal plays and reservoirs. However, the achieved results imply, that only a very small amount of the available believed geothermal resources is already utilized (<1%) and therefore, hydrogeothermal utilization is able to play an important role in the future energy supply in the Transenergy project area.

References

BARNES, R., 2002, *Variogram Tutorial*. http://www.goldensoftware.com/variogram_Tutorial.pdf, status: 03.09.2012.

BECK, A.E., 1976, *An improved method of computing the thermal conductivity of fluid-filled sedimentary rocks*. Geophysics, Volume 41, Issue 1, p. 133 – 145.

BOLDIZSÁR, T., 1959, *Terrestrial heat flow in the Nagylengyel oil field*. Publ. Min. Fac. Sopron, XX: p. 27-34.

CARSLAW, H. S. AND JAEGER, J. C., 1959, *Conduction of heat in solids*. Clarendon Press, Oxford: 1-510.

DEIBERT L., TOOHEY, B. (eds.), 2010, *The Canadian Geothermal Code for Public Reporting. Reporting of Results, Geothermal Resources and Geothermal Reserves – 2010 Edition*. Canadian Geothermal Association (CanGEA). Calgary, Alberta.

DEMETRESCU, C., NIELSEN, S.B., ENE, M., SERBAN, D.Z., POLONIC, G., ANDREESCU, M., POP, A. BALLING, N., 2001, *Lithosphere thermal structure and evolution of the Transylvanian Depression – insights from new geothermal measurements and modelling results*. Phys. Earth and Planet. Inter., 126: 249-267.

DOMBERGER, G., LAPANJE, A., POLTNIG, W., 2008, *Beilage 14 Geothermisches Potenzial (Festgesteinsuntergrund)*; Endbericht der Studie Transthermal; Geologische Bundesanstalt, Wien.

DÖVÉNYI, P., 1994, *Geophysical investigations of the lithosphere of the Pannonian basin*. PhD Thesis, Eötvös Univ., Budapest, pp. 127.

DÖVÉNYI, P., HORVÁTH F., 1988, *A review of temperature, thermal conductivity and heat-flow data from the Pannonian Basin*. In: L.H. Royden and F. Horváth (Editors), The Pannonian Basin, a Study in Basin Evolution. Amer. Assoc. Petr. Geol. Mem., 45: p. 195-233.

DÖVÉNYI, P., HORVÁTH, F., DRAHOS, D., 2002, *Hungary*. In: Hurter, S., Haenel, R. (eds.): Atlas of Geothermal Resources in Europe. - European Commission, Research Directorate-General. Publ. No. EUR 17811, Luxembourg.

DÖVÉNYI, P., HORVÁTH, F., LIEBE, P., GÁLFI, J., ERKI, I., 1983, *Geothermal conditions of Hungary*. Geophys. Transactions, 29/1, p. 3-114.

FERTL, W.H., WICHMANN, P.A., 1977, *How to determine static BHT from well log data*. World Oil, Volume 184, p. 105-106.

FRANKO, O., HALMDOVA, S., REMSLK, A., ZBORIL, L., 1984, *Tektonicka mapa predkriedoveho podlozia komarinanskej kryhy a jej hydrogeotermalny vyznam*. In: Zbornik referatov z VIII. celostatnej hydrogeologickej konJfrencie. Konferencie, sympozia, seminare GUDS, Bratislava, 185-188.

FRANKO, O., FUSÁN, O., KRÁL, M., REMŠÍK, A., FENDEK, M., BODIŠ, D., DROZD, V., VIKA, K., ELEČKO, M., FRANKO, J., GROSS, P., HRUŠECKÝ, I., JANČÍ, J., KALIČIAK,

M., KONEČNÝ, V., LEXA, J., MARCIN, D., MAŤO, J., PERESZLÉNYI, M., PAŠEKOVÁ, P., PÔBIŠ, J., ROHÁČ, J., SLÁVIK, M., VASS, D., ZVARA, I., 1995, *Atlas geotermálnej energie Slovenska*. Franko, O., Remšík, A., Fendek, M. (eds.). - Geologický Ústav Dionýza Štúra, Bratislava, ISBN 80 – 85314 – 38 - X, s. 268.

GOETZL, G., 2007, *Geothermie in Österreich*, aus Geo-Atlas Österreich – Die Vielfalt des geologischen Untergrundes, T. Hofmann & H.P. Schönlaub (Hrsg.), Böhlau Verlag Wien.

GOETZL, G., LAPANJE, A. (eds.), **BAEK, R., BUDKOVIČ, T., DOMBERGER, G., HRIBERNIK, K., LIPIARSKI, P., POLTNIG, W., RAJVER, D., RMAN, N.,** 2008, *Transthermal. Geothermal potential of the border region between Austria and Slovenia – Evaluation of the geothermal potential based on a bilateral database and GIS – maps for the regions of Carinthia, Styria and Northern Slovenia*. INTERREG IIIA Austria-Slovenia, bilateral final report (Austria/Slovenia), 89 p., 47 figs., 6 tab., 15 supplements, Vienna, Graz, Klagenfurt, Ljubljana.

GOETZL, G., FABER, R., JANDA, C., SCHUBERT, G., ZEKIRI, F., 2010, *Coupled geothermal-hydraulic 3D modeling of the Southern Vienna Basin. A state of the art decision planning tool for sustainable hydrothermal exploitation inside an environment of sensitive hydraulic circulation systems*. Proceedings World Geothermal Congress 2010 Bali, Indonesia, 25-29 April 2010.

GOLDBRUNNER, J.E., 2000, *Hydrogeology of Deep Groundwaters in Austria*. Mitt. Österr. Geol. Ges., 92, p. 281-294.

GRINGARTEN, A.C., 1978, *Reservoir lifetime and heat recovery factor in geothermal aquifer used for urban heating*. Pure and Applied Geophysics, 117, Issues 1-2, p. 298-308.

HORNER, D.R., 1951, *Pressure Build-Up in Wells*. Proceedings Third World Petroleum Congress – Section 11, p. 503-521, The Hagues.

HORVÁTH, F., 2005, *Heat flow density map of the Pannonian basin and surrounding region*. Atlas of present-day geodynamics of the Pannonian basin: Euconform maps with explanatory text. http://geophysics.elte.hu/atlas/geodin_atlas.htm

HORVÁTH, F., DÖVÉNYI, P., 1987, *A medencefejlődés modellezése*. GEOS GMK jelentése a KV megbízásából. Budapest, p. 476-672. Translation: *Modelling of basin evolution*. Research report for the Hungarian Oil Research Company, GEOS, Budapest, p 476-672.

HORVÁTH, F., DÖVÉNYI, P., ERKI, I., LENKEY, L., 1989, *A Szombathely-II sz, fúrás geotermikus vizsgálata. Kutatási zárójelentés a MÁFI megbízásából*. ELTE, Budapest, p. 29. Geothermal investigation of well Szombathely-II. Research report for the Hungarian Geological Institute, Eötvös University, Budapest, p. 29.

HORVÁTH, F., ERKI, I., BODRI, L., MARKÓ, L., GELLÉRT, T., 1977, *Hőárammérések*. In: Stegena L. (Ed): Geotermikus rezervoárkutatás III. Kutatási Jelentés a KFH megbízása alapján, ELTE, Budapest, 1-138. Determinations of heat flow density. In: Stegena L. (Ed): Geothermal reservoir research III. Research report for the Central Geological Office, Eötvös University, Budapest, p. 138.

HURTER, S., HAENEL, R. (eds.), 2002, *Atlas of Geothermal Resources in Europe*. - European Commission, Research Directorate-General. Publ. No. EUR 17811, Luxembourg.

HURTIG, E. (ED.-IN-CHIEF), CERMÁK, V., HAENEL, R., ZUI, V., 1992, *Geothermal Atlas. Association for Seismology and Physics of the earth's interior/International Heat Flow Commission/Central Institute for Physics of the Earth*. – In: GeoForschungsZentrum Potsdam Publication. Hermann Haack-Verlag, Gotha.

KAPPELMEYER, O., HAENEL, R., 1974, *Geothermics with special reference to application*. Geoexploration Monographs, Series1, No. 4, Gebrueder Borntraeger, Berlin, Stuttgart.

KOLLMANN, W.F.H. (ED), 1997, *Danube Region Vienna – Bratislava – Budapest Geothermal Potential Map 1:200000*; Geological Institute of Hungary, Budapest.

KOVAC, M., ZLINSKA, A., HALASOVA, E., HOLCOVA, K., HUDACKOVA, N., 2000; *Neogene sequence stratigraphy of the Western Carpathian Basins*; Mitteilungen der Gesellschaft der Geologie- und Bergbaustudenten in Österreich; Nr. 43; S.75.; Wien.

KOVAČ, M., BARÁTH, I., HARZHAUSER, M., HLAVATÝ, I., HUDÁČKOVÁ, N., 2004, *Miocene depositional systems and sequence stratigraphy of the Vienna Basin*. Cour. Forsch. Inst. Senckenberg, Volume 246, p. 187-212.

KRALJIC, M. ET AL., 2005, *Poročilo o izgradnji vrtine Benedikt-2 (Be-2)*. Technical report, Nafta Geoterm, Lendava.

LANKREIJER, A., KOVÁC, M., CLOETINGH, S., PITOSÁK, P., HLOSKA, M., BIERMANN, C., 1995, *Quantitative subsidence analysis and forward modelling of the Vienna and Danube basins: thin-skinned versus thick-skinned extension*. Tectonophysics, 252: 433-451.

LEBLANC, Y., PASCOE, L.J., JONES, F.W., 1982, *A comparison of two methods of estimating static formation temperature from well logs*. Geophysical Prospecting, Volume 30, p. 348-357.

LENKEY, L., 1999, *Geothermics of the Pannonian basin and its bearing on the tectonics of basin evolution*. PhD thesis, Vrije Universiteit, Amsterdam, 215 pp.

LENKEY, L., DÖVÉNYI, P., HORVÁTH, F., CLOETINGH S.A.P.L., 2002, *Geothermics of the Pannonian basin and its bearing on the Neotectonics.* EGU Stephan Mueller Special Publication Series, 3, 29-40.

LUCAZEAU, F. AND LE DOUARAN, S., 1985, *The blanketing effect of sediments in basins formed by extension: a numerical model. Application to the Gulf of Lion and Viking graben*. Earth Planet. Sci. Lett., 74: 92-102.

MÁDLNÉ SZŐNYI, J., RYBACH, L., LENKEY, L., HÁMOR, T., ZSEMLE, F., 2008. *A geotermikus energiahasznosítás nemzetközi és hazai helyzete, jövőbeni lehetőségei Magyarországon. Ajánlások a hasznosítást előmozdító kormányzati lépésekre és háttértanulmány*. Kutatási jelentés az MTA Elnöki Titkársága részére, ELTE, Budapest, p. 105. Actual state of the use of geothermal energy in worldwide and in Hungary, and further perspectives in Hungary. Report for the Hungarian Academy of Sciences, Eötvös University, Budapest, p. 105.

MCKENZIE, D., 1978, *Some remarks on the development of sedimentary basins*. Earth and Planet. Sci. Lett., 40: 25-32.

MUFFLER, P., CATTALDI R., 1978, *Methods for regional assessment of geothermal resources*. Geothermics, Volume 7, Issue 2-4, p. 53–89.

PARSONS, B. AND SCLATER, J.G., 1977, *An analysis of the variation of ocean floor bathymetry and heat flow with age*. J. Geoph. Res., 82: 803-827

PÉCSKAY, Z., LEXA, J., SZAKÁCS, A., BALOGH, K., SEGHEDI, I., KONECNY, V., KOVÁCS, M., MÁRTON, E., KALICIAK M., SZÉKY-FUX, V., PÓKA, T., GYARMATI, P., EDELSTEIN, O., ROSU, E., ZEC, B., 1995, *Space and time distribution of Neogene-Quaternary volcanism in the Carpatho-Pannonian Region*. In: H. Downes and O. Vaselli (Eds), Neogene and related magmatism in the Carpatho-Pannonian Region. Acta Vulcanol., 7: 15-28.

POWELL, W.G., CHAPMAN, D.S., BALLING, N., BECK, A.E., 1988, *Continental heat-flow density*. In: R. Haenel, L. Rybach, L. Stegena (eds.), Handbook of terrestrial heat-flow density determination. Kluwer academic publishers, Dordrecht, Boston, London, p. 167-222.

PRIECHODSKA, Z. AND VASS, D., 1986, *Geologia neogenu centralnej depresie v Podunajskej niiine*. Regionalna geologia Zapadnych Karpat. Spravy 0 vyskumoch GODS, Bratislava, 105-111.

RAÁB, D., 2011, *A Csomád vulkán (Keleti-Kárpátok) alatti magmakamra hűlésének numerikus modellezése. Szakdolgozat. ELTE, Budapest, p. 37. Modelling the cooling of the magmachamber of the volcano Csomád (Eastern Carpathians)*. Thesis work, Eötvös University, Budapest, p. 37.

RAJVER, D., RAVNIK, D., PREMRU, U., MIOČ, P., KRALJ, P., 2002, *Slovenia*. In: S. Hurter and R. Haenel (Editors), Atlas of Geothermal Resources in Europe. European Commission, Research Directorate-General. Publ. No. EUR 17811, Luxembourg.

RAJVER, D., RAVNIK, D., 2002, *Geotermična slika Slovenije - razširjena baza podatkov in izboljšane geotermične karte; Geothermal pattern of Slovenia - enlarged database and improved geothermal maps*. Geologija, 45/2, p. 519-524 (in Slovenian, with English abstract).

RAVNIK, D., 1991, *Geotermične raziskave v Sloveniji; Geothermal investigations in Slovenia*. Geologija 34, 265-303 (in Slovenian, with English summary).

RAVNIK, D., RAJVER, D., POLJAK, M., ŽIVČIĆ, M., 1995, *Overview of the geothermal field between the Alps, the Dinarides and the Pannonian basin*. Tectonophysics, Volume 250, Issues 1-3, p. 135-149.

REMSIK, A., FRANKO, O., 1979, *Zakladny vyskum geotermalnych zdrojov komariianskej vysokej kryhy*. Geofond, Bratislava.

REMSIK, A., FENDEK, M., BODIS, D., 1985, *Geotermalna energia viedenskej panvy - prognozne zasoby*. Geofond, Bratislava.

REMSIK, A., BODIS, D., FENDEK, M., KRAL, M., ZBORIL, L., 1989, *Methods of Research and Evaluation of Geothermal Energy Reserves in a Fissure-Karst Setting of the Slovak part of the Vienna Basin.* Zapadne Karpaty. Seria hydrogeologia a inzinierska geologia,8, GODS, Bratislava, 193-205.

REMSIK, A., FRANKO, O., BODIS, D., 1992, *Geotermalne zdroje komarinanskej kryhy. Zapadne Karpaty*. Seria hydrogeologia a inzinierska geologia, 10, GODS, 159-199.

REZESSY, G., SZANYI, J., HÁMOR, T., 2005, *A geotermikus energiavagyon állami nyilvántartásának előkészítéséről. I. fázis*. Magyar Geológiai Szolgálat. Budapest, p. 85. Report on the registration of geothermal resources in Hungary. First phase. Hungarian Geological Survey, Budapest, p. 85.

ROYDEN, L.H. AND DÖVÉNYI, P., 1988, *Variations in extensional styles at depth across the Pannonian basin system*. In: L.H. Royden and F. Horváth (Editors), The Pannonian Basin, a Study in Basin Evolution. Amer. Assoc. Petr. Geol. Mem., 45: 235-255.

ROYDEN, L.H., HORVÁTH, F. AND RUMPLER, J., 1983a, *Evolution of the Pannonian basin system: 1. Tectonics*. Tectonics, 2: 63-90.

ROYDEN, L.H., HORVÁTH F., NAGYMAROSY A., STEGENA L., 1983b, *Evolution of the Pannonian basin system: 2. Subsidence and thermal history*. Tectonics, 2: 91-137.

ROYDEN, L.H. AND HORVÁTH, F. (eds.), 1988, *The Pannonian Basin, a Study in Basin Evolution*. Amer. Assoc. Petr. Geol. Mem., 45, 394 pp.

ROYDEN, L., KEEN, C.E., 1980, *Rifting process and thermal evolution of the continental margin of Eastern Canada determined from subsidence curves*. Earth and Planet. Sci. Let. 51: 343-361.

RYBACH, L. AND BUNTEBARTH, G., 1984, *The variation of heat generation, density and seismic velocity with rock type in the continental lithosphere*. Tectonophysics, 103: 335-344

RYBACH, L. AND CERMÁK, V., 1982, *Radioactive heat generation in rocks. In: G. Angenheister (Editor), Physical Properties of Rocks*. Springer-Verlag Berlin, Vol. 1b: 353-371.

SACHSENHOFER, R.F., LANKREIJER, A., CLOETINGH, S., EBNER, F., 1997, *Subsidence analysis and quantitative basin modelling in the Styrian Basin (Pannonian Basin System, Austria)*. Tectonophysics, 272: 175-196.

SASS, J.H., LACHENBRUCH, A.H., MOSES, Jr. T.H., MORGAN, P., 1992, *Heat flow from a scientific research well at Cajon Pass, California*. Journal of Geophysical Research, Volume 97, No. B4, p. 5017 – 5030.

SCHOEN, J., 1983, *Petrophysik – Physikalische Eigenschaften von Gesteinen und Mineralien*, Akademie Verlag Berlin.

SCLATER, J.G., JAUPART, C., GALSON, D., 1980, *The heat flow through oceanic and continental crust and the heat loss of the Earth*. Rev. Geophys. Space Phys., 18(1): 269-311.

SEKIGUCHI, K., 1984, *A method for determining terrestrial heat flow in oil and basinal areas*. Tectonophysics, Volume 103, Issues 1-4, p. 67 – 79.

SZALAY, Á., 1982, *A rekonstrukciós szemléletű földtani kutatás lehetőségei szénhidrogén-perspektívák előrejelzésében* (Possibilities in the reconstruction of basin evolution in the prediction of hydrocarbon prospects). Hungarian Academy of Sciences, Budapest, PhD thesis.

VACQUIER, V., 1984, *Oil fields – a source of heat flow data*. Tectonophysics, Volume 103, Issues 1- 4, p. 81 – 98.

ZEKIRI, F., 2011, *Erstellung von Temperaturkarten in verschiedenen Tiefen im südlichen Wiener Becken*. Univ. Wien, Wien, diploma thesis (in German, with English abstract).

ZÖTL, J., ZOJER, H., 1979, *Bericht über die Erstellung einer Karte der geothermischen Tiefenstufe für den Bereich des südlichen Burgenlandes*. Bericht Bund/Bundesländer-Rohstoffprojekt B-A-006/79, Joanneum Research, Graz.

ZOJER, H., 1977, *Untersuchung der geothermischen Tiefenstufe mittels Temperaturmessungen bei artesischen Brunnen in der Oststeiermark und im südlichen Burgenland*. Verhandlungen der Geol. B.A. Bd. 1977, S. 393 – 403, Wien.

ZOTH, G., HAENEL, R., 1988, *Appendix*. In: HAENEL R., RYBACH L., STEGENA L. (eds.), Handbook of terrestrial heat flow density determination. Kluwer academic publishers, Dordrecht, Boston, London, p. 449-466.

Enclosures

- **Enclosure 1:** Surface Heat Flow Density Map, 1:500.000
- **Enclosure 2a:** Temperature at depth of 1000m below surface, 1:500.000
- **Enclosure 2b:** Temperature at depth of 2500m below surface, 1:500.000
- **Enclosure 2c:** Temperature at depth of 5000m below surface, 1:500.000
- **Enclosure 2d:** Temperature at top of pre-tertiary basement, 1:500.000
- **Enclosure 3a:** Depths of 50degC isothermal surface, 1:500.000
- **Enclosure 3b:** Depths of 100degC isothermal surface, 1:500.000
- **Enclosure 3c:** Depths of 150degC isothermal surface, 1:500.000
- **Enclosure 4a:** Specific Heat in Place for Neogene sediments, 1:500.000
- **Enclosure 4b:** Specific Heat in Place at the uppermost 50m of the pre-tertiary basement, 1:500.000
- **Enclosure 4c:** Specific Heat in Place from surface until 5000m.b.s, 1:500.000
- **Enclosure 4d:** Specific Heat in Place from surface until 7000m.b.s, 1:500.000
- **Enclosure 4e:** Specific Identified Resources for Neogene sediments, 1:500.000
- **Enclosure 4f:** Specific Identified Resources at the uppermost 50m of the pre-tertiary basement, 1:500.000
- **Enclosure 4g:** Specific Identified Resources from surface until 5000m.b.s, 1:500.000
- **Enclosure 4h:** Specific Identified Resources from surface until 7000m.b.s., 1:500.000